

**Design and Synthesis of Matrix Metalloproteinase
Inhibitors Derived from a 6*H*-1,3,4-Thiadiazine Scaffold**

Dissertation zur Erlangung des Grades eines
Doktors der Naturwissenschaften
der Universität Bielefeld

vorgelegt von

Jörg Schröder

aus Lage

Bielefeld 2001

Für Sabine

Die vorliegende Arbeit entstand in der Zeit von Januar 1997 bis Juni 2001 an der Fakultät für Chemie der Universität Bielefeld.

Meinem akademischen Lehrer, Herrn Prof. Dr. Harald Tschesche danke ich für die interessante Themenstellung, die er mir zur weitgehend selbständigen Gestaltung überließ, die stete Diskussionsbereitschaft und für das fortwährende Interesse an meiner Arbeit.

Herrn Dr. Hans Brandstetter, Max-Planck-Institut für Biochemie, Martinsried, danke ich für die Röntgenstrukturaufklärung von *N*-Allyl-5-(4-chlorphenyl)-6*H*-1,3,4-thiadiazin-2-amin im Komplex mit der katalytischen Domäne der menschlichen neutrophilen Kollagenase sowie für zahlreiche und wertvolle Diskussionen.

Herrn Dr. Andreas Bergner, Max-Planck-Institut für Biochemie, Martinsried, danke ich für den lehrreichen Aufenthalt im Institut vom 08.12. – 12.12.1997, wo er mir eine Einführung in das "Ligand-Docking" gab.

Herrn Dr. Wolf-Diethard Pfeiffer, Institut für Chemie und Biochemie, Universität Greifswald, danke ich für die Überlassung einiger Testsubstanzen.

Herrn Dr. Achim Krüger, Institut für experimentelle Onkologie und Therapieforschung der technischen Universität München, danke ich für die Durchführung von *in vitro* Zellassays mit (2*S*)-*N*-[5-(4-Chlorphenyl)-6*H*-1,3,4-thiadiazin-2-yl]-2-[(phenylsulfonyl)amino]propanamid.

Der Firma Schering AG, Berlin, sei an dieser Stelle für die Finanzierung der europäischen Patentanmeldung gedankt.

Der Deutschen Forschungsgemeinschaft (DFG) danke ich für die Unterstützung dieser Arbeit im Rahmen des Projektes "Inhibitor design" (Ts 8/37 (HT)).

Mein besonderer Dank gilt Frau Beate Neumann, Frau Anja Stammler und Herrn Hans-Georg Stammler für die Durchführung der vielen Röntgenstrukturanalysen, Herrn Dipl.-Ing. Klaus-Peter Mester für das Messen zahlreicher NMR-Spektren sowie Frau Brigitte Michel für die Durchführung der CHN-Analysen.

Desweiteren danke ich den Mitgliedern des Arbeitskreises von Prof. Dr. em. Hans-Friedrich Grützmacher, Prof. Dr. Jochen Mattay und Prof. Dr. Norbert Sewald für die Aufnahme der Massenspektren.

Ferner danke ich Herrn Christian-Alexander Mast, Herrn Micha Jost, Frau Juliane Grotta und Herrn Kai Jenssen für präperative Arbeiten, die sie im Rahmen eines sechswöchigen Praktikums für diese Arbeit geleistet haben.

Mein aufrichtiger Dank gilt Herrn Dr. Herbert Wenzel und Herrn Rainer Beckmann für zahlreiche Ratschläge und wertvolle Diskussionen; dem gesamten Arbeitskreis BC I danke ich für das angenehme Arbeitsklima und die gute Zusammenarbeit.

Schließlich möchte ich mich ganz besonders bei meiner Familie bedanken, die mir während der gesamten Zeit mit Rat und Tat zur Seite gestanden hat.

Teile des Inhalts dieser Arbeit sind bereits veröffentlicht, zur Publikation angenommen oder von mir auf Symposien vorgestellt worden.

1. Schröder, J. und Tschesche, H. (2000) Thiadiazines and their use as inhibitors of metalloproteinases. *Europäische Patentanmeldung* EP00120727.3.
2. Schröder, J., Henke, A., Wenzel, H., Brandstetter, H., Stammler, H. G., Stammler, A., Pfeiffer, W. D., and Tschesche, H. (2001) Structure-based design and synthesis of potent matrix metalloproteinase inhibitors derived from a 6H-1,3,4-thiadiazine scaffold. *J. Med. Chem.*, im Druck.
3. Schröder, J., Wenzel, H., Tschesche, H. (2001) 3D structure and design of matrix metalloproteinase inhibitors. In: *Proteases and their inhibitors in cancer metastasis* (Muschel R. J. und Foidart, J. M., Hrsg.). Klüver Akademischer Verlag, Dordrecht, im Druck.
4. Schröder, J., Wenzel, H., Stammler, H. G., Stammler, A., Neumann, B., Tschesche, H. (2001) Novel heterocyclic inhibitors of matrix metalloproteinases: three 6H-1,3,4-thiadiazines. *Acta Cryst. C57*, 593-596.
5. Schröder, J. (01.06.1999) Various approaches to the design of synthetic metalloproteinase inhibitors. Vortrag auf dem Workshop "Metalloproteinases and their inhibitors", Schering AG, Berlin.

6. Schröder, J. (09.03.2001) Strukturbasiertes Design von heterocyclischen Matrix Metalloproteinase Inhibitoren auf der Basis von 6*H*-1,3,4-Thiadiazinen. Vortrag auf dem DFG-Workshop "Matrixmetalloproteinasen: Struktur, Funktion und physiologische Bedeutung", Zentrum für interdisziplinäre Forschung (ZIF), Universität Bielefeld.

7. Schröder, J. (14.03.2001) Peptide mimics – The discovery and optimization of potent matrix metalloproteinase inhibitors derived from a 6*H*-1,3,4-thiadiazine scaffold. Vortrag auf dem 5. Deutschen Peptidsymposium, Universität Bielefeld.

***“Upon this gifted age rains from the sky a meteoric shower
of facts... they lie unquestioned, uncombined.
Wisdom enough to leech us of our ills is daily spun, but
there exists no loom to weave it into fabric”.***

(Edria St. Vincent Millay)

List of Abbreviations

Å	angstrom
ACE	angiotensin converting enzyme
ADAM	a disintegrin and metalloproteinase
AG-3340	prinomastat
APMA	p-aminophenylmercuric acetate
aq	aqueous
BB-2516	marimastat
BB-94	batimastat
cd	catalytic domain
CDCl ₃	deutero chloroform
DCI	direct chemical ionization
dec	decomposition
DEI	direct electron impact
DHB	2,5-dihydroxybenzoic acid
DMF	dimethylformamide
DMSO	dimethylsulfoxide
ECM	extracellular matrix
EDC	<i>N</i> -ethyl- <i>N'</i> -(3-dimethyl-aminopropyl)-carbodiimide hydrochloride
EtOH	ethanol
HEPES	<i>N</i> -[2-hydroxyethyl]-piperazine- <i>N'</i> -[2-ethane- sulfonic acid]
HOBt	1-hydroxy-benzotriazole
HTS	high throughput screening
IL-R	interleukin-like receptor
LHS	left-hand side
MALDI	matrix assisted laser desorption/ionization
Mca	(7-methoxy-coumarin-4-yl)acetyl-
MeOH	methanol

List of Abbreviations

MMP	matrix metalloproteinase
MMPI	matrix metalloproteinase inhibitor
mp	melting point
MRB	microfluorogenic reaction buffer
MT-MMP	membrane-type matrix metalloproteinase
NMM	4-methylmorpholine
NMR	nuclear magnetic resonance
p.a.	pro analysi
PDB	protein database
PEG	polyethyleneglycol
PMNL	polymorpho-nuclear neutrophil leucocytes
ppm	parts per million
rdf	receptor description file
RHS	right-hand side
RP-HPLC	reverse phase high performance liquid chromatography
SAR	structure-activity relationship
TFA	trifluoroacetic acid
THF	tetrahydrofurane
TIMP	tissue inhibitor of metalloproteinases
TKI	trypsin kallikrein inhibitor
TLC	thin layer chromatography
TMS	tetramethylsilane
TOF	time of flight
uPA	urokinase plasminogen activator
uPAR	urokinase plasminogen activator receptor
ZBG	zinc-binding group

List of Abbreviations

Aminoacids

A	alanine	Ala
C	cysteine	Cys
D	aspartic acid	Asp
E	glutamic acid	Glu
F	phenylalanine	Phe
G	glycine	Gly
H	histidine	His
I	isoleucine	Ile
K	lysine	Lys
L	leucine	Leu
M	methionine	Met
N	asparagine	Asn
P	proline	Pro
Q	glutamine	Gln
R	arginine	Arg
S	serine	Ser
T	threonine	Thr
V	valine	Val
W	tryptophan	Trp
Y	tyrosine	Tyr

Table of Contents

Chapter 1	Abstract	
1.1	General Introduction	1
1.2	Summary of the Results	2
Chapter 2	Theory	
2.1	Metzincins.....	6
2.2	Matrix Metalloproteinases	7
2.3	Synthetic Matrixin Inhibitors	9
2.3.1	Zinc-Binding Groups	11
2.3.2	First Generation MMPiS	13
2.3.3	Next Generation MMPiS.....	14
2.3.4	Other Inhibitors	17
Chapter 3	Aims of the Study	18
Chapter 4	Results and Discussion	
4.1	Identification of Lead-Structures	19
4.2	Modifications of the Lead-Structures	21
4.3	Chemistry	22
4.4	Structure-Activity Relationship (SAR) Analysis	25
4.4.1	SAR of the Position 5 Substituent	26
4.4.2	SAR of the Sulfonamide Residue	29
4.4.3	SAR of Variations of the α -Carbon Substituents	30
4.5	X-ray Crystallography.....	31

Table of Contents

4.5.1	Crystal Structures of 6 <i>H</i> -1,3,4-Thiadiazine-2-amide-Based MMPIs	31
4.5.2	Binding of <i>N</i> -Allyl-5-(4-chlorophenyl)-6 <i>H</i> -1,3,4-thiadiazine-2-amine Hydrobromide to cdMMP-8.....	38
4.6	Protein/Ligand-Docking Experiments	41
4.7	<i>In vitro</i> Cell-Assay	45
Chapter 5	Conclusions	47
Chapter 6	Experimental Section	
6.1	General Information	49
6.2	Synthetic Methods.....	51
6.2.1	Aryl ω -Halo Ketones	51
6.2.2	Substituted 2-Amino-6 <i>H</i> -1,3,4-thiadiazine Hydrohalides	52
6.2.3	<i>N</i> -Sulfonylated Amino Acids	56
6.2.4	Substituted 6 <i>H</i> -1,3,4-Thiadiazine Amides.....	59
6.3	Enzyme Preparations.....	68
6.4	Crystallography.....	69
6.4.1	Crystallization of the Inhibitors and Structure Analysis	69
6.4.2	Crystallization of the cdMMP-8/Inhibitor Complex and Structure Analysis	70
6.5	Computational Docking and Modeling.....	71
6.6	<i>In Vitro</i> Assays.....	72
6.6.1	MMP Inhibition Assay.....	72
6.6.2	Determination of the K_i -Values.....	72

Table of Contents

Chapter 7	Literature	74
Chapter 8	Appendix	88

1 Abstract

1.1 General Introduction

Pharmaceutical drug development is a long and expensive process. Lacking *a priori* knowledge about which compound might serve as a drug in a certain disease indication, this process traditionally contains a series of distinct steps, including an initial screening assay of low molecular weight compounds against the target enzyme, followed by a selection of a candidate lead compound from the initially identified hits. Early selection of promising molecules can dramatically improve this process, but so far, there are only few well defined criteria to perform this selection.

The shortcoming of traditional drug discovery as well as the appeal of a more deterministic approach to combat diseases has led to the concept of "Rational Drug Design". Detailed information about the disease or infectious process is a requirement for drug design. Hereby, the first necessary step is the identification of a molecular target critical to a disease process or an infectious pathogen. An additional important prerequisite of drug design is the determination of the precise three-dimensional molecular structure of the target by X-ray crystallography, ideally complexed with substrate analogues or (natural) inhibitors. This structure then serves as a blueprint for the design of a lead compound. Selected compounds are modeled for their fit in the active site of the target, considering both steric aspects (*i.e.*, geometric shape complementarity) and functional group interactions, such as hydrogen bonding and hydrophobic interactions. The initial design phase is followed by an iterative refinement procedure which includes the synthesis of the lead compound, quantitative measurements of its ability to interact with the target, and X-ray crystallographic analysis of the compound-target complex. This analysis reveals important empirical information on how the compound actually binds to the target and the nature and extent of changes induced in the target by the binding. These data, in turn, suggest ways to improve the lead compounds binding affinity. The refined lead compound is then synthesized and complexed with the target, and further refined in a reiterative process. Once a sufficiently potent compound has been designed and optimized, its activity is evaluated in a biological system to establish the function in a physiological environment. This process continues until a designed compound exhibits the desired

properties. The compound is then evaluated in an experimental disease model to prove its status as an experimental drug. The experimental drug candidate is then ready for conventional drug development in a clinical trial.

The drug discovery approach by which synthetic compounds are designed from detailed structural knowledge of the active sites of protein targets associated with particular diseases is called "Structure-Based Drug Design".¹⁻⁶ The following figure emphasizes the cyclic and multidisciplinary aspects of this type of drug design.

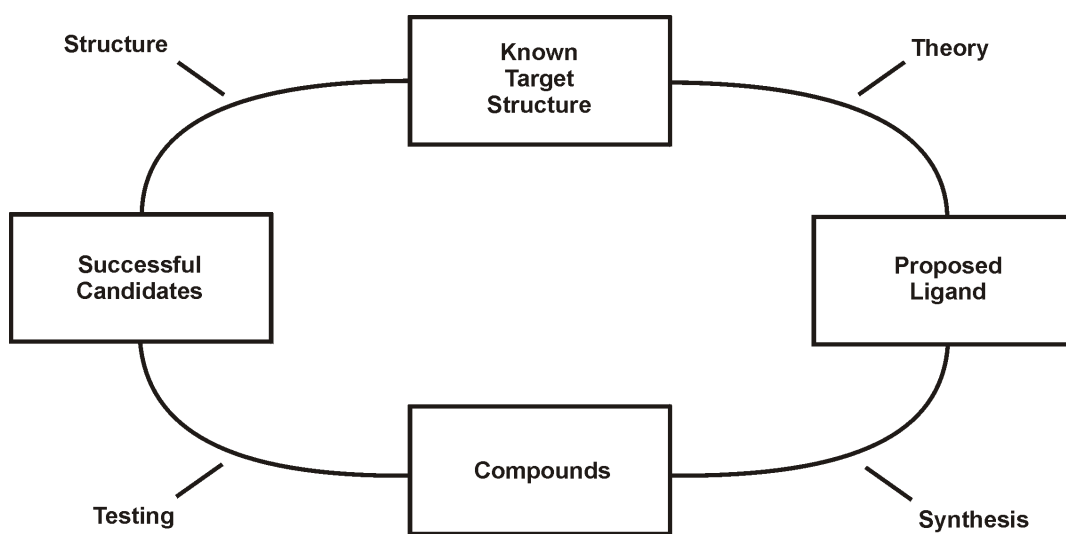


Figure 1.1 *The cycle of structure-based drug design.*

In fact, this method is limited to the availability of a high-resolution target structure with its substrate recognition sites defined at atomic detail. Only with this information "Structure-Based" or "Rational Drug Discovery" will be feasible.

1.2 Summary of the Results

In the last decade the zinc-containing matrix metalloproteinases (MMPs) have become attractive targets for structure-based drug design because of their implication in a variety of diseases in which the destruction of connective tissue is an important pathological event. To date the main focus of the therapeutic applications of MMP inhibitors (MMPi) has been in the areas of cancer and arthritis. An appreciation for the potential role of MMPs in other pathological conditions is ever expanding. The design of MMPi has been

primarily based upon imitation of the binding scheme of natural protein substrates such as collagen to the MMPs. Peptidomimetics, pseudopeptides or non-peptide inhibitors which incorporate a zinc-binding group and side chains which interact with the enzyme subsites form the common structural scaffold. The most ubiquitous type of inhibitor is designed to bind to the primed substrate recognition sites ("right-hand side") of the enzyme using a hydroxamic acid as the zinc chelator. Because of the biologically labile nature of hydroxamates, the low oral bioavailability, and poor duration of action exhibited by most peptide-based compounds, two important aims of the present thesis to the design, synthesis, and biological evaluation of inhibitors of matrix metalloproteinases are highlighted: 1. the invention of alternatives to hydroxamic acid zinc-chelators, and 2. the construction of non-peptide scaffolds.

In this thesis a new generation of heterocyclic non-peptide matrix metalloproteinase inhibitors derived from a 6*H*-1,3,4-thiadiazine scaffold was discovered. A screening effort identified some chiral *N*-alkyl-(6-methyl-5-phenyl-6*H*-1,3,4-thiadiazine-2-yl)-amines which are weak inhibitors ($K_i > 40 \mu\text{M}$) of the catalytic domain of human neutrophil collagenase (cdMMP-8). Further chemical modifications including the removal of the 6-methyl group resulted in novel 5-substituted 6*H*-1,3,4-thiadiazine-2-amides which show promising potency against MMPs. The breakthrough of this compound series was initialized by the incorporation of a *N*-sulfonylated amino acid as the carboxylic acid component to improve right-hand side binding affinity. The new compounds were tested against eight different matrix metalloproteinases, MMP-1, cdMMP-2, cdMMP-8, MMP-9, cdMMP-12, cdMMP-13, cdMMP-14, and the ectodomain of MMP-14. An in-depth examination of structure-activity relationships (SARs) on modifications of the position 5 substituent, on modifications of the sulfonamide residue, and on variations of the α -carbon substituents produced the selective inhibitor (2*R*)-*N*-[5-(4-bromophenyl)-6*H*-1,3,4-thiadiazin-2-yl]-2-[(phenylsulfonyl)amino]propanamide with high affinity for MMP-9 ($K_i = 40 \text{ nM}$) and (2*S*)-*N*-[5-(4-chlorophenyl)-6*H*-1,3,4-thiadiazin-2-yl]-2-[(2-thienylsulfonyl)amino]propanamide with high affinity for cdMMP-8 ($K_i = 60 \text{ nM}$).

The X-ray crystallographic structure determined at 2.7 Å resolution for cdMMP-8 co-crystallized with *N*-allyl-5-(4-chlorophenyl)-6*H*-1,3,4-thiadiazin-2-amine hydrobromide gave detailed design information on key binding interactions for thiadiazine-based MMP

inhibitors. In addition the crystal structure of uncomplexed *N*-allyl-5-(4-chlorophenyl)-6*H*-1,3,4-thiadiazin-2-amine hydrobromide was determined and compared with the complexed structure. This comparison and the calculation of ring puckering parameters for both structures reveal a preferential screw-boat conformation of the thiadiazine system when complexed to cdMMP-8. The coordination to the catalytic zinc cation is surprisingly mediated via the exocyclic nitrogen of the thiadiazine moiety, while the ring nitrogens are involved in specific hydrogen bonds with the backbone of cdMMP-8. These results indicate that 6*H*-1,3,4-thiadiazine-based MMPIs interact with both the primed and the unprimed side of the MMP.

To explore the structures of 6*H*-1,3,4-thiadiazine-2-amide-based MMPIs a method to crystallize these compounds was developed within this thesis. Using X-ray crystallography an amido-imino tautomerism (prototropic shift) shown by different bond lengths within the 6*H*-1,3,4-thiadiazine moiety was elucidated for this compound series. Therefore, the endocyclic N3 of the 6*H*-1,3,4-thiadiazine core fragment acts either as a hydrogen-bond acceptor or a hydrogen-bond donor depending on the state of the tautomeric equilibrium. Since suitable crystals of the cdMMP-8/(2*S*)-*N*-[5-(4-chlorophenyl)-6*H*-1,3,4-thiadiazin-2-yl]-2-[(2-thienylsulfonyl)amino]propanamide complex could not be obtained for X-ray studies, cdMMP-8/inhibitor docking experiments were performed using the program FlexX. The crystal structure of uncomplexed (2*S*)-*N*-[5-(4-chlorophenyl)-6*H*-1,3,4-thiadiazin-2-yl]-2-[(2-thienylsulfonyl)amino]propanamide was determined at 0.84 Å resolution and shows two molecules per asymmetric unit. Within the molecules different ring conformations of the thiadiazine system occur. The atom coordinates of these two structures in combination with coordinates from the complexed reference inhibitor *N*-allyl-5-(4-chlorophenyl)-6*H*-1,3,4-thiadiazin-2-amine were used to perform the virtual docking to cdMMP-8. The comparison of the minimized energies and the best rms-values (best rms means closest to reference structure) for the binding models reveal that the 2-thienyl residue does not fit into the S₁' pocket but is positioned on the normal vector to the catalytic zinc(II)-ion at 5.1 Å distance. These results suggest that cation-aromatic interactions may play a role in stabilizing the enzyme/inhibitor adduct.

To test the anti-tumor activity of the novel thiadiazine-based MMPIs an *in vitro* cell assay with the mamma carcinoma cell-line MDA-231 BAG was performed. The inhibitor

(2*S*)-*N*-[5-(4-chlorophenyl)-6*H*-1,3,4-thiadiazin-2-yl]-2-[(phenylsulfonyl)amino]propanamide was assayed using a potent MMP inhibitor as a reference. It was found that both the thiadiazine-based inhibitor and the reference inhibitor can reduce the gelatinolytic activity of the cell-line by about 20 percent. As an additional benefit, the thiadiazine-based inhibitor displayed this activity at about 50 percent lower concentration compared to the reference inhibitor. Since the reference inhibitor was tested in a synergic mouse lymphoma model with great success, thiadiazine-based MMPIs are now attractive candidates for *in vivo* tumor models.

In summary, a complete drug design work was performed with this thesis. The discovery of 6*H*-1,3,4-thiadiazine-based MMPIs may be regarded as a breakthrough for continued development of inhibitors of matrix metalloproteinases as drugs.

2 Theory

2.1 Metzincins

Proteinases can be subdivided into four major classes: serine-, cysteine-, aspartic- and metalloproteinases due to their residue crucial in catalysis. The majority of zinc containing metalloproteinases exhibit a characteristic HEXXH consensus sequence integrated into an "active-site helix". The two histidine residues serve as zinc ligands, and the glutamic acid residue polarizes a water molecule involved in nucleophilic attack at the scissile peptide bond. These features were first examined in the structure of the gluzincin thermolysin.⁷ The metzincins, classified by Bode *et al.*, have an extended zinc binding consensus sequence HEXHXXGXXH, where the third histidine acts as the third zinc ligand instead of the more distant glutamic acid in thermolysin.⁸ In addition this superfamily has a methionine-containing turn the conformation of which is strictly conserved (the Met-turn).

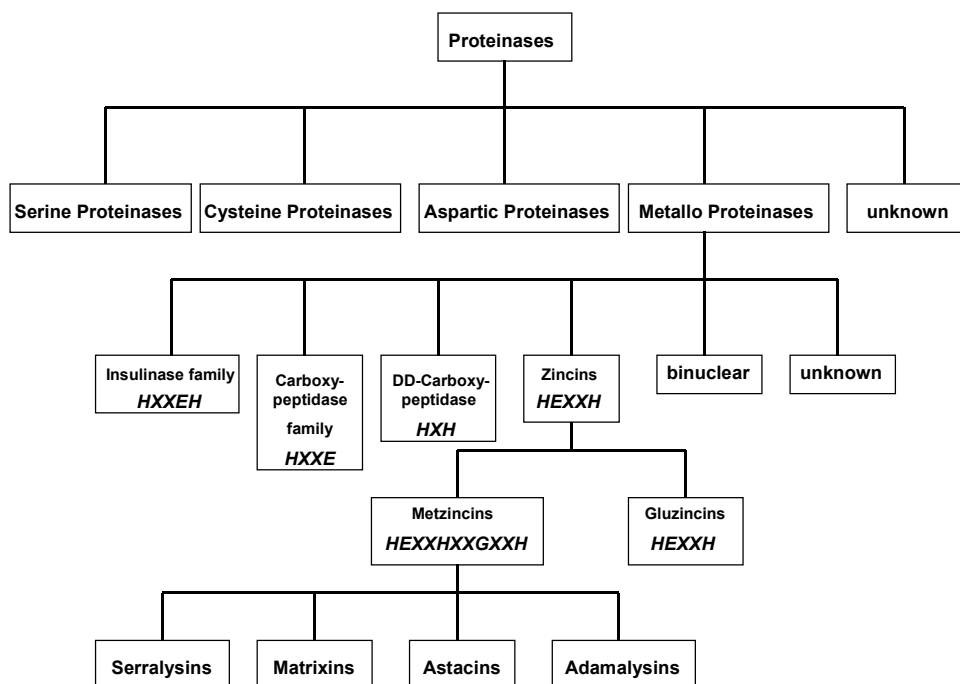


Figure 2.1 Families of proteinases. The families of the zinc metalloproteinases and their inter-relationship based on the sequence around the zinc-binding residues are shown. *Italicised bold letters represent the consensus sequence.*

The metzincin superfamily consists of four subfamilies: the astacins, the serralysins, the snake venom adamalysins (ADAMs: A Disintegrin And Metalloproteinase), and the matrix metalloproteinases (matrixins).

2.2 Matrix Metalloproteinases

The matrix metalloproteinases (MMPs, matrixins) form a subfamily of the metzincins and are structurally and functionally related zinc- and calcium-dependent endopeptidases.

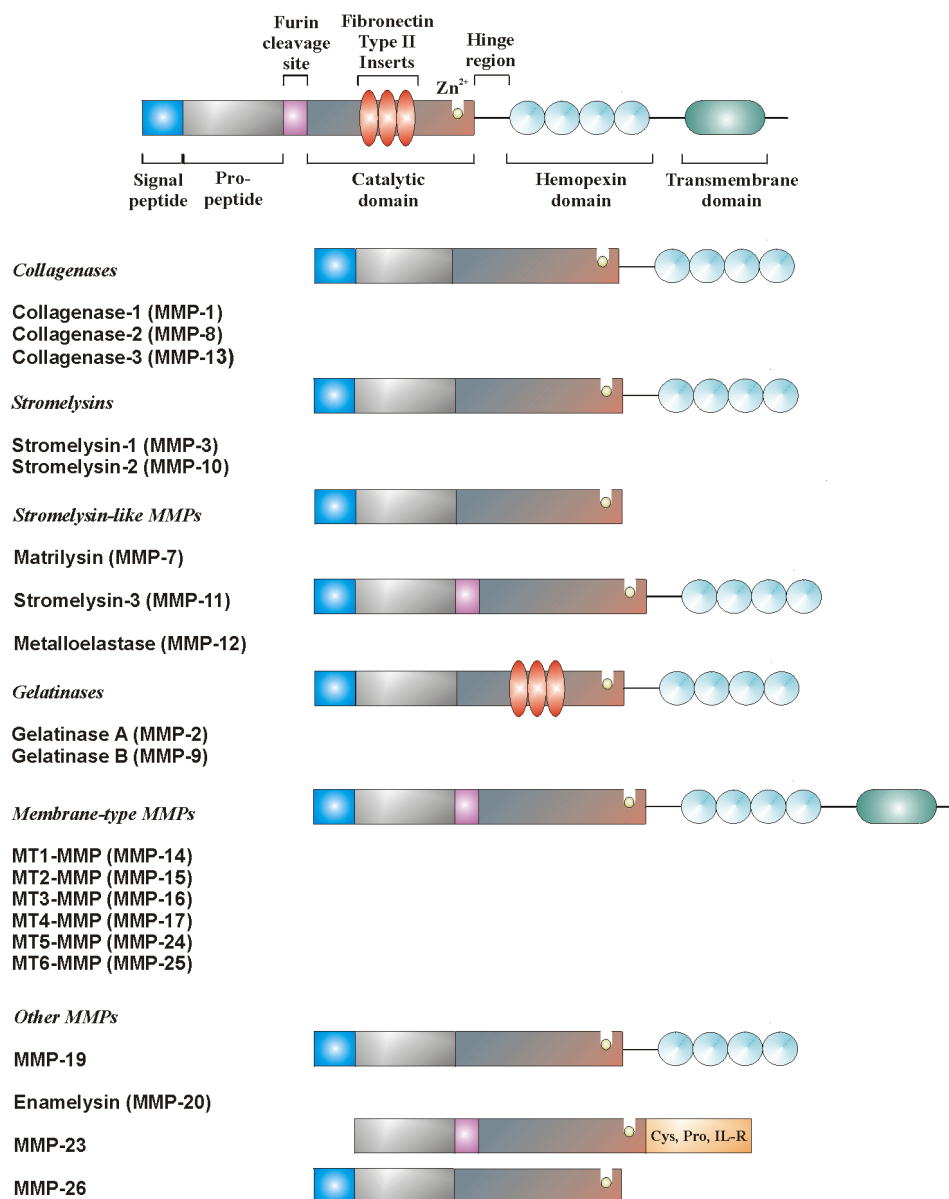


Figure 2.2 Domain structure of matrix metalloproteinases. IL-R = interleukin-like receptor.

The proteolytic activity is directed against most constituents of the extracellular matrix (ECM), like proteoglycans, fibronectin, laminin, and interstitial collagens.^{9,10} At present time, 20 members of the human MMP family have been characterized. Based on their structure and substrate specificity, MMPs are divided into subgroups of collagenases, stromelysins, stromelysin-like MMPs, gelatinases, membrane-type MMPs (MT-MMPs), and other MMPs.¹¹ They all share similar domain structures, which include four major regions: an N-terminal leader sequence involved in secretion, a prodomain that inhibits the enzymatic activity, a catalytic domain, and a hemopexin domain which determines the substrate specificity of MMPs and, in the case of MMP-2, MMP-9 and MMP-13, mediates interactions with their endogenous inhibitors, the tissue inhibitors of metalloproteinases (TIMPs).^{12,13} The hemopexin domain is absent in matrilysin (MMP-7) and MMP-26. In addition, gelatinases A and B (MMP-2 and MMP-9) contain three repeats of the fibronectin-type II domain inserted in the catalytic domain. MT-MMPs contain a transmembrane domain, which anchors these enzymes to the cell surface. MT-MMPs, MMP-11, and MMP-23 also contain a furin cleavage site between the pro-peptide and the catalytic domain, suggesting that these pro-enzymes are activated intracellularly by furin or related enzymes.

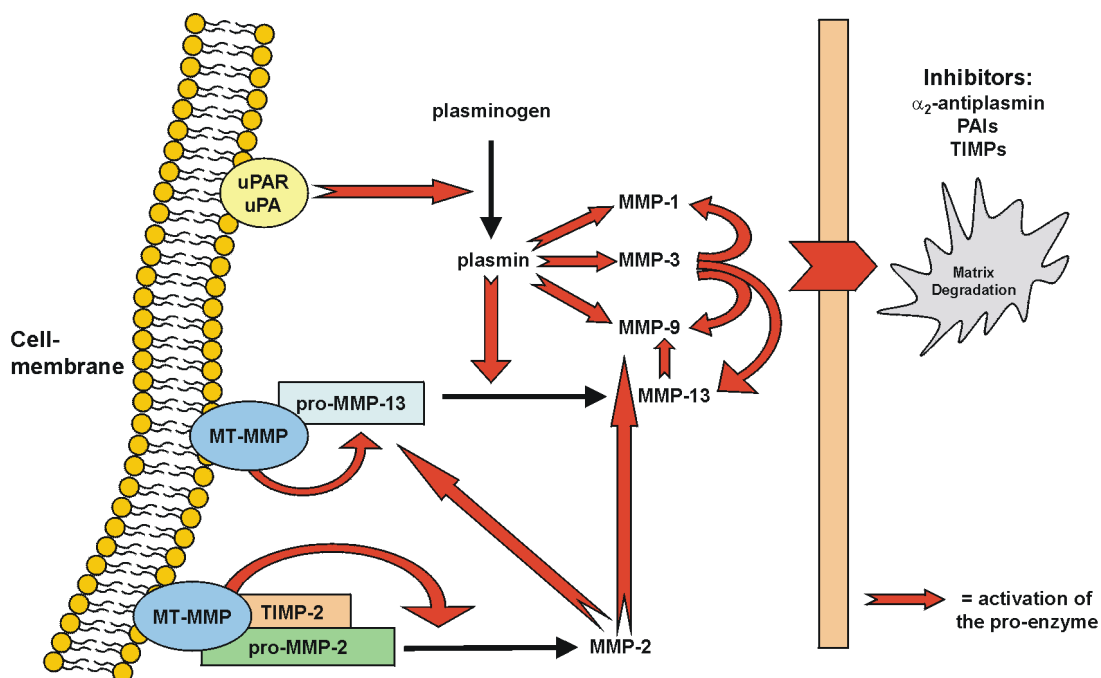


Figure 2.3 Cell surface-associated activation cascades for MMPs.

All MT-MMPs can activate pro-MMP-2. It has been shown that in the process of pro-MMP-2 activation, MT1-MMP is proteolytically activated before it binds the pro-MMP-2/TIMP-2 complex at the cell surface.¹⁴ MT1- and MT2-MMP can also activate pro-MMP-13. This extracellular activation of pro-MMPs is probably limited to the pericellular environment where cell-associated proteinase activities can function in an inhibitor-depleted environment. However, the key initiators of the MMP activation cascades are MT1-MMP and MT2-MMP, which are activated intracellularly, and urokinase-like plasminogen activator (uPA), which is bound to its cell surface receptor (uPAR) (Figure 2.3).¹⁵ At the transcriptional level MMPs are regulated by cytokines and growth factors which stimulate the synthesis and secretion of pro-MMPs as well as of TIMPs. Functionally active forms of pro-MMPs are released via the "cysteine switch" mechanism, whereby the cysteine containing pro-domain is dislocated from the essential zinc of the catalytic module through the proteolytic cleavage of loops necessary for pro-peptide stability.¹⁶ Activated MMPs are thought to play an important role in the physiological degradation of ECM components, *e.g.* during tissue repair, tissue morphogenesis and angiogenesis.¹⁷ In addition, they play a role in pathological conditions characterized by excessive degradation of ECM, such as osteoarthritis, rheumatoid arthritis, periodontal disease, multiple sclerosis, or tumor metastasis.¹⁸⁻²² Therapeutic interventions are possible at one or more biochemical sites of the MMP activation cascades, but direct inhibition of enzyme action by synthetic agents that bind to the catalytic site is a particularly compelling and validated objective.

2.3 Synthetic Matrixin Inhibitors

Two approaches to the identification of matrixin inhibitors have been followed: substrate-based design of pseudopeptide derivatives and random screening of compound libraries and natural products. The design of early matrixin inhibitors was based on the scissile site sequence of peptide substrates. This is the sequence around the glycine-isoleucine and glycine-leucine cleavage sites in the collagen molecules that are hydrolysed by collagenase (Figure 2.4).

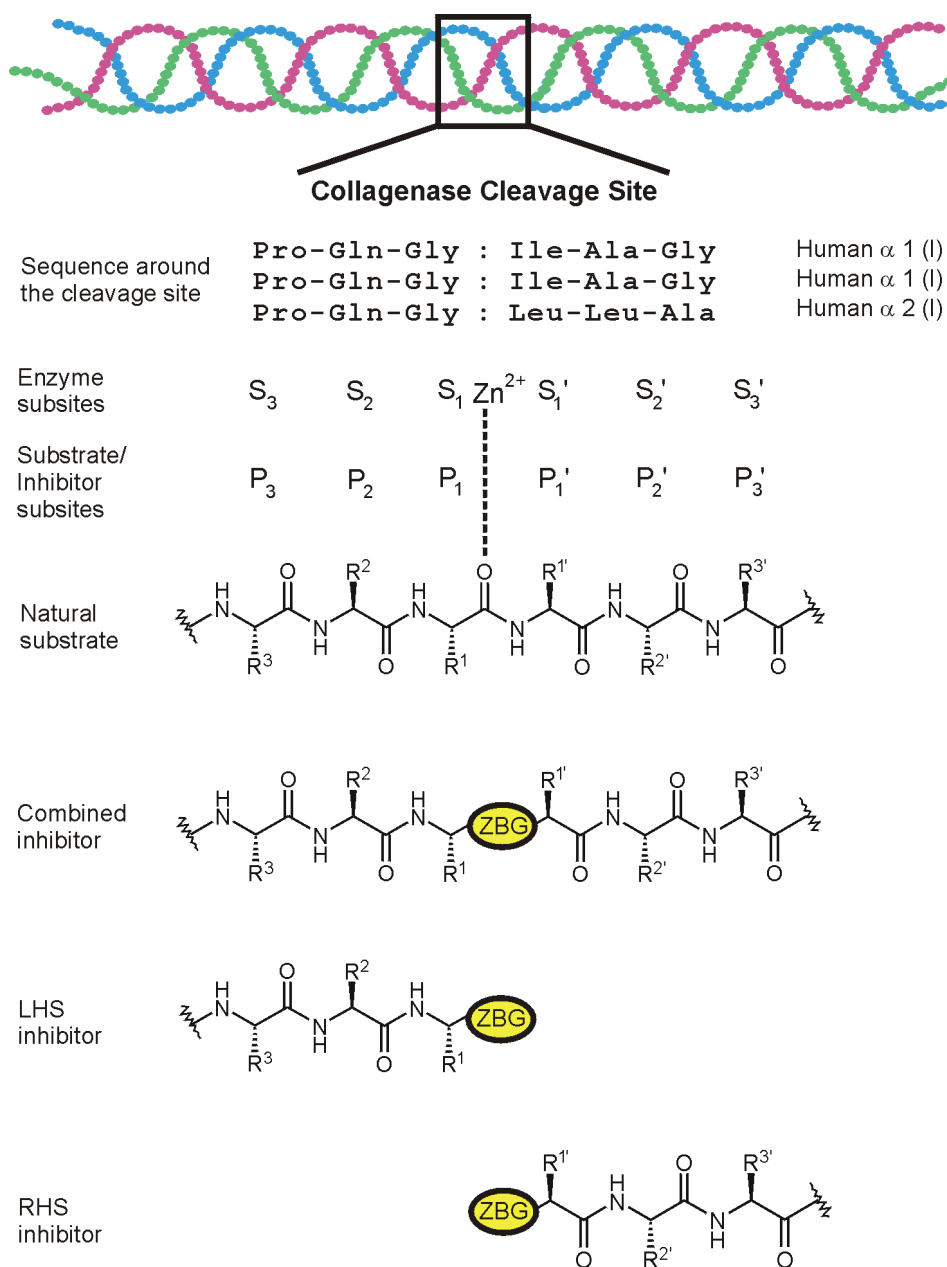


Figure 2.4 Design of matrix metalloproteinase inhibitors based on the cleavage site of collagen.

The key to obtain potent enzyme inhibition has been the incorporation of a zinc-binding group (ZBG) into peptide analogues of the substrate sequence positioned either on the left-hand side (LHS) or the right-hand side (RHS), or in between both sides of the cleavage site. At an early stage, it was found that RHS inhibitors featuring a hydroxamic acid ZBG, are particularly potent in terms of their *in vitro* activity.²³ Considerable insight into MMP/ligand interactions has been obtained from the study of inhibitor structure-

activity relationships (SARs).^{24,25} The use of high-resolution X-ray crystallography and NMR spectroscopy in the elucidation of structures is providing new paradigms for the design of inhibitors in general and selective inhibitors in particular.²⁶⁻³³ From X-ray crystallographic analysis and homology modeling, the MMPs can be divided into two structural classes dependent on the depth of the S₁' pocket. This selectivity pocket is relatively deep for the majority of the enzymes like gelatinase A (MMP-2), stomelysin-1 (MMP-3) or collagenase-3 (MMP-13), but for certain enzymes like human fibroblast collagenase (MMP-1) or matrilysin (MMP-7) it is partially or completely occluded due to an increase in size of the side-chain of amino acid residues that form the pocket.³⁴ Consequently, the main type of selectivity that has been obtained favors the inhibition of the deep pocket enzymes over the short pocket enzymes. This is achieved by the incorporation of an extended P₁' group, whereas the presence of smaller P₁' groups generally leads to broad-spectrum inhibition. This selectivity filter is realised in several MMPI structures which are still under development, including succinyl hydroxamates, sulfonamide hydroxamates and non-hydroxamates.³⁵ This classification for MMPIs further includes the so-called first generation MMPIs, which are pseudopeptide derivatives based on the structure of the collagen molecule at the site of initial cleavage by interstitial collagenase, and the next generation MMPIs, which are non-peptide compounds with selective inhibitory activity against individual MMPs.

2.3.1 Zinc-Binding Groups

The selection of suitable ZBGs has been the subject of intense interest within the research groups. Several different zinc chelators like hydroxamate, carboxylate, sulfhydryl, sulfodiimide and derivatives of phosphoric acid have been identified.³⁶⁻⁴¹ Pseudopeptides, based on phosphorus ZBGs, represented a first interesting inhibitor design alternative. In contrast to peptidic inhibitors containing a thiol or a carboxylate function, these inhibitors act as good mimics of the substrate in the transition state if the zinc-binding function is placed internal at the inhibitor backbone. In this regard, phosphinic chemistry allows the development of transition-state analogues capable to interact with both the primed and unprimed side of the active site cleft. This property can be exploited to optimize inhibitor selectivity.^{42,43}

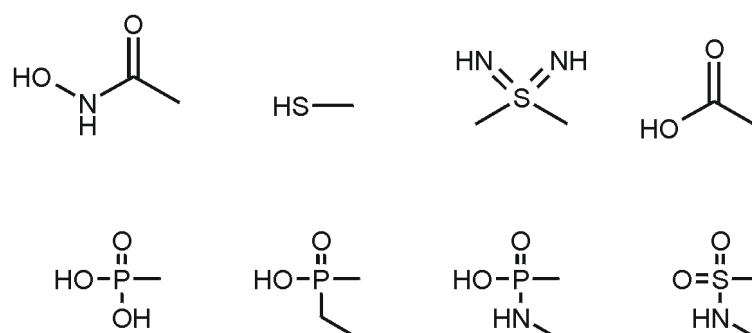


Figure 2.5 Different zinc chelators used in MMP inhibitor templates.

However, the hydroxamates have proved to be the most useful ones and the majority of inhibitors currently under clinical investigation contain this group. The hydroxamate acts as a bidentate ligand with each oxygen at an optimum distance (1.9 – 2.3 Å) from the active site zinc(II)-ion. The position of the hydroxamate nitrogen suggests that it is protonated and forms a hydrogen bond with a carbonyl oxygen of the enzyme backbone.⁴⁴ As shown in Figure 2.6, the hydroxamic acid unit with at least 4-point attachments behaves like a molecular magnet, the significance of which becomes clear as one converts this group to its corresponding carboxylic acid with a concomitant 100 to 1000 fold loss in binding affinity. The remaining residues (R^1 , R^2 etc.) play a significant role in filling specific pockets, endowing the individual inhibitors with unique potency and selectivity.⁴⁵

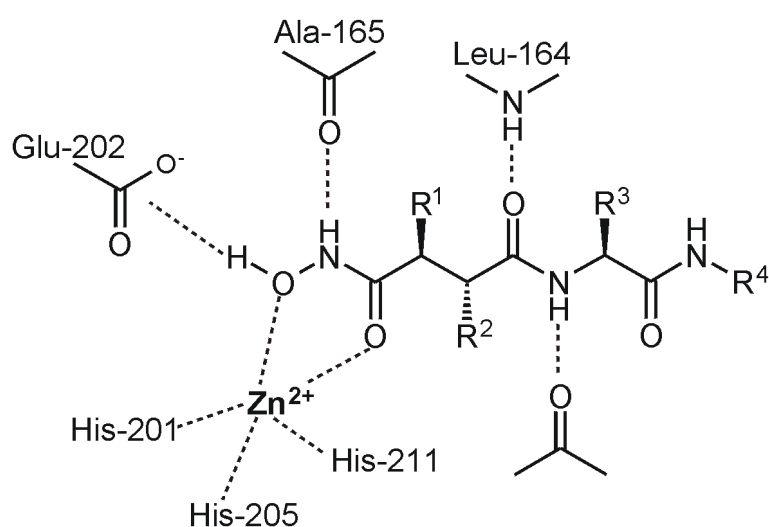


Figure 2.6 Overview of key enzyme/inhibitor interactions of succinyl RHS-hydroxamates (active site of stromelysin-1 is shown).

2.3.2 First Generation MMPIs

Representative examples of this series of MMPIs featuring a succinyl scaffold are the broad-spectrum hydroxamates batimastat (BB-94) and marimastat (BB-2516) developed at British Biotech.⁴⁶

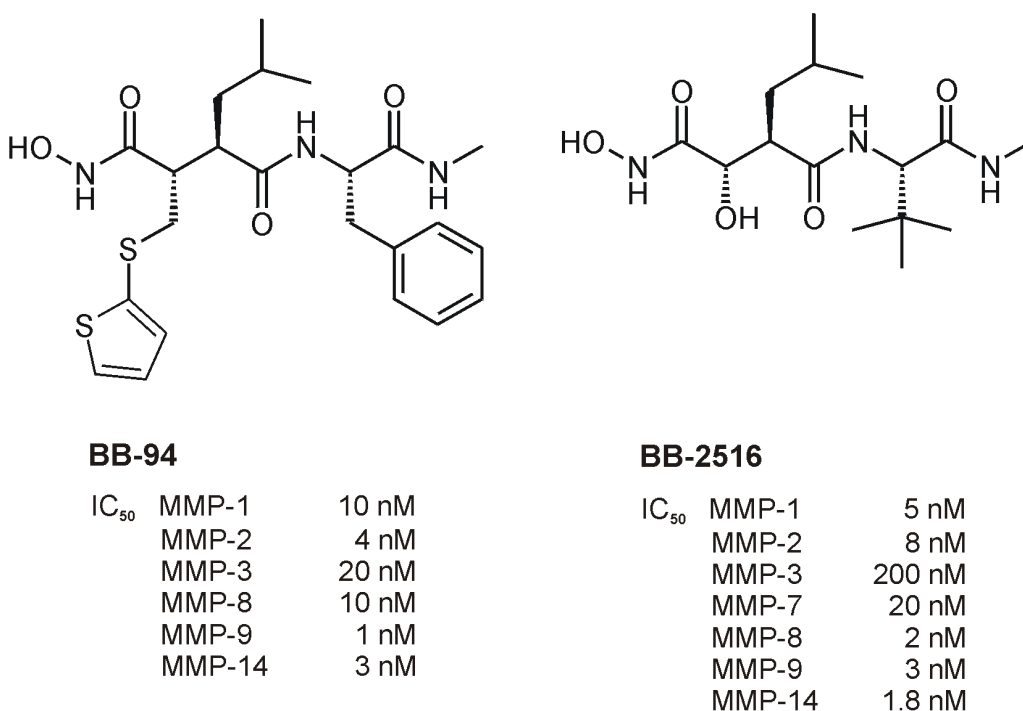


Figure 2.7 Structures of first generation MMPIs reported to be evaluated in clinical trials.

Batimastat was the first compound to enter clinical investigation because of its ability to inhibit primary tumor growth, metastatic spread, and secondary tumor growth *in vivo*.⁴⁷ Despite the effectiveness of batimastat the development of this agent was discontinued because of its low oral bioavailability. The compound's utility is further limited by poor water solubility.⁴⁸ Latest data seem to indicate that batimastat as a hydroxamate-type MMPI promotes liver metastasis.⁴⁹ Structural modification of batimastat resulted in the synthesis of marimastat, which retains the inhibitory activity of its predecessor but shows a species dependent oral bioavailability. It is a potent inhibitor of MMPs, exhibiting K_i -values in the nanomolar range against MMP-1, MMP-2, MMP-3, MMP-7, MMP-8, MMP-9 and MMP-14. Using animal cancer models, marimastat has been observed to inhibit tumor growth and metastasis.^{50,51} Unfortunately, the development of marimastat

was problematic in that, as an anti-tumor drug, it was not expected to induce the reduction in tumor size associated with conventional cytotoxic drugs.⁵²

Batimastat and marimastat are examples of RHS inhibitors with the ZBG on the left end, which has prompted several research groups to establish SAR considerations for this type of MMPIs. Figure 2.8 shows the summary of SARs, which apply to most MMPIs with a succinyl scaffold.⁵³

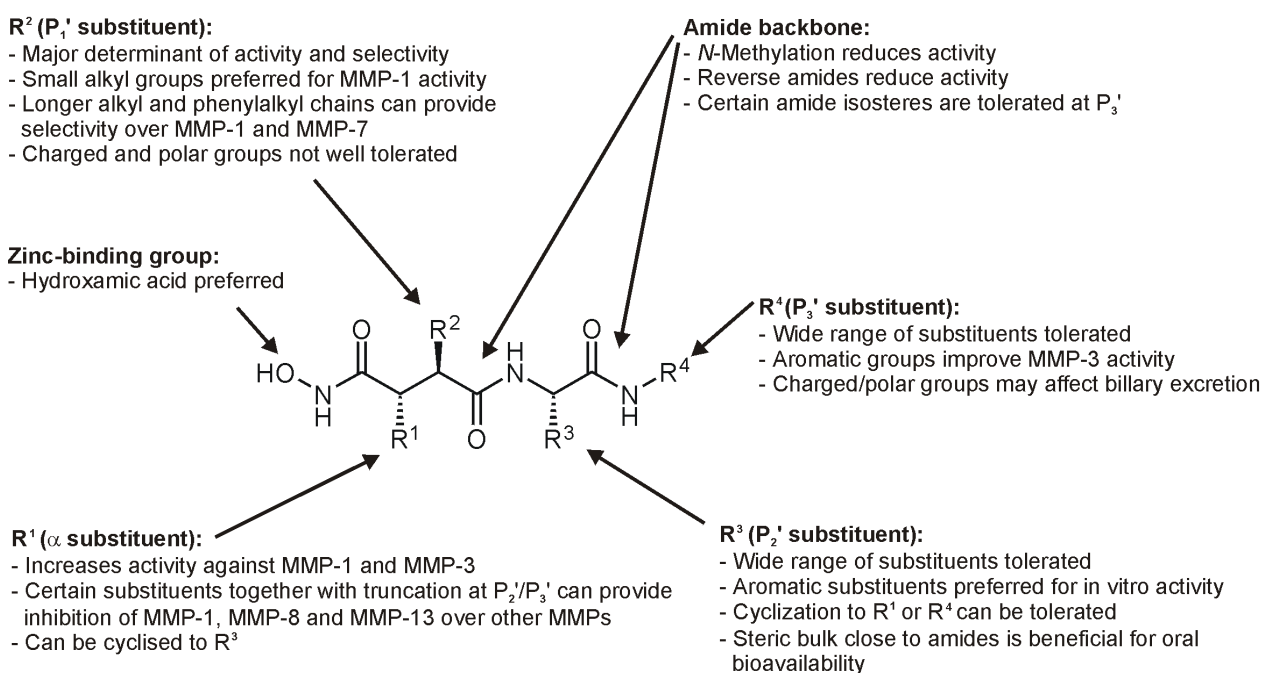


Figure 2.8 Summary of structure-activity relationships for right-hand side MMPIs.

2.3.3 Next Generation MMPIs

In order to develop non-peptidic MMPIs with a selective inhibitory profile, a new concept of inhibitor design has been followed. The discovery and disclosure of CGS-27023A, a small non-peptide MMPI at Ciba-Geigy in the mid-1990's represented a major advance with this concept.^{54,55} The obvious potential of a small molecule inhibitor to overcome the pharmacokinetic problems associated with peptides, such as poor absorption and metabolic lability, attracted the interest of a large number of research groups and has led to several promising compounds based on the sulfonylamino hydroxamic acid scaffold.

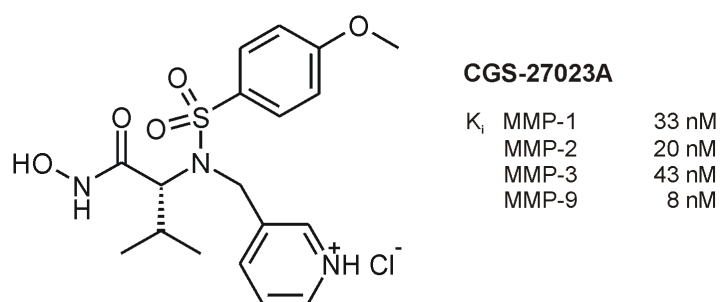


Figure 2.9 Structure of CGS-27023A, a next generation MMPI.

Related compounds have also been independently identified by other research groups through "High-Throughput-Screening" (HTS). In general, these inhibitors have a ZBG like hydroxamic acid, carboxylic acid or thiol and a group capable of acting as a hydrogen bond acceptor (HBA) like sulfone, ketone or ether spaced apart by two atoms.

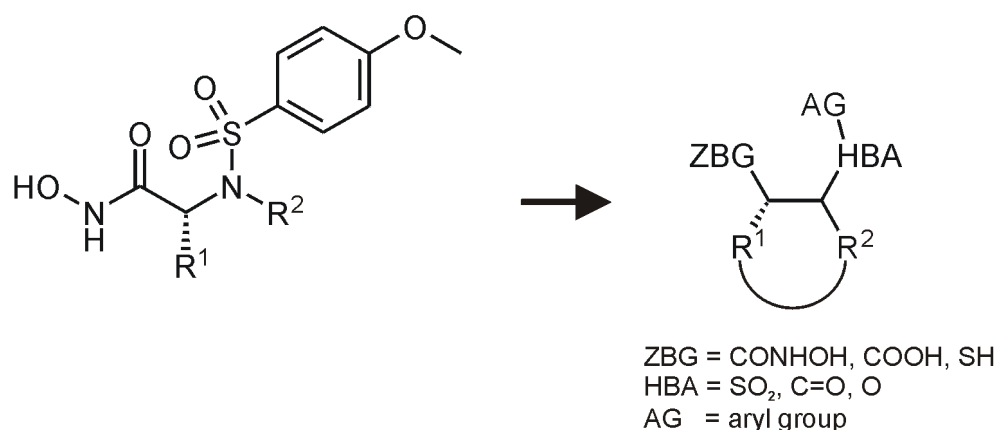


Figure 2.10 Development of non-peptide MMPIs.

The HBA group is typically substituted with an aryl group (AG) which interacts with the S₁' site. In general, the size of this substituent determines selectivity: with monophenyl groups usually resulting in broad-spectrum inhibition and with larger biaryls, which are often linked through an oxygen, providing selective inhibitory activity to MMPs with a deep S₁' pocket.⁵⁶ Exceptions from this rule exist, however. Since the R² residue usually projects towards the open solvent pocket, a short tether can be attached between R¹ and R² to form a small ring.

Representative examples of this series of MMPi are the biphenylbutyric acid derivative BAY-129566 developed at Bayer and the heterocyclic sulfonamide Prinomastat (AG-3340) developed at Agouron (Figure 2.11). The clinical candidate BAY-129566 was derived from a series of related γ -keto carboxylic acids. As with the sulfonamide CGS-27023A, the key to the discovery of this series was HTS, which identified a fenbufen derivative as a micromolar MMP-3 inhibitor. The examination of the SAR of the α -position and of the terminal phenyl substitution of the fenbufen derivative led to BAY-129566.

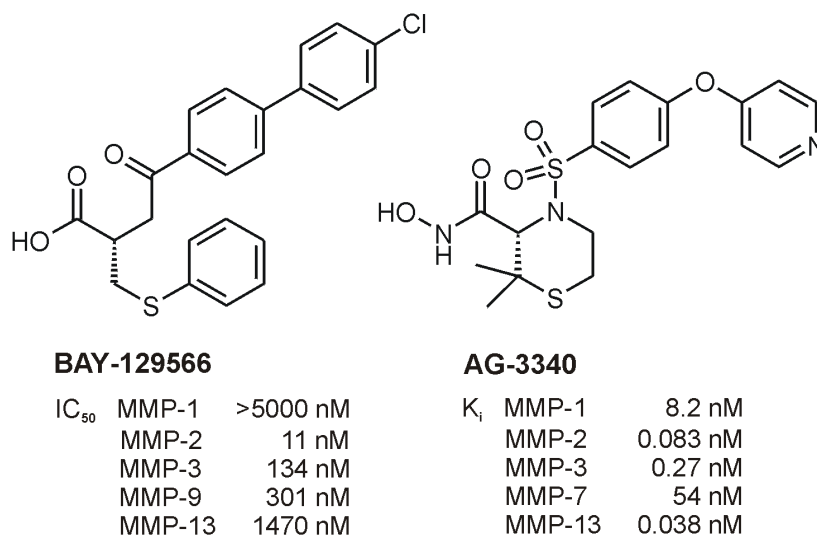


Figure 2.11 Next generation MMPi reported to be evaluated in clinical trials.

It is the only MMPi under clinical investigation that is a carboxylic acid. In preclinical studies, the inhibitory activities in both *in vitro* and *in vivo* models of matrix invasion, malignant angiogenesis and tumor growth were notable.⁵⁷ Preclinical pharmacologic studies in mice, rats, guinea pigs and dogs indicated that the compound is highly bioavailable after oral administration. It is further notable, that the recommended dose for subsequent disease-directed studies is 800 mg twice daily to achieve biologically relevant pharmacologic profiles. Unfortunately, the development of BAY-129566 was abandoned because no positive effects could be revealed in humans in a clinical phase-III trial.⁵⁸

The discovery of CGS-27023A has paved the way to design more potent non-peptide inhibitors of MMP-3, the gelatinases A and B (MMP-2, MMP-9) and collagenase-3

(MMP-13). Agouron has disclosed a series of related aryloxyphenylsulfonyl compounds that display selectivity for certain MMPs.⁵⁹ Ultimately, the choice of Prinomastat (AG-3340) over other candidates was based on pharmacokinetic properties and the efficacy of this compound in animal models of cancer.^{60,61} It is a selective inhibitor, which targets inhibition of gelatinase A and B, collagenase-3, and stromelysin-1 exhibiting K_i -values in the picomolar range. Clinical studies with this promising compound are still under way.

2.3.4 Other Inhibitors

Irreversible MMP-inhibitors⁶², selective MMP-3 inhibitors based on peptide-linked 5-amino-1,3,4-thiadiazole-2-thiones⁶³, non-peptide inhibitors of MMP-8 and bacterial collagenases, based on tetracyclines, anthraquinones and aranciamycin⁶⁴⁻⁶⁷, are also reported in the literature. However, the inhibitory activities of these compounds are generally very weak in comparison to many of the inhibitors described. Thus, these compounds may provide leads for drug design work.

3 Aims of the Study

Matrix metalloproteinases are involved in extracellular matrix remodeling. Under normal physiological conditions, their proteolytic activities are controlled by maintaining a delicate balance of pro-MMP synthesis, activation and their inhibition by endogenous inhibitors. Under pathological conditions, this balance is altered, often resulting in an abnormally high proteolytic activity: in arthritis, there is uncontrolled destruction of cartilage; in cancer, increased matrix turnover is thought to promote tumor cell invasion.⁶⁸ Modulation of the MMP regulation is possible at several biochemical levels such as gene expression or zymogen activation, but direct inhibition of enzyme action provides a particularly attractive target for therapeutic intervention. Thus, the design and synthesis of inhibitors of matrix metalloproteinases continues to be a prominent area of pharmaceutical research. Both peptide- and non-peptide-based inhibitors are in clinical studies for various indications. One key issue in the clinical development of MMPi relates to whether the development of broad-spectrum inhibitors, active against a range of different enzymes, or of selective inhibitors, targeted against a particular subset of the MMPs, represents the optimal strategy. However, since their inception during the eighties, MMPi have undergone several cycles of metamorphosis. Within promising compound classes the hydroxamate moiety plays a decisive role in achieving inhibitor potency. Clinical data suggested that the biologically labile nature of hydroxamates and the low oral bioavailability and poor duration of action exhibited by most peptide-based compounds are responsible for the failure of many compounds in clinical trials.

The aims of the present study were:

- the design, synthesis, and biological evaluation of inhibitors of matrix metalloproteinases.
- the invention of alternatives to hydroxamic acid zinc-chelators.
- the construction of non-peptide scaffolds.

4 Results and Discussion

4.1 Identification of Lead-Structures

In recent years, interest in thiadiazines has increased due to the high biological activity and broad-spectrum action of their derivatives.⁶⁹ Many thiadiazines have been discovered with possible applications in medical practice as sedatives, antianxiety agents, antiasthmatic agents, anticonvulsants, myorelaxants, coronary vasodilators, and spasmolytics. Many thiadiazines have cardiovascular activity.

From the six theoretically possible thiadiazines, the 1,3,4-isomer has been the most thoroughly investigated one.

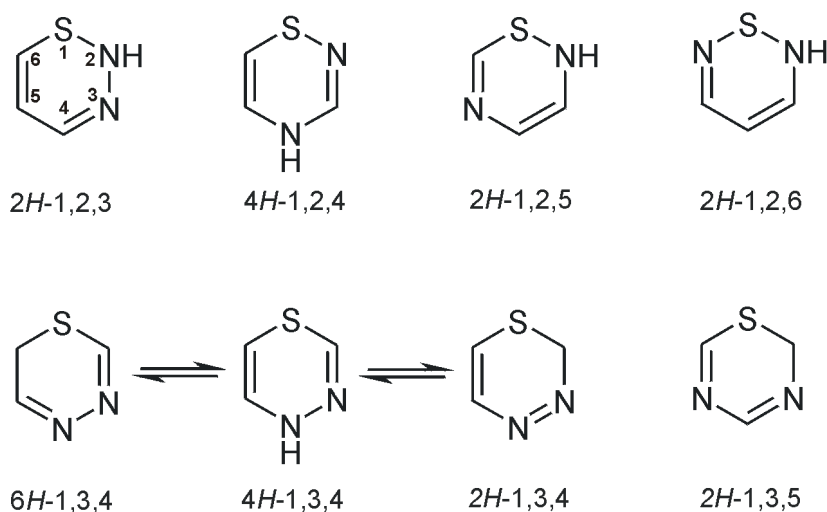


Figure 4.1 The isomeric ring structures of thiadiazines. For the 1,3,4-isomer the tautomeric 6H-1,3,4, 4H-1,3,4 and 2H-1,3,4 forms are shown.

In addition, 1,3,4-thiadiazines may exist in three different tautomeric forms. Spectroscopic investigations suggest that the 6H-form is preferred. The 4H-form represents a potentially anti-aromatic 8π -system which can be transformed by valence isomerization to a thiahomopyrazole and by subsequent extrusion of sulfur to a pyrazole.⁷⁰

Substituted 6H-1,3,4-thiadiazines are reported to be inhibitors of lipoxygenase, phosphodiesterase, and of the angiotensin-converting enzyme (ACE).⁷¹⁻⁷³ The value of 6H-1,3,4-thiadiazine derivatives as MMP inhibitors has, however, not hitherto been

recognized. To explore this issue further a series of chiral 6-methyl-6*H*-1,3,4-thiadiazines⁷⁴⁻⁷⁷ gratefully received from the institute of chemistry and biochemistry at the University of Greifswald, was tested using the catalytic domain of human neutrophil collagenase (cdMMP-8) as the screening enzyme (see the experimental section for complete assay protocol). From this analysis, a small number of compounds **1-3** were determined to be competitive inhibitors with weak ($K_i > 40 \mu\text{M}$) inhibitory activity.

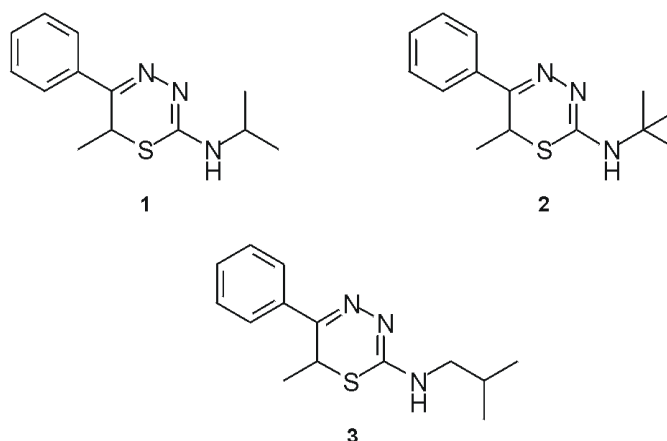


Figure 4.2 Thiadiazine screening leads.

The lead structures consist of a 6-methyl-6*H*-1,3,4-thiadiazine scaffold, a phenyl substituent in position 5, and an *N*-alkyl substituent in position 2. At this design stage, the binding mode of compounds **1-3** to cdMMP-8 was still unclear. With the aid of the visualization program InsightII (MSI, Germany) and the three-dimensional structure of recombinant cdMMP-8 complexed with the hydroxamate inhibitor Pro-Leu-Gly-NHOH, the leads were manually docked into the active site of the enzyme. Several orientations of the energy minimized lead-structures were superimposed upon the reference hydroxamate inhibitor structure to map possible binding distances of the 6*H*-1,3,4-thiadiazine core structure to the catalytic zinc(II)-ion. These results were compared with energy minimized structures of 6-methyl-6*H*-1,3,4-thiadiazine compounds, which showed no inhibitory activity against cdMMP-8. From these trials, the following theoretical binding mode was postulated: the phenyl substituent fits into enzyme pockets on the unprimed side, while the 6-methyl-6*H*-1,3,4-thiadiazine scaffold coordinates to the catalytic zinc(II)-ion and the *N*-alkyl residue is directed towards the S_1' pocket.

4.2 Modifications of the Lead-Structures

In order to prove the binding statement and to get a lead structure for further modifications, the alkyl groups at position 2 and 6 of the 6*H*-1,3,4-thiadiazine scaffold were removed. The resulting 2-amino-5-phenyl-6*H*-1,3,4-thiadiazine is a good starting lead to test the concept of amide-linked 5-substituted 6*H*-1,3,4-thiadiazine derivatives. As a first trial the dihydroorotic acid derivative **11** was synthesized.

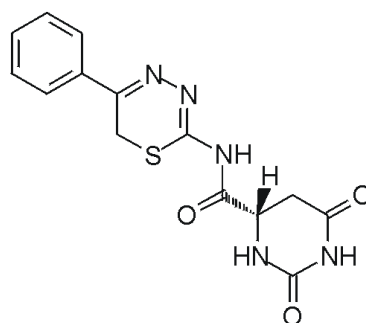


Figure 4.3 The chemical structure of (4*S*)-2,6-dioxo-*N*-(5-phenyl-6*H*-1,3,4-thiadiazin-2-yl)hexahydro-4-pyrimidinecarboxamide **11**.

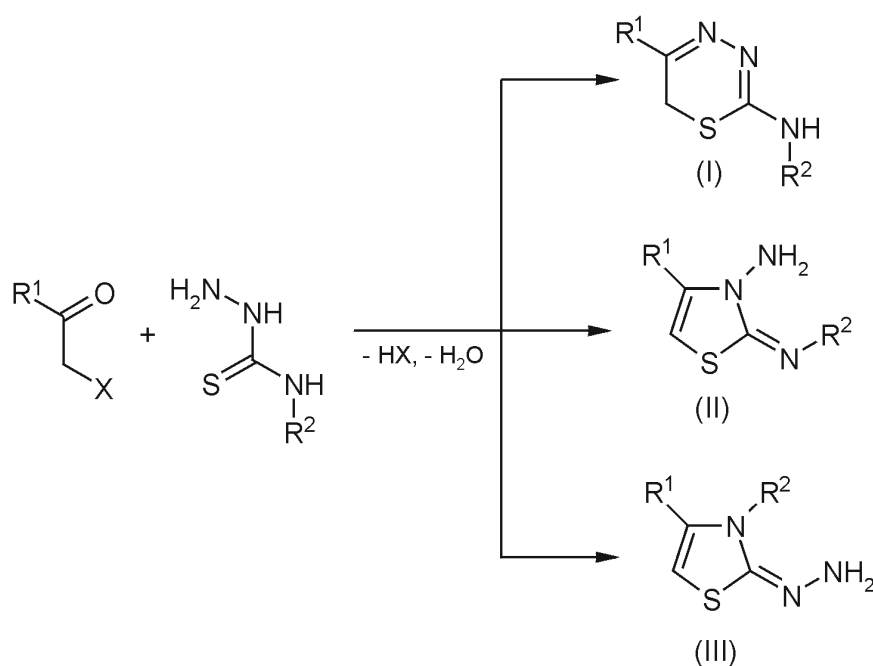
Ultimately, the choice of (*S*)-(+)-dihydroorotic acid over other carboxylic acids was based on the hydrogen bonding interactions, which this heterocycle may provide with the backbone of cdMMP-8. Surprisingly, this compound showed promising potency of $K_i = 6.2 \mu\text{M}$ against cdMMP-8 and $K_i = 1.2 \mu\text{M}$ against MMP-9.

As previously outlined, the most active compounds from the class of non-peptide MMP inhibitors possess an arylsulfonyl group, occupying the specificity S_1' pocket of the enzyme. It was also shown that the $-\text{SO}_2-$ moiety of these inhibitors is involved in several strong hydrogen bonds with amino acid residues from the active site cleft, which considerably stabilize the enzyme-inhibitor adduct.⁷⁸ Assuming that the phenyl ring of **11** occupies the unprimed site of cdMMP-8 or MMP-9, the next effort was the preparation of 5-substituted 6*H*-1,3,4-thiadiazine-2-amines acylated with a *N*-arylsulfonyl substituted amino acid derivative to improve primed side binding affinity.

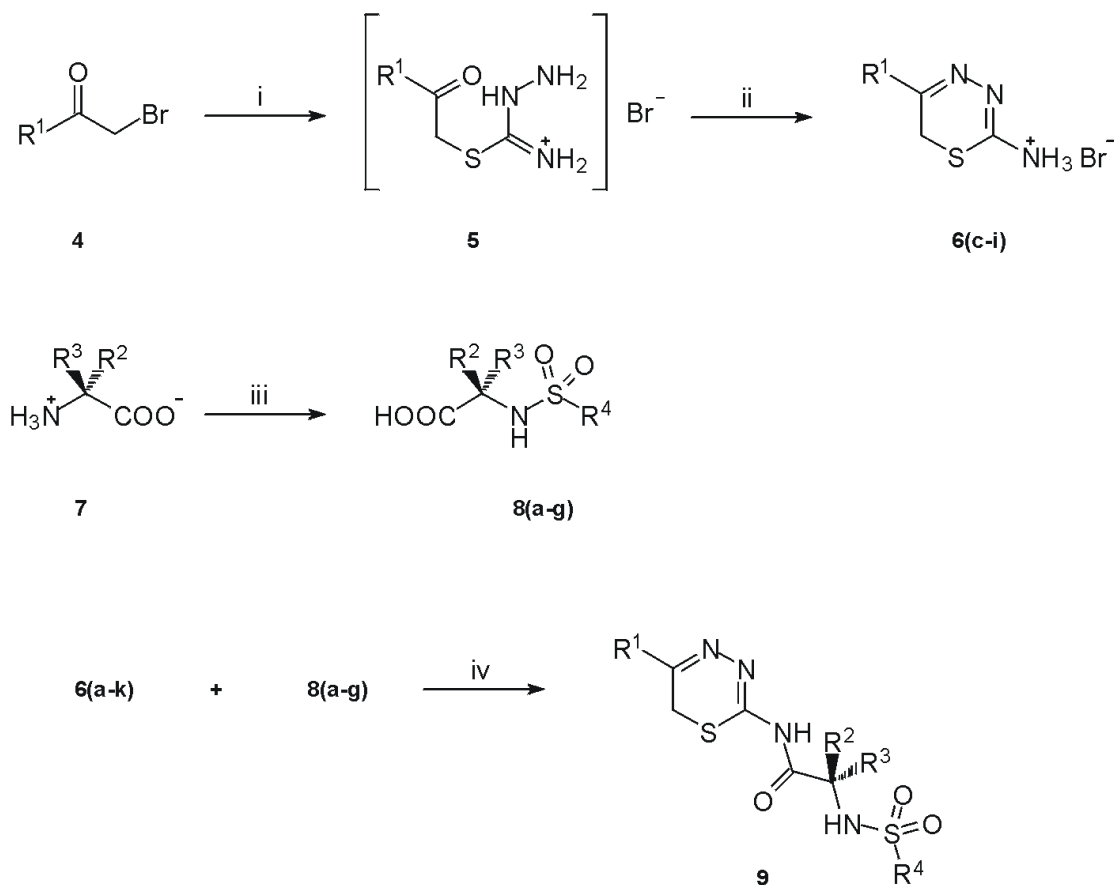
4.3 Chemistry

The 1,3,4-thiadiazine system was first reported by P. K. Bose, employing a reaction of α -bromoacetophenone with thiosemicarbazide.⁷⁹ Depending on whether condensation occurs at the N1, N2, or N4 of the thiosemicarbazide, three different sulfur-containing heterocyclic rings are expected after ring closure: the 6*H*-1,3,4-thiadiazines (I), the 2-substituted imino-2,3-dihydrothiazol-3-amines (II), and the 3-substituted 2-hydrazono-2,3-dihydrothiazoles (III).

Scheme 1.



Which isomer is formed exclusively or preferentially, decisively depends on the respective H⁺-ion concentration, the polarity of the solvent, the reaction temperature and on the substituents R¹ and R². The synthesis of the 6*H*-1,3,4-thiadiazine-based MMPIs was accomplished using two methods. In the first method, a substituted α -bromo-keto compound **4** was allowed to react with thiosemicarbazide in ethanol at 0°C (Scheme 2). The resulting linear intermediate **5** was isolated and then ring-closed by heating this compound in an ethanol/H₂O/HBr mixture to afford preferentially the 5-substituted 6*H*-1,3,4-thiadiazine-2-amines **6(c-i)** as their hydrobromide salts in good isolated yields.⁸⁰

Scheme 2. Method A^a

^a Reagents and conditions: (i) thiosemicarbazide; EtOH; 0 to 20°C; (ii) EtOH, 48% aq. HBr, reflux; (iii) a) K₂CO₃/H₂O, R⁴-SO₂Cl, reflux, b) conc. HCl; (iv) EDC, HOBT, NMM, DMF, 5°C.

To obtain the desired sulfonamides **8(a-g)** a *L*- or *D*-configured amino acid **7** was heated with the appropriate sulfonylchloride in an aqueous potassium carbonate solution. Acylation of the 5-substituted 6H-1,3,4-thiadiazine-2-amine hydrohalides **6(a-k)** (Table 1) with the carboxylic group of the sulfonamides **8(a-g)** (Table 2) was mediated by a mixture of *N*-ethyl-*N'*-(3-dimethyl-aminopropyl)-carbodiimide hydrochloride (EDC), 1-hydroxy-benzotriazole (HOBT) and 4-methylmorpholine (NMM) in DMF at 5°C. The compounds with the general structure **9** were obtained as white or yellow solids which could be crystallized from methanol/acetonitrile mixtures as described in the experimental section. The latter step was also used to synthesize compound **11** from (*S*)-(+)-dihydro-oroctic acid and compound **6a**.

Table 1. Synthesized 5-Substituted 6*H*-1,3,4-Thiadiazine-2-Amine Hydrohalides **6(a-k)**.

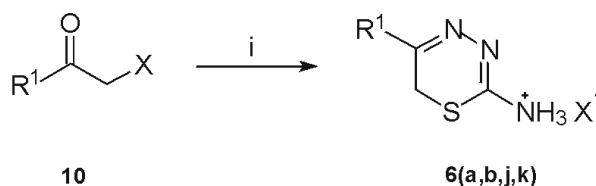
compd	R ¹	formula	mp (°C)
6a	Ph	C ₉ H ₁₀ ClN ₃ S	206
6b	4-F-Ph	C ₉ H ₉ ClFN ₃ S	231
6c	4-Cl-Ph	C ₉ H ₉ BrClN ₃ S	227
6d	4-Br-Ph	C ₉ H ₉ Br ₂ N ₃ S	218
6e	4-O ₂ N-Ph	C ₉ H ₉ BrN ₄ O ₂ S	228
6f	4-NC-Ph	C ₁₀ H ₉ BrN ₄ S	248
6g	4-F ₃ C-Ph	C ₁₀ H ₉ BrF ₃ N ₃ S	224
6h	4-H ₃ CO-Ph	C ₁₀ H ₁₂ BrN ₃ OS	185
6i	4-H ₃ C-Ph	C ₁₀ H ₁₂ BrN ₃ S	220
6j	1-adamantyl	C ₁₃ H ₂₀ BrN ₃ S	251
6k	5-Cl-2-thienyl	C ₇ H ₇ BrClN ₃ S ₂	249

Table 2. Synthesized *N*-Sulfonylated Amino Acids **8(a-g)**.

compd	R ²	R ³	R ⁴	formula	mp (°C)
8a(S)	H	CH ₃	Ph	C ₉ H ₁₁ NO ₄ S	123-125
8b(R)	CH ₃	H	Ph	C ₉ H ₁₁ NO ₄ S	124-126
8c(S)	H	CH ₃	2-thienyl	C ₇ H ₉ NO ₄ S ₂	85-87
8d(S)	H	CH ₃	CH ₂ -Ph	C ₁₀ H ₁₃ NO ₄ S	125-127
8e(S)	H	CH(CH ₃) ₂	Ph	C ₁₁ H ₁₅ NO ₄ S	149
8f(R)	CH(CH ₃) ₂	H	Ph	C ₁₁ H ₁₅ NO ₄ S	148-149
8g	CH ₃	CH ₃	Ph	C ₁₀ H ₁₃ NO ₄ S	146-147

In the second method, the thiadiazine ring was prepared in one step from the substituted α -halogeno-keto compound and thiosemicarbazide hydrochloride or thiosemicarbazide hydrobromide.

Scheme 3. Method B^a



^a Reagents and conditions: (i) thiosemicarbazide hydrohalide; MeOH; reflux.

Compound **10** was slowly heated with the corresponding thiosemicarbazide hydrohalide in methanol to produce the 5-substituted 6H-1,3,4-thiadiazine-2-amine hydrohalides **6(a,b,j,k)** as crystalline precipitates which could be purified by recrystallization from an appropriate solvent as described in the experimental section. Only with this method the novel compound 5-(5-chloro-2-thienyl)-6H-1,3,4-thiadiazin-2-amine hydrobromide could be obtained in an acceptable yield. The remaining transformation leading to compounds with the general structure **9** was performed as illustrated in Scheme 2.

4.4 Structure–Activity Relationship (SAR) Analysis

All compounds were tested *in vitro* for the inhibition of PMNL-gelatinase (MMP-9) and the recombinant catalytic domains of human neutrophil collagenase (cdMMP-8), human gelatinase A (cdMMP-2), macrophage elastase (cdMMP-12), collagenase-3 (cdMMP-13), and membrane-type-1 MMP (cdMMP-14). Selected compounds have also been tested for the inhibition of collagenase-1 (MMP-1) and the ectodomain of membrane-type-1 MMP (MMP-14). The compound class generally inhibits cdMMP-2, cdMMP-8, MMP-9, and cdMMP-14 selectively in the nanomolar range. Depending on functional group manipulations within the compound series the inhibition of these MMPs showed great variability. On the other hand, the inhibition of MMP-1 and cdMMP-12 was less potent relative to the other enzymes and demonstrated very few variations in potency as

functional groups were altered. Surprisingly, the inhibition of cdMMP-13, in general, occurs in the micromolar to submicromolar range within the tested 6*H*-1,3,4-thiadiazine series (Tables 3 to 7). The promising concept of this novel class of MMPIs led to the establishment of SAR which apply to most of the 6*H*-1,3,4-thiadiazines described in this thesis.

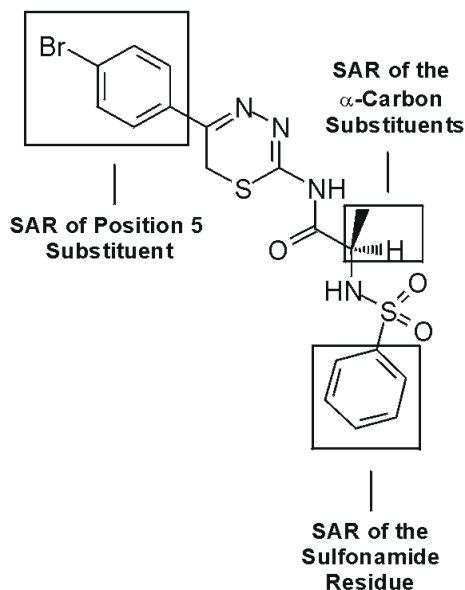
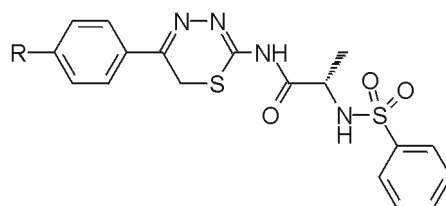


Figure 4.4 Proposed 6*H*-1,3,4-thiadiazine SAR studies.

4.4.1 SAR of the Position 5 Substituent

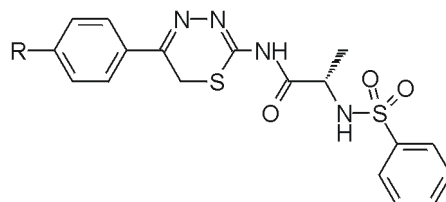
As a first modification, analogues substituting the phenyl ring in position 5 of the 6*H*-1,3,4-thiadiazine moiety with various halogens **12(a-c)**, electron-withdrawing groups **12(d-f)**, and moderately electron-donating groups **12(g,h)** (Tables 3 and 4) were synthesized. As can be seen in Table 3, halogens attached to the 4-position of the phenyl ring increased the potency against cdMMP-8, MMP-9 and cdMMP-14. This increase had the maximum level with an appended chloro substituent in the case of MMP-9, cdMMP-14 and with an appended bromo substituent in the case of cdMMP-8. However, electron-withdrawing groups and moderately electron-donating groups at the 4-position of the phenyl ring were well-tolerated by the tested MMPs (Table 4).

Table 3. *In Vitro* Activity of Halogenated 6*H*-1,3,4-Thiadiazine Derivatives.

compd	R	formula ^a	mp (°C)	method	MMPs K_i (μM) ^b							
					1 ^c	2	8	9 ^c	12	13	14	14E ^d
12a	F	C ₁₈ H ₁₇ FN ₄ O ₃ S ₂	166-167	B	0.44	0.45	0.19	0.16	0.28	0.65	0.44	nt
12b	Cl	C ₁₈ H ₁₇ ClN ₄ O ₃ S ₂	184-185	A	0.65	0.14	0.73	0.06	0.52	0.18	0.10	0.21
12c	Br	C ₁₈ H ₁₇ BrN ₄ O ₃ S ₂	180-181	A	nt	0.27	0.11	0.16	0.44	0.37	0.34	nt

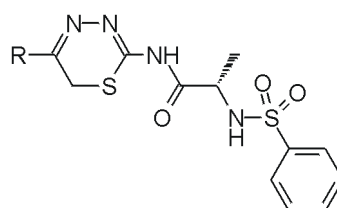
^a Analytical results are within $\pm 0.4\%$ of the theoretical values. ^b MMP inhibition *in vitro*. Assays were run at pH 7 against the catalytic domains of the enzymes. See the Experimental Section for complete protocol. Standard deviations were typically $\pm 15\%$ of the mean or less. ^c Full-length version of the enzyme was used. ^d The ectodomain of the enzyme was used. nt denotes not tested.

Surprisingly, the electron-withdrawing CN group of compound **12e**, which can be described as a pseudohalogen⁸¹, also improved inhibitory activity against MMP-9 comparable to the halogens. With the moderately electron-donating CH₃ group compound **12h** tended to have potency against cdMMP-12. Substitution by electron-withdrawing substituents produces an electron-deficient phenyl ring, which in turn can improve aryl-aryl stacking interactions with aromatic side-chains in the active site. The reduction in affinity, resulting from a reduced aryl-aryl stack by phenyl rings para-substituted by moderate electron-releasing groups (*e.g.* CH₃), appears to be more than offset by the increase in steric bulk/lipophilic contacts that these groups provide in the case of cdMMP-12. Consequently, the replacement of the 4-methyl-phenyl ring in compound **12h** with the bulky adamantyl residue verified in compound **13a** resulted in a 10 to 1000 fold loss of inhibitory activity against the tested MMPs, with the exception of cdMMP-12 (Table 5). This enzyme was inhibited by **13a** very selectively in the submicromolar range.

Table 4. *In Vitro* Activity of 6*H*-1,3,4-Thiadiazine Derivatives Substituted with Electron-Withdrawing or Electron-Donating Functionalities.

compd	R	formula ^a	mp (°C)	method	MMPs K_i (μM) ^b							
					1 ^c	2	8	9 ^c	12	13	14	14E ^d
12d	NO ₂	C ₁₈ H ₁₇ N ₅ O ₅ S ₂	201-202	A	0.26	0.30	0.17	0.13	0.28	0.26	0.29	nt
12e	CN	C ₁₉ H ₁₇ N ₅ O ₃ S ₂	186-187	A	0.39	0.24	0.22	0.08	0.37	0.25	0.24	0.40
12f	CF ₃	C ₁₉ H ₁₇ F ₃ N ₄ O ₃ S ₂	187-188	A	0.43	nt	0.26	0.24	0.30	0.57	0.58	0.39
12g	OCH ₃	C ₁₉ H ₂₀ N ₄ O ₄ S ₂	192-193	A	0.58	0.52	0.18	0.32	0.34	1.33	0.59	nt
12h	CH ₃	C ₁₉ H ₂₀ N ₄ O ₃ S ₂	184-185	A	nt	0.41	0.30	0.16	0.11	0.62	0.38	nt

^{a-d} See footnotes in Table 3. nt denotes not tested.

Table 5. *In Vitro* Activity of 6*H*-1,3,4-Thiadiazine Derivatives with Different Position 5 Residues.

compd	R	formula ^a	mp (°C)	method	MMPs K_i (μM) ^b							
					1 ^c	2	8	9 ^c	12	13	14	14E ^d
13a^e	1-adamantyl	C ₂₂ H ₂₈ N ₄ O ₃ S ₂	183-184	B	nt	>15	>15	>15	0.41	>15	3.07	nt
13b	5-Cl-thienyl	C ₁₆ H ₁₅ ClN ₄ O ₃ S ₃	198-199	B	0.45	1.87	0.18	0.17	0.24	0.47	0.32	0.20

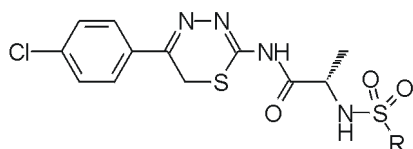
^{a-d} See footnotes in Table 3. ^e At high assay concentrations (>5 μM) the compound showed fluorescence quenching effects. nt denotes not tested.

The bioisosteric⁸² replacement of the 4-chlorophenyl residue with a 5-chlorothieryl moiety represented by compound **13b** demonstrated enzyme selectivity between cdMMP-2 and MMP-9 by a factor of 10.

4.4.2 SAR of the Sulfonamide Residue

The sulfonamide portion of the molecules and the influence of this group on enzyme inhibition was also investigated.

Table 6. Modifications of the Sulfonamide Residue.



compd	R	formula ^a	mp (°C)	method	MMPs K_i (μM) ^b							
					1 ^c	2	8	9 ^c	12	13	14	14E ^d
12b	Ph	C ₁₈ H ₁₇ ClN ₄ O ₃ S ₂	184-185	A	0.65	0.14	0.73	0.06	0.52	0.18	0.10	0.21
14a	CH ₂ Ph	C ₁₉ H ₁₉ ClN ₄ O ₃ S ₂	169-170	A	0.36	0.09	0.20	0.04	0.48	0.12	0.19	0.18
14b	2-thienyl	C ₁₆ H ₁₅ ClN ₄ O ₃ S ₃	175-176	A	1.04	0.55	0.06	0.80	0.36	3.81	0.25	nt

^{a-d} See footnotes in Table 3. nt denotes not tested.

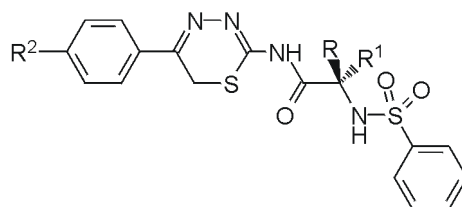
Since halogens attached to the 4-position of the phenyl ring resulted in potent MMPi, the chloro substituent was chosen to be kept constant within the compared structures. The phenylsulfonamide analogue **12b**, was determined to be a broad-spectrum inhibitor. The more flexible benzyisulfonamide **14a** was also prepared and tested for *in vitro* activity. This compound possessed a slight increase of binding affinity with cdMMP-2, cdMMP-13, and MMP-9, all of which are characterized by a deep S₁' pocket. The results obtained with the 2-thienylsulfonamide **14b** were remarkable. Replacement of the phenyl group by a thienyl substituent led to a significant shift in enzyme selectivity. The

compound was found to be even more selective for cdMMP-8 ($K_i = 60$ nM) compared with the other tested MMPs.

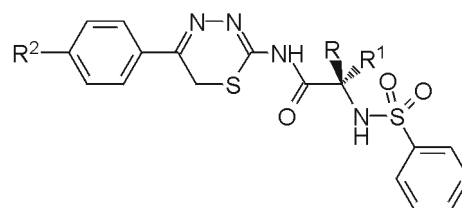
4.4.3 SAR of Variations of the α -Carbon Substituents

The substituents at the α -carbon of the *N*-sulfonylated amino acid residue of the compounds were also modified. In order to determine, if either the *R*- or the *S*-isomer binds tighter to the enzymes, enantiomeric pairs of most of the compounds were synthesized. The results of the *in vitro* tests revealed that the corresponding *R*-isomers were, in general, more potent than the parent *S*-isomers (Table 7). Replacement of the methyl group with the bulky isopropyl substituent (compounds **15f** and **15g**) led to a decrease of inhibitory activity against the tested MMPs. Attachment of a second methyl group at the α -carbon was verified in compound **15h**. This compound is the first example of a potent non-chiral 6*H*-1,3,4-thiadiazine based MMP inhibitor with nanomolar affinity for cdMMP-2 and MMP-9.

Table 7. Modifications of the α -Carbon Substituents.



compd	R;R ¹ ;R ²	formula ^a	mp (°C)	method	MMPs K_i (μM) ^b							
					1 ^c	2	8	9 ^c	12	13	14	14E ^d
12a(S)	H;CH ₃ ;F	C ₁₈ H ₁₇ FN ₄ O ₃ S ₂	166-167	B	0.44	0.45	0.19	0.16	0.28	0.65	0.44	nt
15a(R)	CH ₃ ;H;F	C ₁₈ H ₁₇ FN ₄ O ₃ S ₂	167-168	B	0.63	0.34	0.35	0.05	0.35	0.30	0.39	0.33
12b(S)	H;CH ₃ ;Cl	C ₁₈ H ₁₇ ClN ₄ O ₃ S ₂	184-185	A	0.65	0.14	0.73	0.06	0.52	0.18	0.10	0.21
15b(R)	CH ₃ ;H;Cl	C ₁₈ H ₁₇ ClN ₄ O ₃ S ₂	183-184	A	0.21	0.50	0.15	0.08	0.32	0.14	0.05	0.21
12c(S)	H;CH ₃ ;Br	C ₁₈ H ₁₇ BrN ₄ O ₃ S ₂	180-181	A	nt	0.27	0.11	0.16	0.44	0.37	0.34	nt
15c(R)	CH ₃ ;H;Br	C ₁₈ H ₁₇ BrN ₄ O ₃ S ₂	179-180	A	0.42	0.15	0.21	0.04	0.34	0.13	0.20	0.18

Table 7 (Continued). Modifications of the α -Carbon Substituents.

compd	R;R ¹ ;R ²	formula ^a	mp (°C)	method	MMPs K_i (μ M) ^b							
					1 ^c	2	8	9 ^c	12	13	14	14E ^d
12e(S)	H;CH ₃ ;CN	C ₁₉ H ₁₇ N ₅ O ₃ S ₂	186-187	A	0.39	0.24	0.22	0.08	0.37	0.25	0.24	0.40
15d(R)	CH ₃ ;H;CN	C ₁₉ H ₁₇ N ₅ O ₃ S ₂	185-186	A	0.40	0.21	0.23	0.08	0.36	0.21	0.24	0.40
12h(S)	H;CH ₃ ;CH ₃	C ₁₉ H ₂₀ N ₄ O ₃ S ₂	184-185	A	nt	0.41	0.30	0.16	0.11	0.62	0.38	nt
15e(R)	CH ₃ ;H;CH ₃	C ₁₉ H ₂₀ N ₄ O ₃ S ₂	183-184	A	0.46	0.44	0.22	0.21	0.09	0.32	0.29	0.15
15f(S)^e	H;(CH ₃) ₂ CH;Cl	C ₂₀ H ₂₁ ClN ₄ O ₃ S ₂	201-202	A	nt	0.88	0.78	0.20	0.38	>15	0.74	nt
15g(R)^e	(CH ₃) ₂ CH;H;Cl	C ₂₀ H ₂₁ ClN ₄ O ₃ S ₂	189-190	A	0.55	0.85	4.37	>15	0.35	>15	0.59	0.33
15h	CH ₃ ;CH ₃ ;Cl	C ₁₉ H ₁₉ ClN ₄ O ₃ S ₂	204-205	A	0.30	0.08	0.48	0.09	0.20	0.18	0.15	0.11

^{a-d} See footnotes in Table 3. ^e At high assay concentrations (>5 μ M) the compound showed fluorescence quenching effects. nt denotes not tested.

4.5 X-ray Crystallography

4.5.1 Crystal Structures of 6H-1,3,4-Thiadiazine-2-amide-Based MMPiS

In order to investigate the 6H-1,3,4-thiadiazine system further and to establish the inhibitor structures for protein/ligand-docking experiments, single-crystal X-ray diffraction studies were carried out on (2*S*)-*N*-[5-(4-chlorophenyl)-6H-1,3,4-thiadiazin-2-yl]-2-[(phenylsulfonyl)amino]propanamide **12b**, (2*S*)-*N*-[5-(5-chloro-2-thienyl)-6H-1,3,4-thiadiazin-2-yl]-2-[(phenylsulfonyl)amino]propanamide **13b**, (2*S*)-*N*-[5-(4-chloro-phenyl)-6H-1,3,4-thiadiazin-2-yl]-2-[(2-thienylsulfonyl)amino]propanamide **14b**, and (2*R*)-*N*-[5-(4-fluorophenyl)-6H-1,3,4-thiadiazin-2-yl]-2-[(phenylsulfonyl)amino]propanamide **15a**.

In all four compounds the thiadiazine ring deviates from planarity (Figures 4.5, 4.6, 4.8 and 4.9).⁸³ For conformational analysis the puckering of the ring system may be described as out-of-plane displacements of the vertexes of the symmetric flat polygon using group theory. The method applicable to any real cyclic compound was introduced by Cremer and Pople and refined by Evans and Boeyens.^{84,85} The analysis starts out from crystallographic fractional coordinates and involves transformation first to a set of cartesian coordinates. From these coordinates, a set of three parameters of pucker in the form of polar coordinates (Q , θ , φ) is obtained. These coordinates map out the conformation of the ring on the surface of a sphere with radius Q and with poles at $\theta = 0, 180^\circ$. Three basic conformations (chair, boat and twist-boat) and three highly symmetric intermediate conformations (envelope, half-chair and screw-boat) are located on the sphere, whereby the name screw-boat is proposed for the 1,3-diplanar form.

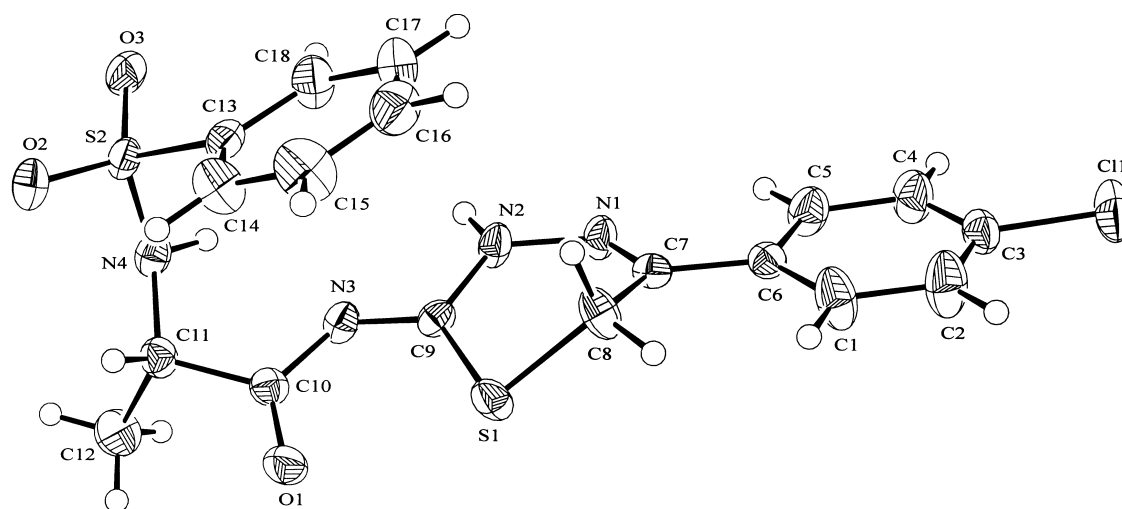


Figure 4.5 The molecular structure of **12b** showing the atom-numbering scheme. Displacement ellipsoids are drawn at the 50% probability level and H atoms are shown as small spheres of arbitrary radii.

Table 8. Selected geometric parameters (Å, °) for **12b**.

S1–C9	1.726 (3)	N2–C9	1.338 (3)
N1–C7	1.284 (4)	N3–C9	1.321 (3)
N1–N2	1.389 (3)		
C9–N2–N1	128.6 (2)		

Table 9. Hydrogen-bonding geometry (Å, °) for **12b**.

D–H···A	D–H	H···A	D···A	D–H···A
N2–H2N···S1 ⁱ	0.82 (4)	2.72 (4)	3.236 (3)	122 (3)
N2–H2N···O1 ⁱ	0.82 (4)	2.56 (4)	3.375 (3)	173 (4)
N4–H4N···N3	0.90 (3)	2.31 (3)	2.661 (3)	103 (2)

Symmetry code: (i) x, y, 1 + z.

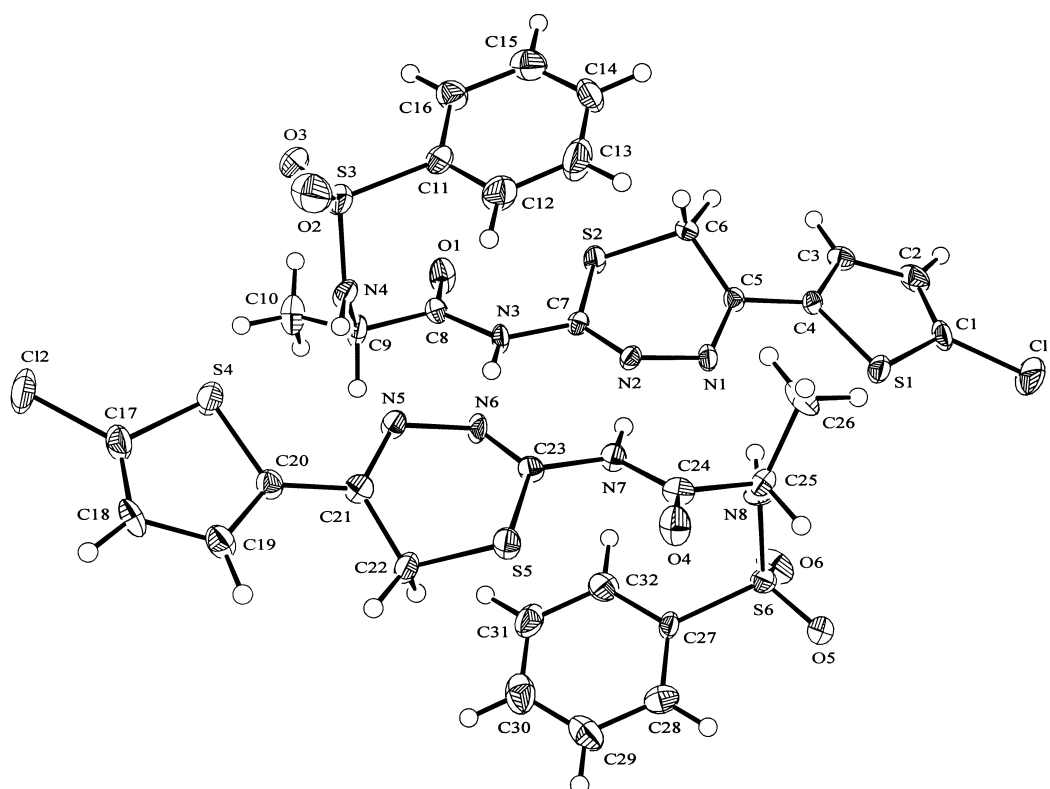
**Figure 4.6** The molecular structure of **13b** showing the two molecules and the atom-numbering scheme. Displacement ellipsoids are drawn at the 50% probability level and H atoms are shown as small spheres of arbitrary radii.

Table 10. Selected geometric parameters (Å, °) for **13b**.

S2–C7	1.750 (6)	S5–C23	1.755 (6)
S2–C6	1.805 (7)	S5–C22	1.817 (7)
N1–C5	1.286 (8)	N5–C21	1.292 (8)
N1–N2	1.407 (7)	N5–N6	1.423 (7)
N2–C7	1.286 (8)	N6–C23	1.288 (8)
N3–C7	1.395 (8)	N7–C23	1.396 (8)

Table 11. Hydrogen-bonding geometry (Å, °) for **13b**.

D–H···A	D–H	H···A	D···A	D–H···A
N3–H3N···N6	0.88	2.09	2.956 (7)	168
N4–H4N···S4	0.88	2.77	3.456 (5)	136
N4–H4N···N5	0.88	2.08	2.842 (7)	145
N7–H7N···N2	0.88	2.11	2.983 (7)	172
N8–H8N···N1	0.88	2.04	2.882 (7)	160

The calculated puckering parameters are shown in Table 12. From this analysis the thiadiazine moiety assumes a screw-boat conformation in all compounds. The large φ value for molecule 1 of **14b** and **13b** indicate that the direction of the ring distortion is towards an inverted screw-boat conformation. The difference between the screw-boat and the inverted screw-boat conformation is illustrated in Figure 4.7.

Table 12. Ring Puckering Parameters for 6*H*-1,3,4-Thiadiazine Amide-Based MMPIs.

compound	Puckering Parameters		
	Q [Å]	θ [°]	φ [°]
12b	0.567(3)	70.6(3)	39.9(3)
13b , molecule 1	0.634	109.5	217.1
13b , molecule 2	0.665	70.5	35.9
14b , molecule 1	0.585	110.5	215.4
14b , molecule 2	0.595	69.7	34.3
15a	0.618(2)	69.9(2)	33.1(3)

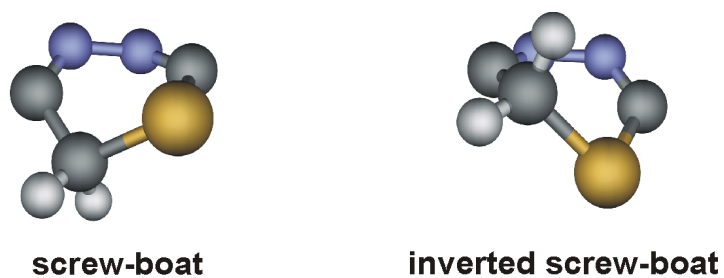


Figure 4.7 Ring conformations of 6H-1,3,4-thiadiazines.

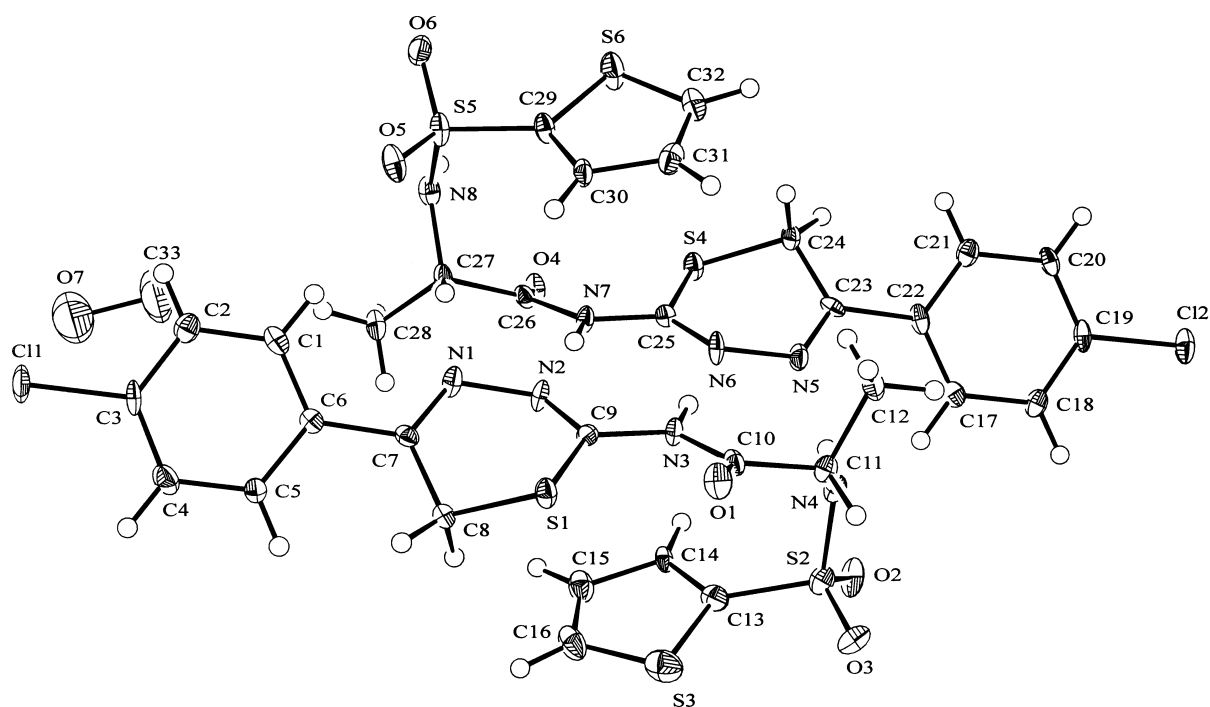


Figure 4.8 The molecular structure of **14b** showing the two molecules, one methanol molecule and the atom-numbering scheme. Displacement ellipsoids are drawn at the 50% probability level and H atoms are shown as small spheres of arbitrary radii.

Table 13. Selected geometric parameters (Å, °) for **14b**.

S1–C9	1.748 (4)	S4–C25	1.746 (4)
S1–C8	1.800 (5)	S4–C24	1.810 (5)
N1–C7	1.275 (5)	N5–C23	1.279 (5)
N1–N2	1.412 (5)	N5–N6	1.400 (5)
N2–C9	1.298 (5)	N6–C25	1.298 (5)
N3–C9	1.379 (5)	N7–C25	1.377 (6)

Table 14. Hydrogen-bonding geometry (Å, °) for **14b**.

D–H···A	D–H	H···A	D···A	D–H···A
N3–H3N···N6	1.03 (5)	1.99 (5)	3.017 (5)	174 (4)
N4–H4N···N5	0.86 (4)	2.04 (4)	2.903 (5)	175 (4)
N7–H7N···N2	1.00 (6)	1.87 (6)	2.865 (5)	170 (6)
N8–H8N···O4 ⁱ	0.76 (5)	2.19 (5)	2.927 (5)	162 (5)

Symmetry code: (i) 1 + y, x – 1, – z

Inspection of the compounds unit cell reveal that the molecules of compound **12b** show a short intramolecular N_{Ala}—H···N_{exo} hydrogen bond [N···N 2.661(3) Å] and are linked into a chain along the *c* axis by N_{endo}—H···S_{endo} and N_{endo}—H···O_{Ala} hydrogen bonds [N···S 3.236(3) and N···O 3.375(3) Å] between neighbouring molecules. The molecules of compound **13b** and **14b** are dimerized through N_{exo}—H···N_{endo} hydrogen bonds [N···N 2.956(7) and 2.983(7) Å (**13b**), N···N 2.865(5) and 3.017(5) Å (**14b**)]. In compound **15a** the molecules are connected antiparallel into a chain along the *a* axis by N_{exo}—H···O_{Ala} and N_{Ala}—H···N_{endo} hydrogen bonds [N···O 2.907(6) and N···N 2.911(6) Å].

Table 15. Selected geometric parameters (Å, °) for **15a**.

S1–C9	1.752 (4)	N1–N2	1.404 (3)
S1–C8	1.816 (3)	N2–C9	1.296 (4)
N1–C7	1.291 (4)	N3–N9	1.403 (3)

Table 16. Hydrogen-bonding geometry (Å, °) for **15a**.

D—H···A	D—H	H···A	D···A	D—H···A
N3—H3N···O1 ⁱ	0.90 (4)	2.01 (4)	2.907 (6)	174 (3)
N4—H4N···N2 ⁱⁱ	0.88 (5)	2.06 (5)	2.911 (6)	163 (4)

Symmetry code: (i) $1/2 + x, 3/2 - y, 1 - z$; (ii) $x - 1/2, 3/2 - y, 1 - z$.

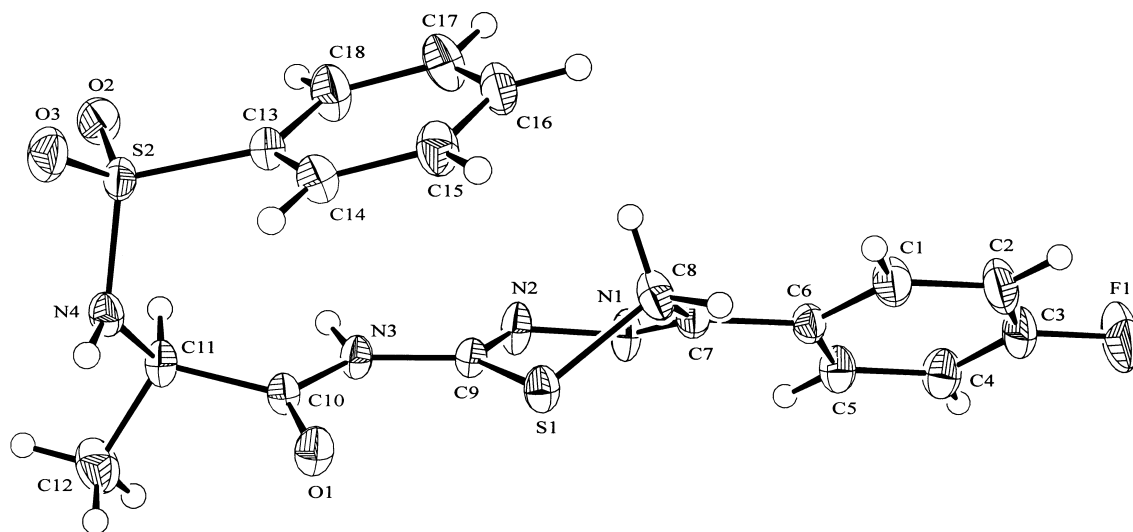
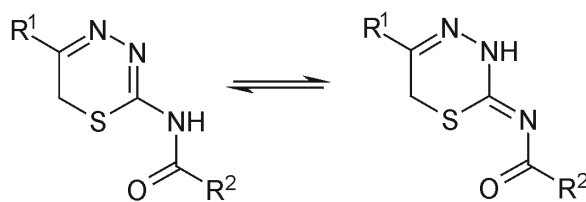


Figure 4.9 The molecular structure of **15a** showing the atom-numbering scheme. Displacement ellipsoids are drawn at the 50% probability level and H atoms are shown as small spheres of arbitrary radii.

In compounds **12b** and **15a**, there are two distinct S1—C8 and S1—C9 bond lengths, which can be attributed to typical S—C sp^3 and S—C sp^2 bonds [average values 1.819(19) and 1.751(17)Å].⁸⁶ The two molecules of compound **13b** and **14b** show similar S—C bond lengths. These results are in accordance with the 6*H* tautomeric form of the thiadiazine system. The endocyclic C9—N2 distance in **15a** is shorter than the exocyclic C9—N3 distance and corresponds to an N=C sp^2 bond. The same applies to the two molecules of compound **13b** and **14b**. In contrast to this trend, the endocyclic C9—N2 distance in **12b** is slightly longer than the exocyclic C9—N3 distance and corresponds to an N—C sp^2 bond. These bond differences resemble the characteristic pattern of bond-length changes introduced by an amido-imino tautomerism (prototropic shift) within the 6*H*-1,3,4-thiadiazine moiety.

Scheme 4. The Prototropic Shift of 6*H*-1,3,4-Thiadiazine-2-amide-Based MMPiS.

As shown in Scheme 4, the geometry of compounds **13b**, **14b** and **15a** is consistent with the tautomer on the left-hand side, while the geometry of **12b** is closer to that of the tautomer on the right-hand side. Consequently, the endocyclic N atom close to the exocyclic N atom is a hydrogen-bond acceptor in **13b**, **14b** and **15a**, and a hydrogen-bond donor in **12b**. The opposite applies to the exocyclic N atom, which is a hydrogen-bond donor in **13b**, **14b** and **15a**, and a hydrogen-bond acceptor in **12b**. This contributes to the different hydrogen-bonding patterns in the crystal structures of the compounds described.

4.5.2 Binding of *N*-Allyl-5-(4-chlorophenyl)-6*H*-1,3,4-thiadiazin-2-amine Hydrobromide to cdMMP-8

With the 5-(4-chlorophenyl)-6*H*-1,3,4-thiadiazine-2-amide-based MMPiS it was shown that the 4-chloro substituent plays a decisive role in archiving binding affinity to the enzymes. To prove this fact with 6*H*-1,3,4-thiadiazine-2-amine-based MMPiS the compound *N*-allyl-5-(4-chlorophenyl)-6*H*-1,3,4-thiadiazin-2-amine hydrobromide **16** was synthesized. This compound shows remarkable potency against MMP-9 ($K_i = 783$ nM) and excellent solubility in water. Thus, the crystal structure of the catalytic domain of human neutrophil collagenase (cdMMP-8) complexed with **16** ($K_i = 41$ μ M) was determined at 2.7 Å resolution (Figure 4.11). This structure provides insights into key enzyme/inhibitor interactions that play a role in the binding of 6*H*-1,3,4-thiadiazine-based MMP inhibitors. These interactions are represented schematically in Figure 4.12.

Notably, the inhibitor is coordinated to the catalytic zinc cation via the exocyclic nitrogen of the thiadiazine moiety. The ring nitrogens are involved in specific hydrogen bonds with the backbone of cdMMP-8. The crystal structure of uncomplexed inhibitor **16** which contains two molecules per asymmetric unit, reveals that the thiadiazine ring deviates from

planarity. The calculated puckering parameters are $Q = 0.651 \text{ \AA}$ for both molecules, $\theta = 109.9^\circ$ (molecule 1) and 109.7° (molecule 2) and $\varphi = 218.8^\circ$ (molecule 1) and 218.3° (molecule 2). Thus, the thiadiazine moiety assumes a screw-boat conformation for both molecules in the asymmetric unit. The large φ values indicate, that the direction of the ring distortion is towards an inverted screw-boat conformation. The space group $P2_1/c$ of the uncomplexed **16** crystals implies an inversion center and thus, an equal subset of molecules with the inverted and non-inverted screw-boat conformation in the crystal structure.

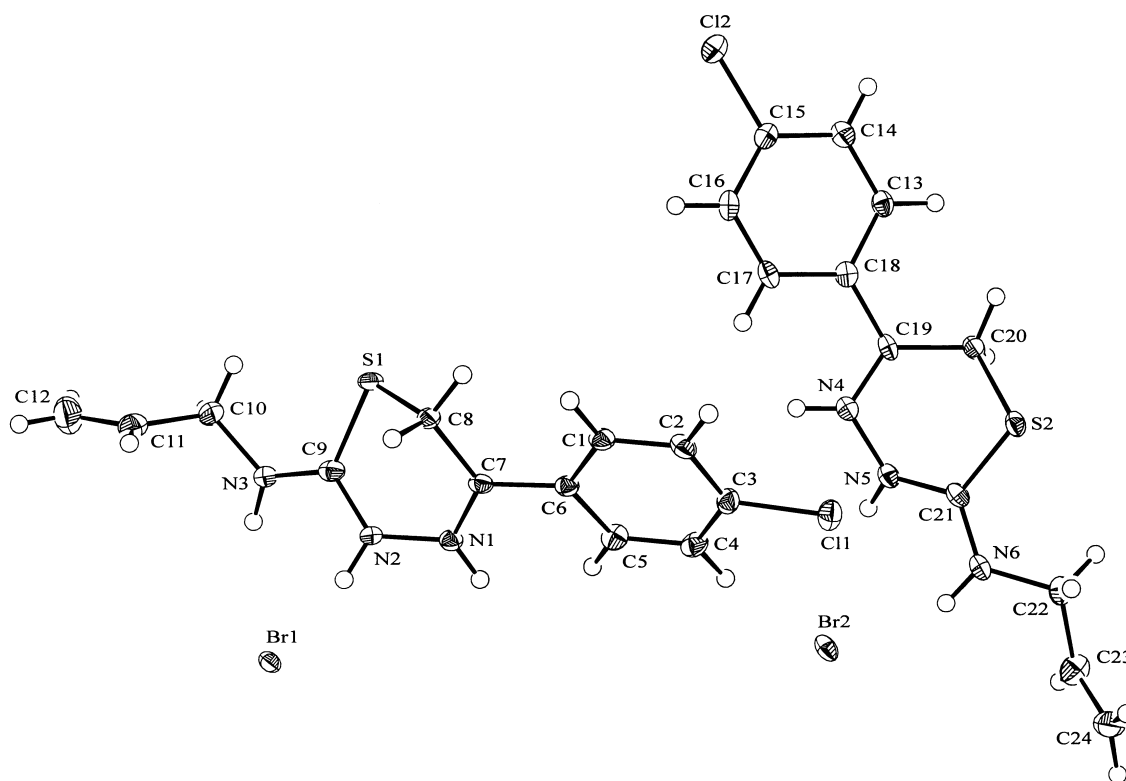


Figure 4.10 *The molecular structure of 16 showing the two molecules and the atom-numbering scheme. Displacement ellipsoids are drawn at the 50% probability level and H atoms are shown as small spheres of arbitrary radii. The hydrogen positions on all endocyclic nitrogens are calculated as half occupied.*

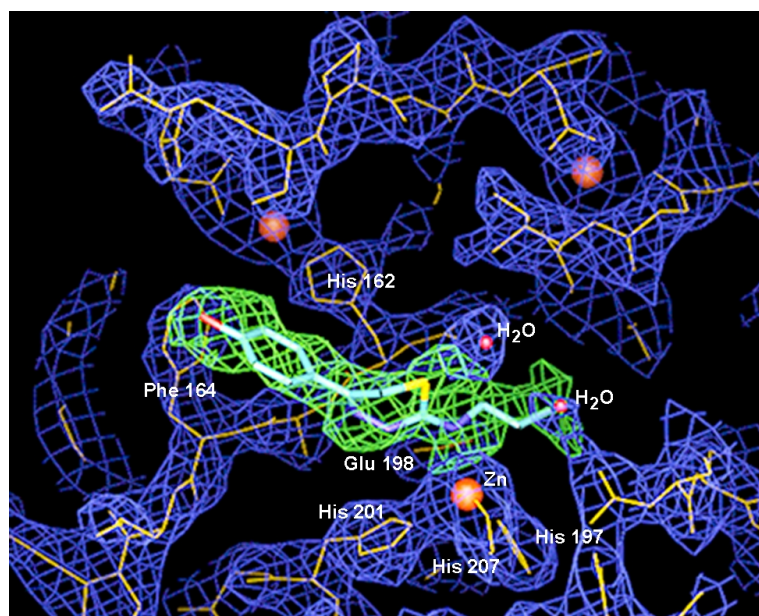


Figure 4.11 The electron density at the active site of the catalytic domain of human neutrophil collagenase (cdMMP-8) complexed with *N*-allyl-5-(4-chlorophenyl)-6*H*-1,3,4-thiadiazin-2-amine.

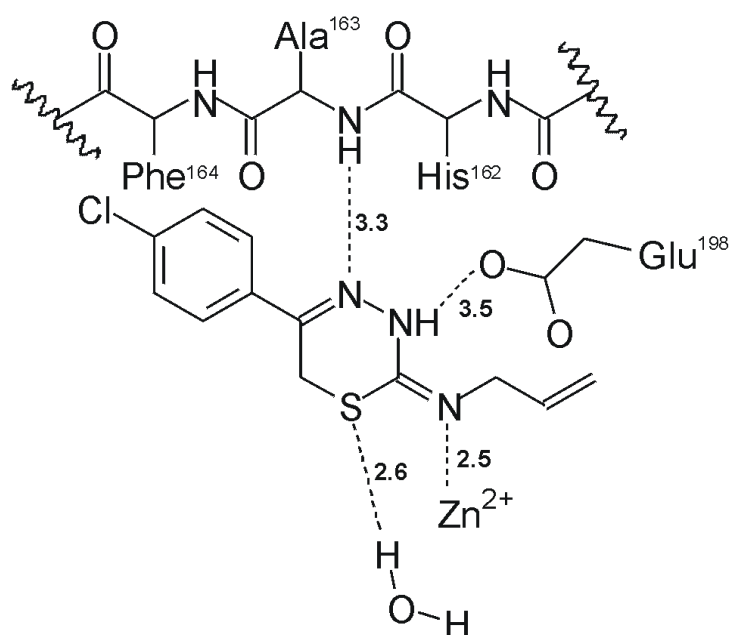


Figure 4.12 Schematic diagram of binding interactions between *N*-allyl-5-(4-chlorophenyl)-6*H*-1,3,4-thiadiazin-2-amine and cdMMP-8. Interatomic distances given in Ångstroms are those observed between protein and inhibitor heteroatoms. Hydrogen positions are inferred from heavier atom positions. Zn^{2+} is the catalytic zinc of cdMMP-8.

By contrast, when complexed with cdMMP-8 the puckering parameters of the thiadiazine ring are $Q = 0.619 \text{ \AA}$, $\theta = 71.3^\circ$ and $\varphi = 36.9^\circ$. This corresponds to the non-inverted screw-boat conformation of the heterocycle and fits the 4-chloro substituted phenyl residue into the S_3 subsite formed by Phe-164, His-162 and Ser-151 on the unprimed side. Thus, stabilization of the non-inverted screw-boat conformation of the thiadiazine core structure is expected to result in an inhibitor with higher affinity. The allyl substituent is directed towards the S_1' pocket of cdMMP-8. The hydrogen on the endocyclic nitrogen closest to the exocyclic nitrogen is prototropically shifted from the exocyclic nitrogen and stabilized by a hydrogen bond to the carboxylate oxygen of Glu-198. This glutamate is conserved in all zinc-proteinases, serving as the general base crucial for catalysis.⁸⁷ The other double bond nitrogen accepts a hydrogen bond from the backbone amide of Ala-163. The endocyclic sulfur does not appear to interact with any protein group, but makes a specific hydrogen bond to a structural water molecule. It is further required for electronic delocalisation of charge within the thiadiazine ring, which is necessary for zinc(II)-ion coordination. The electron density of the exocyclic nitrogen is directed to the catalytic zinc and does not interact with the backbone. The unique hydrogen bonding of the thiadiazine core explains why other related thiadiazines were not identified through the screening effort. Furthermore, the complex structure rationalizes the selectivity profile of compound **16** towards certain MMPs. Significant enzyme differences are found for the MMPs at the unprimed side of the enzyme cleft (S_1 - S_3), as compared to the primed side (S_1' - S_3') where most of the known inhibitors bind. In fact, the potency of *N*-allyl-5-(4-chlorophenyl)-6*H*-1,3,4-thiadiazin-2-amine hydrobromide is remarkable, given that the inhibitor lacks a substituent capable of filling the S_1' pocket. Consequently, it makes sense to attach a sulfonamide moiety to the thiadiazine core structure to improve primed side binding affinity.

4.6 Protein/Ligand–Docking Experiments

To understand the observed SARs and to rationalize the specificity profile, the interaction of compound **14b** with the active site of cdMMP-8 was examined. Since suitable crystals of a cdMMP-8/compound **14b** complex could not be obtained for X-ray studies, compound **14b** was modeled with the help of the docking tool FlexX⁸⁸ into the protein by

using coordinates from the above described cdMMP-8/inhibitor complex structure as a reference. The overall strategy for docking of flexible ligands within FlexX is incremental, as described below. The only interactive step during a complex prediction run is the selection of a base fragment. Conformations of the ligand are generated according to a discrete raster. Bond lengths and angles are kept invariant as given in the input structure. A set of up to 12 discrete torsion angle values is assigned to each acyclic single bond by matching representative torsional fragments onto the ligand. Conformational preferences are determined for each fragment by a statistical evaluation employing an experimental database of small molecule structures while the receptor is regarded as rigid. The docking algorithm in FlexX is based on the incremental construction strategy, which consists of three phases: 1. Base selection. The first phase of the docking algorithm is the selection of a connected part of the ligand, the base fragment. 2. Base placement. In the second phase, the base fragment is placed into the active site independently of the rest of the ligand. 3. Complex construction. In the last phase, called the construction phase, the ligand is constructed in an incremental way, starting with the different placements of the base fragment. The base fragment selection is performed interactively and the determined fragment is regarded as a rigid object.

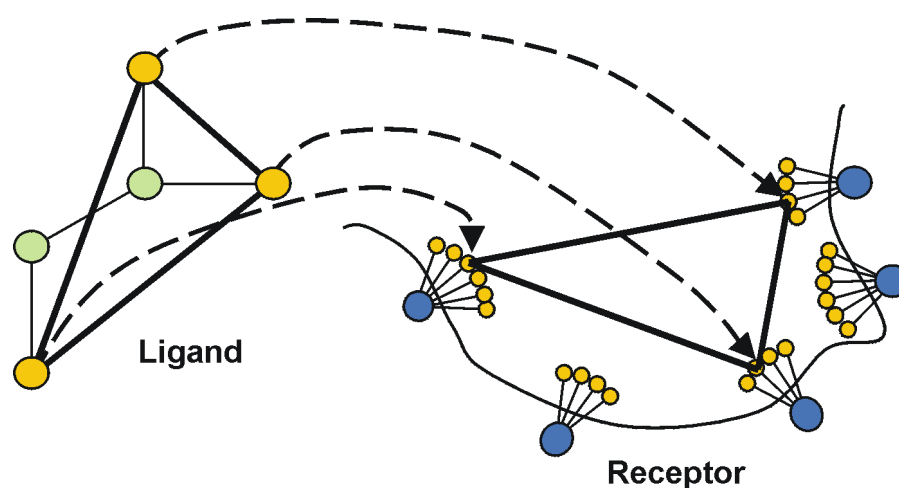


Figure 4.13 *The fragment placing algorithm: mapping three interaction centers (yellow spheres) of the ligand onto three discrete interaction points (yellow dots) in the active site defines a unique transformation of the ligand into the active site.*

The interaction surfaces on the receptor side are approximated by finite sets of interaction points. A transformation of the base fragment into the active site is uniquely defined by mapping three interaction centers of the fragment onto three interaction points of the receptor by simply superposing the three point pairs onto each other (assuming that the points sets are not collinear). Two of these triangles are regarded δ -compatible, if the corresponding edge lengths differ by at most δ and the corresponding corners have compatible interaction types. Therefore, in the first step the base placement algorithm has to solve the following problem: For each triangle of interaction centers of the base fragment have to be found all δ -compatible triangles of interaction points in the active site of the receptor. The second step of the base placement algorithm clusters the placements according to an appropriate distance function. For this purpose, the rms deviation between two placements was used. All placements inside the same cluster are combined to one solution by merging the lists of interactions and recomputing a superposition of all interaction centers of the ligand onto the interaction points of the receptor. In a third step, a final overlap test is performed and for the non overlapping placements energies are computed. The resulting free binding energy of the protein-ligand complex is estimated in FlexX as the sum of free energy contributions from hydrogen bonds, ion-pair interactions, hydrophobic and π -stacking interactions of aromatic groups, and lipophilic interactions.

The underlying assumption for the docking experiment performed here is, that the orientation of the 5-(4-chlorophenyl)-6*H*-1,3,4-thiadiazin-2-amine moiety in the binding site of cdMMP-8 is highly conserved. This assumption appears to be reasonable, since the interactions of this residue (Zn^{2+} coordination, a.o.) are highly favorable and specific. The flexible ligand docking results (highest scoring binding modes) for **14b** in cdMMP-8 were calculated in the form of rms values between the crystallographic binding mode and the docked binding mode of the core fragment. In Table 17 the first 10 placements produced by the docking algorithm are shown. The highest-ranking solution no. 73 has a free binding energy of $\Delta G = -24.2$ kJ/mol and an rms value of 3.6 Å.

Table 17. List of Docking Results generated by FlexX.

No.	Total Score	Match-Score	Lipo-Score	Ambig-Score	Overl-Score	RMS-Value	Simil. Index	#Match	Avg. Volume	Max. Volume	Frag. No.
73	-24.159	-26.349	-8.672	-7.268	7.129	3.550	3.670	7	0.449	2.069	1
95	-23.703	-25.370	-10.006	-6.570	7.243	3.774	3.581	7	0.464	2.026	1
265	-21.264	-23.916	-9.010	-7.623	8.286	3.810	3.645	9	0.488	1.848	2
82	-24.007	-26.155	-10.260	-6.678	8.087	3.821	3.420	7	0.492	1.433	1
245	-21.688	-24.707	-8.707	-6.834	7.560	3.833	3.702	7	0.435	1.926	2
100	-23.633	-26.349	-8.933	-6.700	7.349	3.868	3.655	7	0.480	2.069	1
237	-21.776	-24.707	-9.035	-6.634	7.600	3.886	3.669	7	0.431	1.926	2
202	-22.172	-24.454	-7.678	-7.418	6.378	3.937	3.833	7	0.360	1.954	2
268	-21.259	-23.107	-7.364	-6.669	4.881	3.999	3.519	6	0.281	1.554	2
249	-21.655	-23.084	-7.598	-6.888	4.914	4.007	3.489	6	0.316	2.487	2

Surprisingly, in this binding prediction the thiophene ring does not occupy the S_1' pocket, but is positioned above the catalytic zinc. Such electrostatic interactions between the positive charge of a cation and the negative partial charge of aromatic π clouds have been proposed in molecular recognition processes and recently explored by experimental and theoretical works.⁸⁹ A physical model of this interaction has been reported in a review.⁹⁰ The catalytic zinc ion is positioned on the normal vector to the aromatic thiophene ring at 5.1 Å distance.

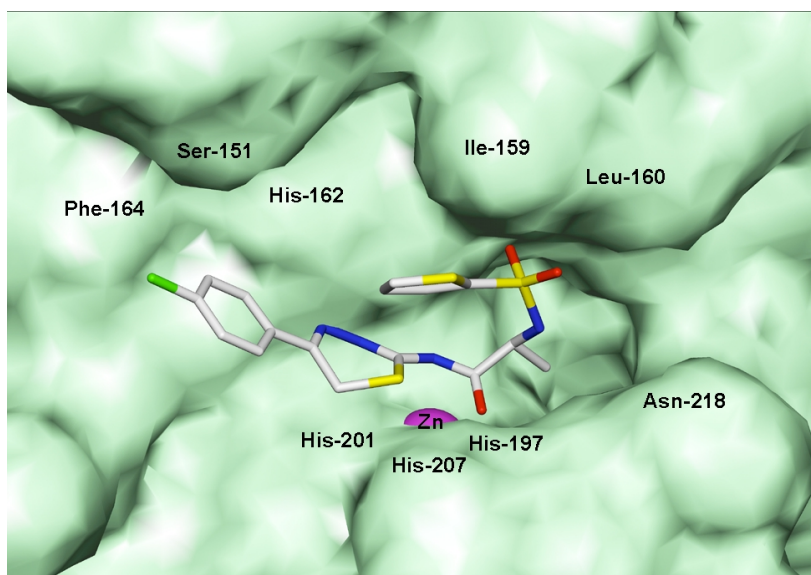


Figure 4.14 View of the highest-ranking binding prediction of compound **14b** in the active site of *cdMMP-8*. Amino acid residues that form the binding cleft are labeled, and a solid surface has been added.

A similar interaction involving the catalytic zinc ion has already been described for the complex between cdMMP-8 and batimastat, where the thiophene aromatic ring of the inhibitor faces the cation at a distance of 4.5 Å.

The contribution of these attractive electrostatic interactions, albeit at a relatively large distance, should not be neglected in the evaluation of the stabilization of the complex model but has to be taken into account in the selectivity of compound **14b** as well as other compounds of this series. Further interactions contributing to the tight binding of **14b** may include oxygen- and sulfur-zinc ligation and specific hydrogen bonds. These occur between the endocyclic N4 and Ala-163, one of the sulfonyl oxygen atoms and Ala-161 and the sulfonamide nitrogen of the inhibitor and Pro-217.

4.7 *In Vitro* Cell-Assay

The ability of mamma carcinoma cells to invade the surrounding tissue and form distant metastases is closely related to their ability to disintegrate components of the surrounding extracellular matrix. As outlined in chapter 2 several types of proteinases contribute to the degradation of the ECM, namely, serine proteinases (*e.g.* plasmin, uPA), cysteine proteinases (*e.g.* cathepsins B and L), and matrix metalloproteinases. Increased expression of uPA and its membrane-bound receptor uPAR is closely correlated with an increase in disease recurrence and with early death of mamma carcinoma patients. Cell membrane-associated uPAR is a key molecule for the induction of pericellular proteolysis, as plasminogen is efficiently activated to plasmin by cell surface-associated interactions with uPAR-bound uPA. Plasmin is a broad-range serine protease that cleaves a variety of extracellular matrix proteins. In addition plasmin can also activate MMPs such as MMP-2 and MMP-9.⁹¹ On this basis, it was postulated and shown at the "Institut für Experimentelle Onkologie und Therapieforchung, TU München" that the inhibitor (2*S*)-*N*-[5-(4-chlorophenyl)-6*H*-1,3,4-thiadiazin-2-yl]-2-[(phenylsulfonyl)amino]propanamide **12b** inhibits the activity of MMP-2 and MMP-9 expressed by MDA-231 BAG mamma carcinoma cells.⁹² The active and latent forms of MMP-9 and the latent form of MMP-2 were detected in the supernatants of the tumor cells by zymography. Compound **12b** was tested using a potent MMP inhibitor as a reference. The compounds were incubated under cell culture conditions in a 5% CO₂ atmosphere at 37°C for 24 hours. The final

gelatinolytic activity of the tumor cells was measured using DQTM-gelatin (Molecular probes, Eugene, OR, USA), which serves as a fluorescein-conjugated but fluorescence-quenched protease substrate. On degradation of the substrate by gelatinases, the released fluorescent peptides are quantified by a fluorescence reader (Wallac, Victor² 1420, Perkin Elmer, Überlingen, Germany) at excitation and emission wavelengths of 485 nm and 535 nm, respectively. The increase in fluorescence is proportional to the gelatinolytic activity. These results were compared to the gelatin degrading activity of the cell-line without inhibitor. It was found, that the reference MMP-inhibitor reduced the gelatinolytic activity by about 20 percent at 21 μM final assay concentration, while compound **12b** showed the same reduction at 10 μM final assay concentration.

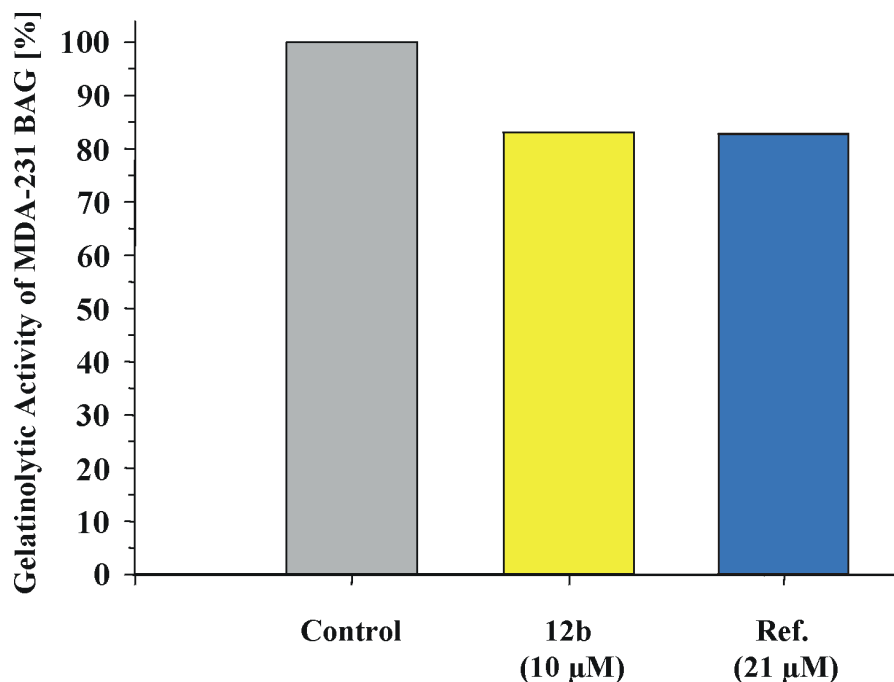


Figure 4.15 *Inhibition of the gelatinolytic activity of the mamma carcinoma cell-line MDA-231 BAG by **12b** in comparison with a potent reference MMPI.*

Since the reference MMP inhibitor was already tested in a synergic mouse lymphoma model with great success, thiadiazine-based MMPIs are now attractive candidates for *in vivo* tumor models.

5 Conclusions

A series of potent matrix metalloproteinase inhibitors based on a 6*H*-1,3,4-thiadiazine scaffold was discovered and optimized. The new compounds lacking a typical zinc-coordinating group were tested against eight different matrix metalloproteinases, MMP-1, cdMMP-2, cdMMP-8, MMP-9, cdMMP-12, cdMMP-13, cdMMP-14, and the ectodomain of MMP-14. From a small number of screening hits exhibiting K_i -values in the micromolar range against cdMMP-8, the optimization strategy led to compounds with nanomolar inhibitory activity against cdMMP-2, cdMMP-8, MMP-9, and cdMMP-14. This was primarily achieved by the attachment of a *N*-sulfonylated amino acid derivative to the 6*H*-1,3,4-thiadiazine core fragment. From in-depth SAR examinations, optimum enzyme inhibitory activity in the series generally was associated with the *R* configuration at the amino acid chiral center. The non-chiral variant *N*-[5-(4-chlorophenyl)-6*H*-1,3,4-thiadiazine-2-yl]-2-methyl-2-[(phenylsulfonyl)amino]propanamide was synthesized as well and shows nanomolar affinity for cdMMP-2 and MMP-9. Variations of substituents attached to the *para*-position of the phenyl ring in position 5 of the thiadiazine moiety revealed a preference for halogens to produce potent and selective inhibitors. On the other hand, the inhibition of MMP-1 and cdMMP-12 demonstrated very few variations in potency as functional groups were altered. Inhibition of cdMMP-13 generally occurred in the micromolar to submicromolar range within the tested compound series. The most potent inhibitors were readily prepared by standard peptide coupling reactions from 5-substituted 6*H*-1,3,4-thiadiazine-2-amine hydrohalides and *N*-sulfonylated amino acid derivatives.

Using X-ray crystallography, a novel binding mode of *N*-allyl-5-(4-chloro-phenyl)-6*H*-1,3,4-thiadiazin-2-amine in the active site of the catalytic domain of human neutrophil collagenase was elucidated. In contrast to the established MMP-inhibitors, which exclusively bind to the primed side, *N*-allyl-5-(4-chlorophenyl)-6*H*-1,3,4-thiadiazin-2-amine interact with both the primed and the unprimed side. The zinc-ligation is mediated via the exocyclic nitrogen while the endocyclic nitrogens of the thiadiazine system are involved in specific hydrogen bonds with cdMMP-8. These results are in good agreement with the postulated binding mode of the inhibitors. Analysis of the puckering parameters of the 6*H*-1,3,4-thiadiazine system bound to cdMMP-8 reveal a preferential screw-boat

conformation of the heterocycle. This is important in comparison with the crystal structure of uncomplexed *N*-allyl-5-(4-chlorophenyl)-6*H*-1,3,4-thiadiazin-2-amine hydrobromide which consists of an equal subset of molecules with the inverted- and non-inverted screw-boat conformation. Similar thiadiazine ring conformations were observed in the crystal structures of the uncomplexed 6*H*-1,3,4-thiadiazin-2-amide-based MMPiS. Docking experiments of (2*S*)-*N*-[5-(4-chlorophenyl)-6*H*-1,3,4-thiadiazin-2-yl]-2-[(2-thienylsulfonyl)amino]propanamide to cdMMP-8 reveal an unexpected binding mode of the highest ranking binding prediction. In this prediction the thiophene ring may stabilize the enzyme-inhibitor adduct by cation-aromatic interactions. Furthermore, the conformational rigidity of the compound and specific hydrogen bonds with the enzyme's backbone may be advantageous as a means to obtain the observed selectivity.

On the basis of its *in vitro* activity (2*S*)-*N*-[5-(4-chlorophenyl)-6*H*-1,3,4-thiadiazin-2-yl]-2-[(phenylsulfonyl)amino]propanamide was used for an *in vitro* cell assay with the mamma carcinoma cell-line MDA-231 BAG to elucidate the anti-tumor activity of the compound class. The promising results imply that 6*H*-1,3,4-thiadiazine-based MMPiS are now attractive candidates for *in vivo* tumor models and further pharmacological trials.

6 Experimental Section

6.1 General Information

All moisture-free operations were performed in oven dried glassware under a positive pressure of argon. Sensitive liquids and solutions were transferred via syringe or cannula and introduced into reaction vessels through rubber septa.

Proton (^1H) nuclear magnetic resonance (NMR) spectra were measured with a Bruker DRX-500 (500.1 MHz) spectrometer, and carbon thirteen (^{13}C) NMR spectra were measured with a Bruker DRX-500 (125.8 MHz) spectrometer, both at 22°C and with TMS as an external standard. Chemical shifts are reported in parts per million (ppm, δ units). Coupling constants are reported in units of hertz (Hz).

Mass spectral (MS) data were obtained on a Fisons Autospec VG spectrometer by the DCI/methane and DEI/isobutane method. MALDI-TOF mass spectral data were obtained on a PerSeptive Biosystems Voyager-DE spectrometer with DHB as the matrix and PEG 200 as the calibration standard.

Elemental analyses were performed on a Leco CHNS-932 elemental analyzer (microanalytical laboratory of the University of Bielefeld). All inhibitors synthesized in the experiments below were analyzed by elemental analysis and the compounds had values within the range of $\pm 0.4\%$ for CHN.

Melting points (mp) were determined with a Büchi 510 melting point apparatus and are uncorrected.

Analytical purity was assessed by RP-HPLC using an Applied Biosystems 130A Separation System. Compounds were detected at 230 nm. The stationary phase was an Aquapore OD-300 C_{18} column (2.1 mm x 220 mm). The mobile phase employed aqueous trifluoroacetic acid with acetonitrile as the organic modifier and a flow rate of 250 $\mu\text{L}/\text{min}$. Solvent A = 0.1% TFA in water. Solvent B = 0.09% TFA and 80% acetonitrile in water.

The following gradient was used: $t = 0$ min (0% B), $t = 5$ min (40% B), $t = 25$ min (60% B), $t = 30$ min (100% B), $t = 35$ min (0% B). Analytical data is reported as retention time, t_R , in minutes.

Analytical TLC was performed on Alugram Sil G/UV₂₅₄ pre-coated aluminium-backed silica gel plates (Macherey-Nagel, Düren). Visualization of spots was effected by one of the following techniques: (a) ultraviolet illumination and (b) immersion of the plate in a 3% solution of ninhydrin in ethanol followed by heating. Analytical data is reported as "ratio of front"-values (R_f -values).

P.a. grade reagents and solvents were used without further purification except that methylene chloride was distilled under argon from calcium hydride, and DMF was distilled under argon on molecular sieve 3 Å. Most of the special organic starting materials and reagents were obtained from Sigma-Aldrich, Deisenhofen, and Lancaster-Synthesis, Mühlheim. Solvents were generally obtained from Merck, Darmstadt and Baker, Groß-Gerau.

6.2 Synthetic Methods

6.2.1 Aryl ω -Halo Ketones

2-Bromo-1-(5-chloro-2-thienyl)ethanone

A solution of 2-acetyl-5-chlorothiophene (1.28 g, 8 mmol) in 20 mL chloroform was cooled to 0°C. Pyridinium bromide perbromide (3.2 g, 10 mmol) was added in four portions to the stirred solution over a period of 30 min. Upon completion of the reaction (indicated by TLC) the solution was poured into ice water and extracted with ether. The combined ether fractions were finally washed with water and saturated saline solution, dried over MgSO₄, and concentrated. The oily residue was triturated with petrolether (40/80) and the resulting 2-bromo-1-(5-chloro-2-thienyl)ethanone was recrystallized from petrolether giving 1.16 g (61%) of the pure product as colorless plates; mp: 70-72°C; R_f = 0.78 (eluent: methanol/THF 3 : 1); ¹H-NMR (DMSO-*d*₆): δ 4.80 (s, 2H), 7.34 (d, ³J = 4.1 Hz, 1H), 7.98 (d, ³J = 4.2 Hz, 1H); ¹³C-NMR (DMSO-*d*₆): δ 32.16 (CH₂), 129.22, 135.18 (CH), 138.85, 139.45 (C), 184.45 (C=O).

2-Bromo-1-[4-(trifluoromethyl)phenyl]ethanone

A solution of 4-trifluoromethyl-acetophenone (1.88 g, 10 mmol) in 40 mL methylene chloride was heated to reflux. Within 1 h a solution of bromine (1.6 g, 10 mmol) in 20 mL methylene chloride was added dropwise to the boiling solution under rapid stirring. During reaction the resulting HBr gas was removed by a positive argon pressure. The orange reaction mixture was stirred overnight at room temperature within which time it becomes clear. The mixture was then evaporated under reduced pressure to give an off-white solid. Recrystallization from petrolether/n-hexane afforded 2.36 g (88%) of the desired product as colorless plates; mp: 53-54°C; R_f = 0.81 (eluent: methanol/THF 3 : 1); ¹H-NMR (CDCl₃): δ 4.43 (s, 2H), 7.74 (d, ³J = 8.3 Hz, 2H), 8.08 (d, ³J = 8.2 Hz, 2H); ¹³C-NMR (CDCl₃): δ 30.31 (CH₂), 123.37 (q, ¹J_{CF} = 272.9 Hz, CF₃), 125.90, 129.31 (CH), 135.05 (q, ²J_{CF} = 33.09 Hz, C-CF₃), 136.56 (C-CO), 190.40 (C=O).

6.2.2 Substituted 2-Amino-6H-1,3,4-thiadiazine Hydrohalides

General Procedure for Preparing Substituted 2-Amino-6H-1,3,4-thiadiazine Hydrohalides (Method A)

2-Amino-5-(4-chlorophenyl)-6H-1,3,4-thiadiazine Hydrobromide (6c)

4-Chlorophenacylbromide (2.34 g, 10 mmol) and thiosemicarbazide (0.91 g, 10 mmol) were suspended in 30 mL ethanol at 0°C. The mixture was allowed to warm up to room temperature overnight under stirring. The resulting slurry was cooled to -20°C and the precipitate was collected by filtration, washed with cold ethanol, and dried in vacuo. The pale yellow solid was again suspended in 20 mL ethanol which contained 1 mL of 48% aqueous hydrobromic acid. The mixture was heated to reflux for 30 min and then allowed to cool down to room temperature overnight. The precipitate was filtered, recrystallized from ethanol, and dried in high-vacuo at 40°C over phosphorus pentoxide. Yield: 1.84 g (60%); colorless needles; mp: 227°C; $R_f = 0.52$ (eluent: chloroform/methanol/glacial acetic acid/ethylacetate 5 : 3 : 1 : 4); $^1\text{H-NMR}$ (DMSO- d_6): δ 4.31 (s, 2H), 7.59 (d, $^3J = 8.6$ Hz, 2H), 7.90 (d, $^3J = 8.7$ Hz, 2H), 9.46 (br s, 1H), 10.11 (br s, 1H), 13.32 (br s, 1H); $^{13}\text{C-NMR}$ (DMSO- d_6): δ 22.10 (CH₂), 128.81, 129.11 (CH_{arom.}), 131.86, 136.22, 150.24, 164.17 (C). DEI MS: m/z 225 [M - HBr]⁺.

2-Amino-5-(4-bromophenyl)-6H-1,3,4-thiadiazine Hydrobromide (6d)

The compound was prepared starting from 4-bromophenacylbromide as described for compound **6c**. Yield: 2.33 g (66%); colorless crystals; mp: 218°C; $R_f = 0.54$ (eluent: chloroform/methanol/glacial acetic acid/ethylacetate 5 : 3 : 1 : 4); $^1\text{H-NMR}$ (DMSO- d_6): δ 4.30 (s, 2H), 7.73 (d, $^3J = 8.6$ Hz, 2H), 7.83 (d, $^3J = 8.6$ Hz, 2H), 9.34 (br s, 1H), 10.09 (br s, 1H), 13.31 (br s, 1H); $^{13}\text{C-NMR}$ (DMSO- d_6): δ 22.04 (CH₂), 125.16 (C), 128.96, 132.03 (CH_{arom.}), 132.21, 150.34, 164.16 (C). DEI MS: m/z 270 [M - HBr]⁺.

2-Amino-5-(4-nitrophenyl)-6H-1,3,4-thiadiazine Hydrobromide (6e)

The title compound was prepared starting from 4-nitrophenacylbromide as described for compound **6c**. Yield: 1.58 g (49%); orange crystals; mp: 228°C; $R_f = 0.53$ (eluent:

chloroform/methanol/glacial acetic acid/ethylacetate 5 : 3 : 1 : 4); $^1\text{H-NMR}$ (DMSO- d_6): δ 4.38 (s, 2H), 8.14 (d, $^3J = 8.9$ Hz, 2H), 8.34 (d, $^3J = 8.9$ Hz, 2H), 9.61 (br s, 1H), 10.21 (br s, 1H), 13.42 (br s, 1H); $^{13}\text{C-NMR}$ (DMSO- d_6): δ 22.22 (CH₂), 124.07, 128.36 (CH_{arom.}), 139.00, 148.76, 149.34, 164.25 (C). DEI MS: m/z 236 [M - HBr]⁺.

2-Amino-5-(4-cyanophenyl)-6H-1,3,4-thiadiazine Hydrobromide (6f)

The compound was prepared starting from 4-cyanophenacylbromide as described for compound **6c**. Yield: 1.80 g (61%); yellow needles; mp: 248°C; R_f = 0.49 (eluent: chloroform/methanol/glacial acetic acid/ethylacetate 5 : 3 : 1 : 4); $^1\text{H-NMR}$ (DMSO- d_6): δ 4.35 (s, 2H), 8.00 (d, $^3J = 8.4$ Hz, 2H), 8.05 (d, $^3J = 8.4$ Hz, 2H), 9.93 (br s, 1H), 10.19 (br s, 1H), 13.33 (br s, 1H); $^{13}\text{C-NMR}$ (DMSO- d_6): δ 22.08 (CH₂), 113.41, 118.30 (C), 127.74, 132.92 (CH_{arom.}), 137.30, 149.68, 164.22 (C). DEI MS: m/z 216 [M - HBr]⁺.

2-Amino-5-(4-(trifluoromethyl)phenyl)-6H-1,3,4-thiadiazine Hydrobromide (6g)

The compound was prepared starting from 2-bromo-1-[4-(trifluoromethyl)phenyl]ethanone as described for compound **6c**. Yield: 1.54 g (45%); colorless crystals; mp: 224°C; R_f = 0.56 (eluent: chloroform/methanol/glacial acetic acid/ethylacetate 5 : 3 : 1 : 4); $^1\text{H-NMR}$ (DMSO- d_6): δ 4.36 (s, 2H), 7.90 (d, $^3J = 8.3$ Hz, 2H), 8.10 (d, $^3J = 8.2$ Hz, 2H), 9.92 (br s, 1H), 10.12 (br s, 1H), 13.13 (br s, 1H); $^{13}\text{C-NMR}$ (DMSO- d_6): δ 22.17 (CH₂), 123.88 (q, $^1J_{\text{CF}} = 272.3$ Hz, CF₃), 125.92, 127.86 (CH_{arom.}), 130.97 (q, $^2J_{\text{CF}} = 32.2$ Hz, C-CF₃), 137.01, 149.92, 164.18 (C). DEI MS: m/z 259 [M - HBr]⁺.

2-Amino-5-(4-methoxyphenyl)-6H-1,3,4-thiadiazine Hydrobromide (6h)

The title compound was prepared starting from 4-methoxyphenacylbromide as described for compound **6c**. Yield: 1.65 g (55%); pale yellow needles; mp: 185°C; R_f = 0.54 (eluent: chloroform/methanol/glacial acetic acid/ethylacetate 5 : 3 : 1 : 4); $^1\text{H-NMR}$ (DMSO- d_6): δ 3.81 (s, 3H), 4.27 (s, 2H), 7.06 (d, $^3J = 8.9$ Hz, 2H), 7.85 (d, $^3J = 8.9$ Hz, 2H), 9.26 (br s, 1H), 9.85 (br s, 1H), 13.10 (br s, 1H); $^{13}\text{C-NMR}$ (DMSO- d_6): δ 22.07 (CH₂), 55.54 (CH₃),

114.46 (CH_{arom.}), 125.06 (C), 128.82 (CH_{arom.}), 151.04, 161.85, 163.99 (C). DEI MS: *m/z* 221 [M - HBr]⁺.

2-Amino-5-(4-methylphenyl)-6H-1,3,4-thiadiazine Hydrobromide (6i)

The compound was prepared starting from 4-methylphenacylbromide (20 mmol) as described for compound **6c**. Yield: 3.13 g (55%); colorless crystals; mp: 220°C; R_f = 0.52 (eluent: chloroform/methanol/glacial acetic acid/ethylacetate 5 : 3 : 1 : 4); ¹H-NMR (DMSO-*d*₆): δ 2.35 (s, 3H), 4.29 (s, 2H), 7.33 (d, ³J = 8.0 Hz, 2H), 7.78 (d, ³J = 8.1 Hz, 2H), 9.31 (br s, 1H), 10.04 (br s, 1H), 13.23 (br s, 1H); ¹³C-NMR (DMSO-*d*₆): δ 21.01 (CH₂), 22.11 (CH₃), 126.96, 129.61 (CH_{arom.}), 130.13, 141.60, 151.28, 164.19 (C). DEI MS: *m/z* 205 [M - HBr]⁺.

N-Allyl-5-(4-chlorophenyl)-6H-1,3,4-thiadiazin-2-amine Hydrobromide (16)

4-Chlorophenacylbromide (2.34 g, 10 mmol) and 4-allylthiosemicarbazide (1.31 g, 10 mmol) were suspended in 30 mL ethanol at 0°C. The mixture was allowed to warm up to room temperature overnight under stirring. The yellow solution was added dropwise to 50 mL ethylacetate at 0°C, and the precipitate was collected by filtration, washed with cold ethanol, and dried in vacuo. The yellow solid was again suspended in 20 mL ethanol which contained 1 mL of 48% aqueous hydrobromic acid. The mixture was heated to reflux for 30 min and then allowed to cool down to room temperature overnight. After addition of cold ethylacetate, the precipitate was filtered, recrystallized from ethanol/ethylacetate (1 : 3), and dried in high-vacuo at 40°C over phosphorus pentoxide. Yield: 1.49 g (43%); colorless crystals; mp: 210°C; R_f = 0.66 (eluent: chloroform/methanol/glacial acetic acid/ethylacetate 5 : 3 : 1 : 4); HPLC (*t*_R: 11.97); ¹H-NMR (DMSO-*d*₆): δ 4.17 (br s, 2H), 4.31 (s, 2H), 5.24-5.31 (m, 2H), 5.89 (m, 1H), 7.61 (d, ³J = 8.6 Hz, 2H), 7.92 (d, ³J = 8.6 Hz, 2H), 10.71 (br s, 1H), 12.87 (br s, 1H); ¹³C-NMR (DMSO-*d*₆): δ 22.23 (CH₂), 46.01 (CH₂), 117.95 (=CH₂), 128.82, 129.16 (CH_{arom.}), 131.53 (=CH), 131.86, 136.28, 151.29 (C). DEI MS: *m/z* 265 [M - HBr]⁺; MALDI-TOF-MS: *m/z* calculated for [M - Br]⁺: 266.1, found: 266.1. Analysis calculated

for C₁₂H₁₃BrClN₃S: C, 41.58%; H, 3.78%; N, 12.12%. Found: C, 41.59%; H, 3.67%; N, 12.10%.

General Procedure for Preparing 2-Amino-6*H*-1,3,4-thiadiazine Hydrohalides (Method B)

2-Amino-5-phenyl-6*H*-1,3,4-thiadiazine Hydrochloride (6a)

Thiosemicarbazide Hydrochloride: This compound was obtained as colorless crystals by evaporation of a hydrochloric acid solution of thiosemicarbazide.

A suspension of phenacylchloride 1.55 g (10 mmol) and thiosemicarbazide hydrochloride 1.72 g (10 mmol) in 25 mL methanol was heated to reflux for 15 min. After cooling down to room temperature the white crystalline solid was filtered, recrystallized from methanol, and dried in high-vacuo at 40°C over phosphorus pentoxide. Yield: 0.99 g (43%); colorless needles; mp: 206°C; R_f = 0.43 (eluent: chloroform/methanol/glacial acetic acid/ethylacetate 5 : 3 : 1 : 4); ¹H-NMR (DMSO-*d*₆): δ 4.29 (s, 2H), 7.50-7.56 (m, 3H), 7.87-7.89 (m, 2H), 9.63 (br s, 1H), 10.51 (br s, 1H), 13.73 (br s, 1H); ¹³C-NMR (DMSO-*d*₆): δ 21.97 (CH₂), 126.97, 129.03, 131.40 (CH_{arom.}), 133.06, 150.85, 164.95 (C). DEI MS: *m/z* 225 [M - HCl]⁺.

2-Amino-5-(4-fluorophenyl)-6*H*-1,3,4-thiadiazine Hydrochloride (6b)

The compound was prepared starting from 4-fluorophenacylchloride as described for compound **6a**. Yield: 1.79 g (73%); colorless crystals; mp: 231°C; R_f = 0.50 (eluent: chloroform/methanol/glacial acetic acid/ethylacetate 5 : 3 : 1 : 4); ¹H-NMR (DMSO-*d*₆): δ 4.28 (s, 2H), 7.34-7.38 (m, 2H), 7.92-7.96 (m, 2H), 9.59 (br s, 1H), 10.54 (br s, 1H), 13.74 (br s, 1H); ¹³C-NMR (DMSO-*d*₆): δ 22.02 (CH₂), 116.11 (d, ²J_{CF} = 21.4 Hz, CH_{arom.}), 129.57 (d, ³J_{CF} = 8.8 Hz, CH_{arom.}), 129.64, 149.95, 162.92, 164.94 (C). DEI MS: *m/z* 209 [M - HCl]⁺.

2-Amino-5-(2-adamantyl)-6H-1,3,4-thiadiazine Hydrobromide (6j)

Thiosemicarbazide Hydrobromide: This compound was obtained as colorless crystals by evaporation of a 48% hydrobromic acid solution of thiosemicarbazide.

A suspension of 1-(2-bromoacetyl)-adamantane 2.57 g (10 mmol) and thiosemicarbazide hydrobromide 1.72 g (10 mmol) in 25 mL methanol was heated to reflux for 15 min. After cooling down to room temperature the white crystalline solid was filtered, recrystallized from methanol, and dried in high-vacuo at 40°C over phosphorus pentoxide. Yield: 1.97 g (60%); colorless crystals; mp: 251°C; $R_f = 0.60$ (eluent: chloroform/methanol/glacial acetic acid/ethylacetate 5 : 3 : 1 : 4); $^1\text{H-NMR}$ (DMSO- d_6): δ 1.61-1.68 (m, 6H), 1.75 (s, 6H), 1.98 (s, 3H), 3.79 (s, 2H), 9.11 (br s, 1H), 9.84 (br s, 1H), 12.91 (br s, 1H); $^{13}\text{C-NMR}$ (DMSO- d_6): δ 20.39 (CH₂), 27.21 (CH), 35.82 (CH₂), 38.18 (C), 162.87 (C), 164.84 (C). DEI MS: m/z 249 [M - HBr]⁺.

2-Amino-5-(5-chloro-2-thienyl)-6H-1,3,4-thiadiazine Hydrobromide (6k)

The title compound was prepared starting from 2-bromo-1-(5-chloro-2-thienyl)ethanone as described for compound **6j**. Yield: 0.35 g (11%); off-white solid; mp: 249°C; $R_f = 0.47$ (eluent: chloroform/methanol/glacial acetic acid/ethylacetate 5 : 3 : 1 : 4); $^1\text{H-NMR}$ (DMSO- d_6): δ 4.35 (s, 2H), 7.28 (d, $^3J = 4.1$ Hz, 1H), 7.68 (d, $^3J = 4.1$ Hz, 1H), 9.63 (br s, 1H), 10.03 (br s, 1H), 13.19 (br s, 1H); $^{13}\text{C-NMR}$ (DMSO- d_6): δ 21.69 (CH₂), 128.36, 131.47 (CH), 133.86, 135.94, 146.13, 163.71 (C). DEI MS: m/z 231 [M - HBr]⁺.

6.2.3 N-Sulfonylated Amino Acids**General Procedure for Preparing N-Sulfonylated Amino Acids****(2S)-2-[(Phenylsulfonyl)amino]propanoic Acid (8a)**

Benzenesulfonylchloride (1.80 g, 10 mmol) was added to a solution of *L*-alanine (1.07 g, 12 mmol) in aqueous potassium carbonate (20 mL, 1.1 M). Under vigorous stirring, the mixture was carefully heated to 70°C for 30 min. The resulting clear solution was cooled

in an ice bath and then acidified to pH 2.5 by the dropwise addition of concentrated hydrochloric acid under stirring. The precipitate was collected by filtration and washed with a minimum amount of ice-cold water. Recrystallization from distilled water yielded 1.42 g (62%) (2*S*)-2-[(phenylsulfonyl)amino]propanoic acid as a white crystalline solid; mp: 123-125°C; $R_f = 0.47$ (eluent: chloroform/acetone/glacial acetic acid 9 : 1 : 0.3); $^1\text{H-NMR}$ (DMSO- d_6): δ 1.13 (d, $^3J = 7.2$ Hz, 3H), 3.76 (m, 1H), 7.54-7.61 (m, 3H), 7.78 (d, $^3J = 7.4$ Hz, 2H), 8.14 (d, $^3J = 8.3$ Hz, NH), 12.64 (s, COOH); $^{13}\text{C-NMR}$ (DMSO- d_6): δ 18.43 (CH₃), 51.15 (CH), 126.40, 129.06, 132.35 (CH_{arom.}), 141.34 (C), 173.22 (COOH).

(2*R*)-2-[(Phenylsulfonyl)amino]propanoic Acid (8b)

This compound was prepared starting from *D*-alanine as described for compound **8a**. Yield: 1.65 g (72%); white solid; mp: 124-126°C; $R_f = 0.47$ (eluent: chloroform/acetone/glacial acetic acid 9 : 1 : 0.3); $^1\text{H-NMR}$ (DMSO- d_6): δ 1.13 (d, $^3J = 7.1$ Hz, 3H), 3.76 (m, 1H), 7.54-7.62 (m, 3H), 7.78 (d, $^3J = 7.5$ Hz, 2H), 8.15 (d, $^3J = 8.3$ Hz, NH), 12.65 (s, COOH).

(2*S*)-2-[(2-Thienylsulfonyl)amino]propanoic Acid (8c)

The title compound was prepared starting from thiophene-2-sulfonylchloride as described for compound **8a**. Yield: 1.57 g (67%); white solid; mp: 85-87°C; $R_f = 0.45$ (eluent: chloroform/acetone/glacial acetic acid 9 : 1 : 0.3); $^1\text{H-NMR}$ (DMSO- d_6): δ 1.17 (d, $^3J = 7.3$ Hz, 3H), 7.14 (m, 1H), 7.56 (d, $^3J = 3.1$ Hz, 1H), 7.89 (d, $^3J = 4.8$ Hz, 1H), 8.35 (d, $^3J = 8.2$ Hz, NH), 12.71 (s, COOH); $^{13}\text{C-NMR}$ (DMSO- d_6): δ 27.81 (CH₃), 60.83 (CH), 137.09, 141.07, 141.99 (CH_{arom.}), 151.69 (C), 182.67 (COOH).

(2*S*)-2-[(Benzylsulfonyl)amino]propanoic Acid (8d)

This compound was prepared starting from benzylsulfonylchloride as described for compound **8a**. Yield: 1.97 g (81%); white solid; mp: 125-127°C; $R_f = 0.49$ (eluent: chloroform/acetone/glacial acetic acid 9 : 1 : 0.3); $^1\text{H-NMR}$ (DMSO- d_6): 1.23 (d, $^3J = 7.3$ Hz, 3H), 3.79 (m, 1H), 4.30 (d, $^2J_{AB} = 13.7$ Hz, 1H), 4.35 (d, $^2J_{AB} = 13.6$ Hz, 1H),

7.33-7.39 (m, 5H), 7.55 (d, $^3J = 7.9$ Hz, NH), 12.71 (s, COOH); ^{13}C -NMR (DMSO- d_6): δ 18.67 (CH₃), 51.30 (CH), 58.55 (CH₂), 128.01, 128.26 (CH_{arom.}), 130.40 (C), 130.91 (CH_{arom.}), 174.20 (COOH).

(2S)-3-Methyl-2-[(phenylsulfonyl)amino]butyric Acid (8e)

The compound was prepared starting from *L*-valine as described for compound **8a**. Yield: 1.75 g (68%); colorless needles; mp: 149°C; $R_f = 0.56$ (eluent: chloroform/acetone/glacial acetic acid 9 : 1 : 0.3); ^1H -NMR (DMSO- d_6): δ 0.77 (d, $^3J = 6.7$ Hz, 3H), 0.80 (d, $^3J = 6.7$ Hz, 3H), 1.92 (m, 1H), 3.51 (m, 1H), 7.52-7.60 (m, 3H), 7.77 (d, $^3J = 7.5$ Hz, 2H), 8.02 (d, $^3J = 9.2$ Hz, NH), 12.58 (s, COOH); ^{13}C -NMR (DMSO- d_6): δ 17.85 (CH₃), 19.03 (CH₃), 30.41 (CH), 61.26 (CH), 126.52, 128.90, 132.27 (CH_{arom.}), 141.19 (C), 172.21 (COOH).

(2R)-3-Methyl-2-[(phenylsulfonyl)amino]butyric Acid (8f)

This compound was prepared starting from *D*-valine as described for compound **8a**. Yield: 1.73 g (67%); colorless needles; mp: 148-149°C; $R_f = 0.56$ (eluent: chloroform/acetone/glacial acetic acid 9 : 1 : 0.3); ^1H -NMR (DMSO- d_6): δ 0.77 (d, $^3J = 6.7$ Hz, 3H), 0.80 (d, $^3J = 6.7$ Hz, 3H), 1.92 (m, 1H), 3.51 (m, 1H), 7.52-7.60 (m, 3H), 7.77 (d, $^3J = 7.5$ Hz, 2H), 8.02 (d, $^3J = 9.2$ Hz, NH), 12.58 (s, COOH).

2-Methyl-*N*-(phenylsulfonyl)alanine (8g)

The title compound was prepared starting from 2-aminoisobutyric acid as described for compound **8a**. Yield: 1.84 g (76%); colorless crystals; mp: 146-147°C; $R_f = 0.53$ (eluent: chloroform/acetone/glacial acetic acid 9 : 1 : 0.3); ^1H -NMR (DMSO- d_6): δ 1.25 (s, 6H), 7.52-7.59 (m, 3H), 7.79-7.83 (m, 2H), 7.99 (s, NH), 12.55 (s, COOH); ^{13}C -NMR (DMSO- d_6): δ 25.76 (CH₃), 57.77 (C), 126.13, 128.92, 131.99 (CH_{arom.}), 143.73 (C), 175.32 (COOH).

6.2.4 Substituted 6*H*-1,3,4-Thiadiazine Amides

General Procedure for Preparing Substituted 6*H*-1,3,4-Thiadiazine Amides

(4*S*)-2,6-Dioxo-*N*-(5-phenyl-6*H*-1,3,4-thiadiazin-2-yl)hexahydro-4-pyrimidinecarboxamide (**11**)

To a suspension of 2-amino-5-phenyl-6*H*-1,3,4-thiadiazine hydrochloride (**6a**) (314 mg, 1.38 mmol), (*S*)-2,6-dioxohexahydropyrimidine-4-carboxylic acid (221 mg, 1.40 mmol), and 1-hydroxybenzotriazole (190 mg, 1.40 mmol) in 5 mL of DMF at 0°C was added 4-methylmorpholine (190 μ L, 1.72 mmol) followed by the addition of *N*-ethyl-*N'*-(3-dimethyl-aminopropyl)-carbodiimide hydrochloride (275 mg, 1.43 mmol). After 48 h at 5°C, the mixture was diluted with 20 mL of 0.1 M hydrochloric acid and stirred for 30 min at room temperature. The precipitate was filtered and washed successively with water, ice-cold methanol and diethylether. After drying in vacuo the solid was recrystallized from methanol to yield 225 mg (49%) of the title compound as colorless crystals; mp: 198°C (dec.); HPLC (t_R : 11.30); $^1\text{H-NMR}$ (DMSO- d_6): δ 2.61 (m, 1H), 2.93 (m, 1H), 3.80 (s, 2H), 4.18 (m, 1H), 7.48-7.50 (m, 3H), 7.63 (s, 1H), 7.88-7.90 (m, 2H), 10.07 (s, 1H), 12.45 (br s, 1H); $^{13}\text{C-NMR}$ (DMSO- d_6): δ 21.63, 33.27 (CH₂), 51.64 (CH), 126.95, 128.87, 130.61 (CH_{arom.}), 133.97, 148.58, 153.63, 163.32 (C), one (C) and (C=O) were not detected. DCI MS: m/z 332 [M + H]⁺; MALDI-TOF-MS: m/z calculated for [M + H]⁺: 332.1, found: 332.2; calculated for [M + Na]⁺: 354.1, found: 354.2, calculated for [M + K]⁺: 370.0, found: 370.1. Analysis calculated for C₁₄H₁₃N₅O₃S: C, 50.75%; H, 3.95%; N, 21.14%. Found: C, 50.55%; H, 3.79%; N, 20.96%.

The following compounds were prepared according to the general procedure as described for the preparation of compound **11** starting from compounds **6a-k** (1.38 mmol) by coupling with compounds **8a-g** (1.40 mmol).

(2S)-N-[5-(4-Fluorophenyl)-6H-1,3,4-thiadiazine-2-yl]-2-[(phenylsulfonyl)amino]propanamide (12a)

Yield: 229 mg (40%); colorless needles from methanol/acetonitrile (5 : 1); mp: 166-167°C; HPLC (t_R : 13.18); $^1\text{H-NMR}$ (DMSO- d_6): δ 1.15 (d, $^3J = 7.1$ Hz, 3H), 3.60 (d, $^2J_{AB} = 14.4$ Hz, 1H), 3.70 (d, $^2J_{AB} = 14.5$ Hz, 1H), 4.02 (m, 1H), 7.30-7.34 (m, 2H), 7.53-7.61 (m, 3H), 7.78-7.79 (m, 2H), 7.94-7.97 (m, 2H), 8.09 (d, $^3J = 8.3$ Hz, 1H), 12.02 (br s, 1H); $^{13}\text{C-NMR}$ (DMSO- d_6): δ 18.91 (CH₃), 21.22 (CH₂), 53.10 (CH), 115.83 (d, $^2J_{CF} = 21.4$ Hz, CH_{arom.}), 126.46, 129.03 (CH_{arom.}), 129.43 (d, $^3J_{CF} = 8.8$ Hz, CH_{arom.}), 130.80 (C), 132.31 (CH_{arom.}), 141.15, 147.44, 162.40, 164.38 (C), one (C=O) was not detected. DCI MS: m/z 421 [M + H]⁺; MALDI-TOF-MS: m/z calculated for [M + H]⁺: 421.1, found: 421.0; calculated for [M + Na]⁺: 443.1, found: 443.0. Analysis calculated for C₁₈H₁₇FN₄O₃S₂: C, 51.42%; H, 4.08%; N, 13.32%. Found: C, 51.11%; H, 4.19%; N, 13.02%.

(2S)-N-[5-(4-Chlorophenyl)-6H-1,3,4-thiadiazine-2-yl]-2-[(phenylsulfonyl)amino]propanamide (12b)

Yield: 294 mg (49%); colorless needles from methanol/acetonitrile (5 : 1); mp: 184-185°C; HPLC (t_R : 13.70); $^1\text{H-NMR}$ (DMSO- d_6): δ 1.15 (d, $^3J = 7.1$ Hz, 3H), 3.60 (d, $^2J_{AB} = 14.6$ Hz, 1H), 3.70 (d, $^2J_{AB} = 14.6$ Hz, 1H), 4.01 (m, 1H), 7.53-7.61 (m, 5H), 7.78-7.80 (m, 2H), 7.92 (d, $^3J = 8.6$ Hz, 2H), 8.09 (d, $^3J = 8.2$ Hz, 1H), 12.05 (br s, 1H); $^{13}\text{C-NMR}$ (DMSO- d_6): δ 18.88 (CH₃), 21.04 (CH₂), 53.07 (CH), 126.46, 128.76, 128.87, 129.02, 132.30 (CH_{arom.}), 133.12, 135.18, 141.12, 147.34 (C), one (C) and (C=O) were not detected. DCI MS: m/z 437 [M + H]⁺; MALDI-TOF-MS: m/z calculated for [M + H]⁺: 437.1, found: 437.1; calculated for [M + Na]⁺: 459.0, found: 459.1. Analysis calculated for C₁₈H₁₇ClN₄O₃S₂: C, 49.48%; H, 3.92%; N, 12.82%. Found: C, 49.20%; H, 3.90%; N, 12.67%.

(2S)-N-[5-(4-Bromophenyl)-6H-1,3,4-thiadiazine-2-yl]-2-[(phenylsulfonyl)amino]propanamide (12c)

Yield: 340 mg (51%); colorless crystals from methanol/acetonitrile (10 : 1); mp: 180-181°C; HPLC (t_R : 13.92); $^1\text{H-NMR}$ (DMSO- d_6): δ 1.15 (d, $^3J = 7.1$ Hz, 3H), 3.60 (d,

$^2J_{AB} = 14.5$ Hz, 1H), 3.70 (d, $^2J_{AB} = 14.6$ Hz, 1H), 4.00 (m, 1H), 7.53-7.61 (m, 3H), 7.69 (d, $^3J = 8.4$ Hz, 2H), 7.78 (d, $^3J = 7.3$ Hz, 2H), 7.84 (d, $^3J = 8.4$ Hz, 2H), 8.09 (d, $^3J = 8.0$ Hz, 1H), 12.01 (br s, 1H); $^{13}\text{C-NMR}$ (DMSO- d_6): δ 18.89 (CH₃), 21.01 (CH₂), 53.07 (CH), 124.05 (C), 126.46, 128.98, 129.03, 131.80, 132.31 (CH_{arom.}), 133.48, 141.11, 147.45 (C), one (C) and (C=O) were not detected. DCI MS: m/z 481 [M + H]⁺; MALDI-TOF-MS: m/z calculated for [M + H]⁺: 481.0, found: 481.0; calculated for [M + Na]⁺: 503.0, found: 503.0; calculated for [M + K]⁺: 519.0, found: 519.0. Analysis calculated for C₁₈H₁₇BrN₄O₃S₂: C, 44.91%; H, 3.56%; N, 11.64%. Found: C, 44.96%; H, 3.53%; N, 11.58%.

(2S)-N-[5-(4-Nitrophenyl)-6H-1,3,4-thiadiazine-2-yl]-2-[(phenylsulfonyl)amino]-propanamide (12d)

Yield: 278 mg (45%); yellow crystals from methanol/acetonitrile (5 : 1); mp: 201-202°C; HPLC (t_R : 13.30); $^1\text{H-NMR}$ (DMSO- d_6): δ 1.15 (d, $^3J = 7.0$ Hz, 3H), 3.68 (d, $^2J_{AB} = 14.6$ Hz, 1H), 3.78 (d, $^2J_{AB} = 14.7$ Hz, 1H), 4.03 (m, 1H), 7.53-7.61 (m, 3H), 7.79 (d, $^3J = 7.4$ Hz, 2H), 8.15 (m, 3H), 8.31 (m, 2H), 12.15 (br s, 1H); $^{13}\text{C-NMR}$ (DMSO- d_6): δ 18.82 (CH₃), 20.99 (CH₂), 53.04 (CH), 123.93, 126.47, 128.19, 129.04, 132.33 (CH_{arom.}), 140.32, 141.09, 146.65, 148.17 (C), one (C) and (C=O) were not detected. DCI MS: m/z 448 [M + H]⁺; MALDI-TOF-MS: m/z calculated for [M + H]⁺: 448.1, found: 448.0; calculated for [M + Na]⁺: 470.1, found: 470.1; calculated for [M + K]⁺: 486.0, found: 486.0. Analysis calculated for C₁₈H₁₇N₅O₅S₂: C, 48.31%; H, 3.83%; N, 15.65%. Found: C, 48.29%; H, 4.04%; N, 15.80%.

(2S)-N-[5-(4-Cyanophenyl)-6H-1,3,4-thiadiazine-2-yl]-2-[(phenylsulfonyl)amino]-propanamide (12e)

Yield: 375 mg (64%); yellow crystals from methanol; mp: 186-187°C; HPLC (t_R : 12.98); $^1\text{H-NMR}$ (DMSO- d_6): δ 1.15 (d, $^3J = 7.1$ Hz, 3H), 3.64 (d, $^2J_{AB} = 14.7$ Hz, 1H), 3.75 (d, $^2J_{AB} = 14.7$ Hz, 1H), 4.02 (m, 1H), 7.53-7.61 (m, 3H), 7.78-7.83 (m, 2H), 7.95 (d, $^3J = 8.4$ Hz, 2H), 8.07 (d, $^3J = 8.3$ Hz, 2H), 8.12 (d, $^3J = 7.6$ Hz, 1H), 12.11 (br s, 1H); $^{13}\text{C-NMR}$ (DMSO- d_6): δ 18.83 (CH₃), 20.89 (CH₂), 53.03 (CH), 112.48, 118.51 (C), 126.46, 127.69, 129.03, 132.32, 132.74 (CH_{arom.}), 138.55, 141.09, 146.96 (C), one (C) and (C=O) were not

detected. DCI MS: m/z 428 $[M + H]^+$; MALDI-TOF-MS: m/z calculated for $[M + H]^+$: 428.1, found: 428.0; calculated for $[M + Na]^+$: 450.1, found: 450.0; calculated for $[M + K]^+$: 466.0, found: 466.0. Analysis calculated for $C_{19}H_{17}N_5O_3S_2$: C, 53.38%; H, 4.01%; N, 16.38%. Found: C, 53.38%; H, 4.08%; N, 16.35%.

(2S)-2-[(Phenylsulfonyl)amino]-N-[5-[4-(trifluoromethyl)phenyl]-6H-1,3,4-thiadiazine-2-yl]propanamide (12f)

Yield: 396 mg (61%); colorless needles from methanol/acetonitrile (5 : 1); mp: 187-188°C; HPLC (t_R : 14.17); 1H -NMR (DMSO- d_6): δ 1.17 (d, $^3J = 7.0$ Hz, 3H), 3.66 (d, $^2J_{AB} = 14.7$ Hz, 1H), 3.76 (d, $^2J_{AB} = 14.6$ Hz, 1H), 4.03 (m, 1H), 7.54-7.61 (m, 3H), 7.79 (d, $^3J = 7.4$ Hz, 2H), 7.84 (d, $^3J = 8.2$ Hz, 2H), 8.10-8.12 (m, 3H), 12.10 (br s, 1H); ^{13}C -NMR (DMSO- d_6): δ 18.85 (CH₃), 21.07 (CH₂), 53.07 (CH), 122.14 (C), 124.03 (q, $^1J_{CF} = 272.3$ Hz, CF₃), 125.11, 125.69, 127.76, 129.03 (CH_{arom.}), 130.14 (q, $^2J_{CF} = 31.9$ Hz, C-CF₃), 132.32 (CH_{arom.}), 138.55, 141.09, 146.96 (C), one (C=O) was not detected. DCI MS: m/z 471 $[M + H]^+$; MALDI-TOF-MS: m/z calculated for $[M + H]^+$: 471.1, found: 471.1; calculated for $[M + Na]^+$: 493.1, found: 493.1. Analysis calculated for $C_{19}H_{17}F_3N_4O_3S_2$: C, 48.50%; H, 3.64%; N, 11.91%. Found: C, 48.62%; H, 3.33%; N, 12.00%.

(2S)-N-[5-(4-Methoxyphenyl)-6H-1,3,4-thiadiazine-2-yl]-2-[(phenylsulfonyl)amino]propanamide (12g)

Yield: 345 mg (58%); colorless plates from methanol/acetonitrile (5 : 1); mp: 192-193°C; HPLC (t_R : 12.95); 1H -NMR (DMSO- d_6): δ 1.15 (d, $^3J = 7.0$ Hz, 3H), 3.57 (d, $^2J_{AB} = 14.5$ Hz, 1H), 3.67 (d, $^2J_{AB} = 14.5$ Hz, 1H), 3.80 (s, 3H), 3.99 (m, 1H), 7.03 (d, $^3J = 8.6$ Hz, 2H), 7.53-7.61 (m, 3H), 7.79 (d, $^3J = 7.4$ Hz, 2H), 7.86 (d, $^3J = 8.6$ Hz, 2H), 8.06 (d, $^3J = 7.3$ Hz, 1H), 11.99 (br s, 1H); ^{13}C -NMR (DMSO- d_6): δ 18.98 (CH₃), 21.22 (CH₂), 53.22 (CH), 55.38 (CH₃), 114.22, 126.47, 128.69, 129.02 (CH_{arom.}), 129.70 (C), 132.30 (CH_{arom.}), 141.15, 148.03, 161.11 (C), one (C) and (C=O) were not detected. DCI MS: m/z 433 $[M + H]^+$; MALDI-TOF-MS: m/z calculated for $[M + H]^+$: 433.1, found: 433.2; calculated for $[M + Na]^+$: 455.1, found: 455.2. Analysis calculated for $C_{19}H_{20}N_4O_4S_2$: C, 52.76%; H, 4.66%; N, 12.95%. Found: C, 52.67%; H, 4.53%; N, 13.00%.

(2S)-N-[5-(4-Methylphenyl)-6H-1,3,4-thiadiazine-2-yl]-2-[(phenylsulfonyl)amino]propanamide (12h)

Yield: 314 mg (55%); colorless needles from methanol; mp: 186-187°C; HPLC (t_R : 13.44); $^1\text{H-NMR}$ (DMSO- d_6): δ 1.15 (d, $^3J = 7.0$ Hz, 3H), 2.34 (s, 3H), 3.58 (d, $^2J_{AB} = 14.5$ Hz, 1H), 3.68 (d, $^2J_{AB} = 14.5$ Hz, 1H), 4.00 (m, 1H), 7.29 (d, $^3J = 7.9$ Hz, 2H), 7.53-7.61 (m, 3H), 7.78-7.80 (m, 4H), 8.06 (d, $^3J = 7.9$ Hz, 1H), 12.02 (br s, 1H). DCI MS: m/z 417 $[\text{M} + \text{H}]^+$. Analysis calculated for $\text{C}_{19}\text{H}_{20}\text{N}_4\text{O}_3\text{S}_2$: C, 54.79%; H, 4.84%; N, 13.45%. Found: C, 54.78%; H, 4.86%; N, 13.42%.

(2S)-N-[5-(1-Adamantyl)-6H-1,3,4-thiadiazin-2-yl]-2-[(phenylsulfonyl)amino]propanamide (13a)

Yield: 420 mg (66%); colorless prisms from methanol/acetonitrile (5 : 1); mp: 183-184°C; HPLC (t_R : 14.70); $^1\text{H-NMR}$ (DMSO- d_6): δ 1.11 (d, $^3J = 7.1$ Hz, 3H), 1.64-1.70 (m, 6H), 1.77 (s, 6H), 1.99 (s, 3H), 3.14 (d, $^2J_{AB} = 14.5$ Hz, 1H), 3.18 (d, $^2J_{AB} = 14.9$ Hz, 1H), 3.91 (m, 1H), 7.51-7.59 (m, 3H), 7.77 (d, $^3J = 7.2$ Hz, 2H), 7.95 (d, $^3J = 7.5$ Hz, 1H), 11.89 (br s, 1H); $^{13}\text{C-NMR}$ (DMSO- d_6): δ 18.99 (CH₃), 20.07 (CH₂), 27.32 (CH), 35.95 (CH₂), 38.55 (C), 53.59 (CH), 126.38, 128.91, 132.14 (CH_{arom.}), 141.19, 159.80 (C), one (C) and (C=O) were not detected. DCI MS: m/z 461 $[\text{M} + \text{H}]^+$; MALDI-TOF-MS: m/z calculated for $[\text{M} + \text{H}]^+$: 461.2, found: 461.0; calculated for $[\text{M} + \text{Na}]^+$: 483.2, found: 483.1. Analysis calculated for $\text{C}_{22}\text{H}_{28}\text{N}_4\text{O}_3\text{S}_2$: C, 57.37%; H, 6.13%; N, 12.16%. Found: C, 57.19%; H, 6.24%; N, 11.92%.

(2S)-N-[5-(5-Chloro-2-thienyl)-6H-1,3,4-thiadiazin-2-yl]-2-[(phenylsulfonyl)amino]propanamide (13b)

Yield: 216 mg (35%); colorless needles from methanol/acetonitrile (5 : 1); mp: 198-199°C; HPLC (t_R : 13.67); $^1\text{H-NMR}$ (DMSO- d_6): δ 1.13 (d, $^3J = 6.9$ Hz, 3H), 3.56 (d, $^2J_{AB} = 16.1$ Hz, 1H), 3.65 (d, $^2J_{AB} = 16.0$ Hz, 1H), 4.03 (m, 1H), 7.22 (d, $^3J = 3.7$ Hz, 1H), 7.53-7.61 (m, 4H), 7.77-7.79 (m, 2H), 8.13 (d, $^3J = 7.5$ Hz, 1H), 11.85 (br s, 1H); $^{13}\text{C-NMR}$ (DMSO- d_6): δ 18.80 (CH₃), 20.27 (CH₂), 52.54 (CH), 127.30, 127.97, 129.04, 129.83, 132.35 (CH_{arom.}), 132.49, 138.18, 141.03, 143.49 (C), one (C) and (C=O) were not detected. DCI MS: m/z 443 $[\text{M} + \text{H}]^+$; MALDI-TOF-MS: m/z calculated for $[\text{M} + \text{H}]^+$:

443.0, found: 443.0; calculated for $[M + Na]^+$: 465.0, found: 465.0. Analysis calculated for $C_{16}H_{15}ClN_4O_3S_3$: C, 43.38%; H, 3.41%; N, 12.65%. Found: C, 43.18%; H, 3.04%; N, 12.46%.

(2S)-2-[(Benzylsulfonyl)amino]-N-[5-(4-chlorophenyl)-6H-1,3,4-thiadiazin-2-yl]-propanamide (14a)

Yield: 288 mg (46%); colorless needles from methanol/acetonitrile (5 : 1); mp: 169-170°C; HPLC (t_R : 14.03); 1H -NMR (DMSO- d_6): δ 1.26 (d, $^3J = 7.1$ Hz, 3H), 3.68 (d, $^2J_{AB} = 14.1$ Hz, 1H), 3.81 (d, $^2J_{AB} = 14.5$ Hz, 1H), 4.00 (m, 1H), 4.32 (d, $^2J_{AB} = 14.0$ Hz, 1H), 4.35 (d, $^2J_{AB} = 14.0$ Hz, 1H), 7.33-7.39 (m, 5H), 7.50 (d, $^3J = 6.2$ Hz, 1H), 7.56 (d, $^3J = 8.5$ Hz, 2H), 7.93 (d, $^3J = 8.4$ Hz, 2H), 12.12 (br s, 1H); ^{13}C -NMR (DMSO- d_6): δ 19.18 (CH₃), 21.19 (CH₂), 53.12 (CH), 58.64 (CH₂), 127.98, 128.24, 128.74, 128.90 (CH_{arom.}), 130.32 (C), 130.86 (CH_{arom.}), 133.10, 135.20, 147.41 (C), one (C) and (C=O) were not detected. DCI MS: m/z 451 $[M + H]^+$; MALDI-TOF-MS: m/z calculated for $[M + H]^+$: 451.1, found: 451.3; calculated for $[M + Na]^+$: 473.1, found: 473.3; calculated for $[M + K]^+$: 489.0, found: 489.3. Analysis calculated for $C_{19}H_{19}ClN_4O_3S_2$: C, 50.60%; H, 4.25%; N, 12.42%. Found: C, 50.67%; H, 3.90%; N, 12.49%.

(2S)-N-[5-(4-Chlorophenyl)-6H-1,3,4-thiadiazine-2-yl]-2-[(2-thienylsulfonyl)amino]-propanamide (14b)

Yield: 301 mg (49%); colorless plates from methanol/acetonitrile (5 : 1); mp: 175-176°C; HPLC (t_R : 13.62); 1H -NMR (DMSO- d_6): δ 1.19 (d, $^3J = 7.1$ Hz, 3H), 3.61 (d, $^2J_{AB} = 14.5$ Hz, 1H), 3.76 (d, $^2J_{AB} = 14.6$ Hz, 1H), 4.08 (m, 1H), 7.14 (m, 1H), 7.55-7.56 (m, 3H), 7.89 (d, $^3J = 4.9$ Hz, 1H), 7.90 (d, $^3J = 8.5$ Hz, 2H), 8.30 (d, $^3J = 6.9$ Hz, 1H), 12.07 (br s, 1H); ^{13}C -NMR (DMSO- d_6): δ 18.81 (CH₃), 21.11 (CH₂), 53.12 (CH), 127.54, 128.75, 128.88, 131.62, 132.51 (CH_{arom.}), 133.11, 135.18, 142.02, 147.37 (C), one (C) and (C=O) were not detected. DCI MS: m/z 443 $[M + H]^+$; MALDI-TOF-MS: m/z calculated for $[M + H]^+$: 443.0, found: 443.0; calculated for $[M + Na]^+$: 465.0, found: 465.0. Analysis calculated for $C_{16}H_{15}ClN_4O_3S_3 \cdot 0.25 CH_3OH$: C, 43.40%; H, 3.57%; N, 12.40%. Found: C, 43.40%; H, 3.62%; N, 12.55%.

(2R)-N-[5-(4-Fluorophenyl)-6H-1,3,4-thiadiazine-2-yl]-2-[(phenylsulfonyl)amino]-propanamide (15a)

Yield: 225 mg (39%); colorless needles from methanol/acetonitrile (5 : 1); mp: 167-168°C; HPLC (t_R : 13.17); $^1\text{H-NMR}$ (DMSO- d_6): δ 1.15 (d, $^3J = 7.1$ Hz, 3H), 3.60 (d, $^2J_{AB} = 14.4$ Hz, 1H), 3.70 (d, $^2J_{AB} = 14.5$ Hz, 1H), 4.02 (m, 1H), 7.30-7.34 (m, 2H), 7.53-7.61 (m, 3H), 7.78-7.79 (m, 2H), 7.94-7.97 (m, 2H), 8.09 (d, $^3J = 8.3$ Hz, 1H), 12.02 (br s, 1H). DCI MS: m/z 421 $[\text{M} + \text{H}]^+$. Analysis calculated for $\text{C}_{18}\text{H}_{17}\text{FN}_4\text{O}_3\text{S}_2$: C, 51.42%; H, 4.08%; N, 13.32%. Found: C, 51.27%; H, 4.25%; N, 13.22%.

(2R)-N-[5-(4-Chlorophenyl)-6H-1,3,4-thiadiazine-2-yl]-2-[(phenylsulfonyl)amino]-propanamide (15b)

Yield: 308 mg (51%); colorless needles from methanol/acetonitrile (5 : 1); mp: 183-184°C; HPLC (t_R : 13.18); $^1\text{H-NMR}$ (DMSO- d_6): δ 1.15 (d, $^3J = 7.1$ Hz, 3H), 3.60 (d, $^2J_{AB} = 14.6$ Hz, 1H), 3.70 (d, $^2J_{AB} = 14.6$ Hz, 1H), 4.01 (m, 1H), 7.53-7.61 (m, 5H), 7.78-7.80 (m, 2H), 7.92 (d, $^3J = 8.6$ Hz, 2H), 8.09 (d, $^3J = 8.2$ Hz, 1H), 12.04 (br s, 1H). DCI MS: m/z 437 $[\text{M} + \text{H}]^+$. Analysis calculated for $\text{C}_{18}\text{H}_{17}\text{ClN}_4\text{O}_3\text{S}_2$: C, 49.48%; H, 3.92%; N, 12.82%. Found: C, 49.22%; H, 3.53%; N, 12.86%.

(2R)-N-[5-(4-Bromophenyl)-6H-1,3,4-thiadiazine-2-yl]-2-[(phenylsulfonyl)amino]-propanamide (15c)

Yield: 365 mg (55%); colorless crystals from methanol/acetonitrile (10 : 1); mp: 179-180°C; HPLC (t_R : 13.90); $^1\text{H-NMR}$ (DMSO- d_6): δ 1.15 (d, $^3J = 7.1$ Hz, 3H), 3.60 (d, $^2J_{AB} = 14.5$ Hz, 1H), 3.70 (d, $^2J_{AB} = 14.6$ Hz, 1H), 4.00 (m, 1H), 7.53-7.61 (m, 3H), 7.69 (d, $^3J = 8.4$ Hz, 2H), 7.78 (d, $^3J = 7.3$ Hz, 2H), 7.84 (d, $^3J = 8.4$ Hz, 2H), 8.10 (d, $^3J = 8.0$ Hz, 1H), 12.05 (br s, 1H). DCI MS: m/z 481 $[\text{M} + \text{H}]^+$. Analysis calculated for $\text{C}_{18}\text{H}_{17}\text{BrN}_4\text{O}_3\text{S}_2$: C, 44.91%; H, 3.56%; N, 11.64%. Found: C, 45.24%; H, 3.62%; N, 11.40%.

(2R)-N-[5-(4-Cyanophenyl)-6H-1,3,4-thiadiazine-2-yl]-2-[(phenylsulfonyl)amino]-propanamide (15d)

Yield: 386 mg (65%); yellow crystals from methanol; mp: 185-186°C; HPLC (t_R : 13.02); $^1\text{H-NMR}$ (DMSO- d_6): δ 1.15 (d, $^3J = 7.1$ Hz, 3H), 3.64 (d, $^2J_{AB} = 14.7$ Hz, 1H), 3.75 (d, $^2J_{AB} = 14.7$ Hz, 1H), 4.02 (m, 1H), 7.53-7.61 (m, 3H), 7.78-7.83 (m, 2H), 7.95 (d, $^3J = 8.4$ Hz, 2H), 8.07 (d, $^3J = 8.3$ Hz, 2H), 8.12 (d, $^3J = 7.6$ Hz, 1H), 12.11 (br s, 1H). DCI MS: m/z 428 $[\text{M} + \text{H}]^+$. Analysis calculated for $\text{C}_{19}\text{H}_{17}\text{N}_5\text{O}_3\text{S}_2$: C, 53.38%; H, 4.01%; N, 16.38%. Found: C, 53.42%; H, 4.05%; N, 16.41%.

(2R)-N-[5-(4-Methylphenyl)-6H-1,3,4-thiadiazine-2-yl]-2-[(phenylsulfonyl)amino]-propanamide (15e)

Yield: 308 mg (54%); colorless needles from methanol; mp: 183-184°C; HPLC (t_R : 13.42); $^1\text{H-NMR}$ (DMSO- d_6): δ 1.15 (d, $^3J = 7.0$ Hz, 3H), 2.34 (s, 3H), 3.58 (d, $^2J_{AB} = 14.5$ Hz, 1H), 3.68 (d, $^2J_{AB} = 14.5$ Hz, 1H), 4.00 (m, 1H), 7.29 (d, $^3J = 7.9$ Hz, 2H), 7.53-7.61 (m, 3H), 7.78-7.80 (m, 4H), 8.06 (d, $^3J = 7.9$ Hz, 1H), 12.02 (br s, 1H); $^{13}\text{C-NMR}$ (DMSO- d_6): δ 18.94 (CH_3), 20.94 (CH_3), 21.23 (CH_2), 53.22 (CH), 126.46, 126.94, 129.01, 129.40 ($\text{CH}_{\text{arom.}}$), 131.41 (C), 132.29 ($\text{CH}_{\text{arom.}}$), 140.37, 141.15, 148.30 (C), one (C) and (C=O) were not detected. DCI MS: m/z 417 $[\text{M} + \text{H}]^+$; MALDI-TOF-MS: m/z calculated for $[\text{M} + \text{H}]^+$: 417.1, found: 417.1; calculated for $[\text{M} + \text{Na}]^+$: 439.1, found: 439.1; calculated for $[\text{M} + \text{K}]^+$: 455.1, found: 455.1. Analysis calculated for $\text{C}_{19}\text{H}_{20}\text{N}_4\text{O}_3\text{S}_2$: C, 54.79%; H, 4.84%; N, 13.45%. Found: C, 54.77%; H, 4.88%; N, 13.43%.

(2S)-N-[5-(4-Chlorophenyl)-6H-1,3,4-thiadiazine-2-yl]-3-methyl-2-[(phenylsulfonyl)amino]butanamide (15f)

Yield: 324 mg (51%); colorless needles from methanol/acetonitrile (5 : 1); mp: 201-202°C; HPLC (t_R : 14.42); $^1\text{H-NMR}$ (DMSO- d_6): 0.77 (d, $^3J = 6.8$ Hz, 3H), 0.80 (d, $^3J = 6.7$ Hz, 3H), 1.93 (m, 1H), 3.54 (d, $^2J_{AB} = 14.5$ Hz, 1H), 3.64 (d, $^2J_{AB} = 14.6$ Hz, 1H), 3.76 (m, 1H), 7.49-7.57 (m, 5H), 7.76 (d, $^3J = 7.2$ Hz, 2H), 7.91-7.93 (m, 3H), 11.95 (br s, 1H); $^{13}\text{C-NMR}$ (DMSO- d_6): 17.95 (CH_3), 19.11 (CH_3), 21.00 (CH_2), 30.90 (CH), 50.66 (CH), 126.55, 128.82, 132.18 ($\text{CH}_{\text{arom.}}$), 133.18, 135.15, 140.99, 147.31 (C), one (C)

and (C=O) were not detected. DCI MS: m/z 465 $[M + H]^+$; MALDI-TOF-MS: m/z calculated for $[M + H]^+$: 465.1, found: 465.0; calculated for $[M + Na]^+$: 487.1, found: 487.0. Analysis calculated for $C_{20}H_{21}ClN_4O_3S_2$: C, 51.66%; H, 4.55%; N, 12.05%. Found: C, 51.70%; H, 4.34%; N, 12.03%.

(2R)-N-[5-(4-Chlorophenyl)-6H-1,3,4-thiadiazine-2-yl]-3-methyl-2-[(phenylsulfonyl)-amino]butanamide (15g)

Yield: 359 mg (56%); colorless needles from methanol/acetonitrile (5 : 1); mp: 189-190°C; HPLC (t_R : 14.45); 1H -NMR (DMSO- d_6): 0.77 (d, $^3J = 6.8$ Hz, 3H), 0.80 (d, $^3J = 6.7$ Hz, 3H), 1.93 (m, 1H), 3.54 (d, $^2J_{AB} = 14.5$ Hz, 1H), 3.64 (d, $^2J_{AB} = 14.6$ Hz, 1H), 3.76 (m, 1H), 7.49-7.57 (m, 5H), 7.76 (d, $^3J = 7.2$ Hz, 2H), 7.91-7.93 (m, 3H), 11.95 (br s, 1H). DCI MS: m/z 465 $[M + H]^+$. Analysis calculated for $C_{20}H_{21}ClN_4O_3S_2$: C, 51.66%; H, 4.55%; N, 12.05%. Found: C, 51.75%; H, 4.53%; N, 12.07%.

N-[5-(4-Chlorophenyl)-6H-1,3,4-thiadiazine-2-yl]-2-methyl-2-[(phenylsulfonyl)-amino]propanamide (15h)

Yield: 239 mg (38%); colorless needles from methanol/acetonitrile (5 : 1); mp: 204-205°C; HPLC (t_R : 14.17); 1H -NMR (DMSO- d_6): 1.31 (s, 3H), 1.78 (s, 3H), 3.57 (m, 1H), 3.75 (m, 1H), 7.42 (m, 1H), 7.54-7.57 (m, 3H), 7.67 (m, 1H), 7.74 (m, 1H), 7.82 (m, 1H), 7.90 (m, 1H), 8.05-8.10 (m, 2H), 12.11 (br s, 1H); ^{13}C -NMR (DMSO- d_6): 21.63 (CH₂), 24.13 (CH₃), 66.85 (C), 126.30, 127.77, 128.15, 128.88, 129.04, 129.36 (CH_{arom.}), 133.82 (C), 134.01 (CH_{arom.}), 134.52, 135.16, 139.09, 149.85, 160.63, 173.79 (C). DCI MS: m/z 451 $[M + H]^+$; MALDI-TOF-MS: m/z calculated for $[M + H]^+$: 451.1, found: 451.7; calculated for $[M + Na]^+$: 473.1, found: 473.7. Analysis calculated for $C_{19}H_{19}ClN_4O_3S_2$: C, 50.60%; H, 4.25%; N, 12.42%. Found: C, 50.69%; H, 4.33%; N, 12.31%.

6.3 Enzyme Preparations

MMP-1 from human rheumatoid synovial fibroblasts was purchased from Calbiochem-Novabiochem Corporation, La Jolla.

Preparation of the recombinant catalytic domain of human gelatinase A (cdMMP-2): The catalytic domain of pro-gelatinase A was prepared using an *E. coli* expression system.⁹³ The proenzyme was activated with 0.5 mM APMA at 37°C prior to use in the assay.

Preparation of the recombinant catalytic domain of human neutrophil collagenase (cdMMP-8): The enzyme was expressed in *E. coli* as an active variant.⁹⁴

Preparation of PMNL-gelatinase (MMP-9): Latent PMNL-pro-gelatinase was prepared from human plasma buffy coat as described by Tschesche *et al.*⁹⁵ PMNL-pro-gelatinase was activated prior to use by incubation with trypsin at 37°C for 10 min. Inactivation of trypsin was accomplished with TKI.

Preparation of the recombinant catalytic domain of human macrophage elastase (cdMMP-12): The catalytic domain of MMP-12 was expressed in *E. coli*. The over-expressed protein was isolated as inclusion bodies, and the renatured protein was purified by affinity column chromatography with an immobilized hydroxamate inhibitor.⁹⁶

Preparation of the recombinant catalytic domain of human collagenase-3 (cdMMP-13): Human pro-cdMMP-13 was prepared using an *E. coli* expression system.⁹⁷ The isolated pro-cdMMP-13 was activated prior to use by incubation with 5 mM HgCl₂ for 2 h at 37°C.

Preparation of the recombinant catalytic domain of membrane-type-1 MMP (cdMMP-14): The catalytic domain of MMP-14 was expressed in *E. coli* and was activated by autocatalysis.⁹⁸

Preparation of the recombinant human ectodomain of membrane-type-1 MMP (MMP-14): The ectodomain of MMP-14 was expressed in *Pichia Pastoris* by the method of Roderfeld *et al.* and activated by yeast proteinases (furin-like proteinases) during maturation.⁹⁹

6.4 Crystallography

6.4.1 Crystallization of the Inhibitors and Structure Analysis

Crystals of (2*S*)-*N*-[5-(4-chlorophenyl)-6*H*-1,3,4-thiadiazin-2-yl]-2-[(phenylsulfonyl)amino]propanamide **12b**, (2*S*)-*N*-[5-(5-chloro-2-thienyl)-6*H*-1,3,4-thiadiazin-2-yl]-2-[(phenylsulfonyl)amino]propanamide **13b**, (2*S*)-*N*-[5-(4-chlorophenyl)-6*H*-1,3,4-thiadiazin-2-yl]-2-[(2-thienylsulfonyl)amino]propanamide **14b**, and (2*R*)-*N*-[5-(4-fluorophenyl)-6*H*-1,3,4-thiadiazin-2-yl]-2-[(phenylsulfonyl)amino]propanamide **15a** suitable for diffraction analysis were obtained by slow crystallization in a Dewar environment from solutions in methanol/acetonitrile (5 : 1).

All H atoms on N atoms in **12b**, **14b** and **15a** were refined isotropically. Other H atoms in **12b**, **14b** and **15a**, and all H atoms in **13b**, were included in calculated positions using a riding model, with $U(\text{H}) = 1.2U_{eq}(\text{C})$ for CH₂ and CH groups, and $U(\text{H}) = 1.5U_{eq}(\text{C})$ for CH₃ groups, and C–H distances in the range 0.95–1.00 Å. The torsion angles of the CH₃ groups were refined.

Data were collected under cryogenic conditions (100K) on the Siemens P2(1) diffractometer (graphite monochromator, Mo–K_α radiation, $\lambda = 0.71073$ Å) with the exception of compound **14b**, which was examined on the Nonius Kappa CCD station (see below). For all other compounds, data collection: *P3/VMS*¹⁰⁰. Cell refinement: *P3/VMS*. Data reduction: *SHELXTL-Plus*¹⁰¹. Program used to solve the structures: *SHELXS-97*¹⁰². Program used to refine the structures: *SHELXL-97*¹⁰³. Program for molecular graphics: *ORTEP-III*¹⁰⁴.

Crystals of *N*-allyl-5-(4-chlorophenyl)-6*H*-1,3,4-thiadiazin-2-amine hydrobromide **16** suitable for diffraction analysis were obtained by slow crystallization in a Dewar environment from an ethanol/ethylacetate (1 : 3) solution.

All H atoms in **16**, were included in calculated positions using a riding model, with $U(\text{H}) = 1.2U_{eq}(\text{C})$ for CH_2 and CH groups, and C–H distances in the range 0.95–1.00 Å. The H atoms on endocyclic N atoms were calculated as half occupied.

Diffraction data were collected under cryogenic conditions (100K) on the Nonius Kappa CCD station. All calculations were performed using *maXus*.¹⁰⁵ Data reduction: *Denzo and Scalepak*.¹⁰⁶ Program used to solve the structure: *SHELXS-97*. Program used to refine the structure: *SHELXL-97*. Program for molecular graphic: *ORTEP-III*. Ring puckering parameters were calculated using the program *PLATON*.¹⁰⁷

6.4.2 Crystallization of the cdMMP-8/Inhibitor Complex and Structure Analysis

The catalytic domain of human neutrophil collagenase (cdMMP-8) was concentrated to 8 mg/mL and then mixed with 3-fold molar excess of an aqueous solution of *N*-allyl-5-(4-chlorophenyl)-6*H*-1,3,4-thiadiazin-2-amine hydrobromide for a final cdMMP-8 concentration of 6 mg/mL. Three microliter of protein/inhibitor complex were mixed with 2 μL precipitant solution containing 100 mM cacodylate pH 5.5–6.5, 10 mM CaCl_2 , 100 mM NaCl, and 10% PEG 6000. The hanging drop was equilibrated by vapor diffusion at 22°C against a reservoir containing 1.0–1.5 M phosphate buffer. The obtained crystals belong to the orthorhombic space group $\text{P2}_1\text{2}_1\text{2}_1$, and exhibit lattice constants $a = 33.67$ Å, $b = 69.64$ Å, $c = 73.40$ Å, $\alpha = \beta = \gamma = 90^\circ$. The asymmetric unit contains one monomer.

X-ray data were collected on an imaging plate detector (MAR Research, Hamburg) to 2.7 Å resolution and processed using CCP4 data reduction software yielding an agreement of redundant measurements of $R_{\text{merge}} = 9.3\%$ over all data and 41% in the outer resolution shell (completeness 98% and 87%, respectively). The orientation and translation of the molecule within the crystallographic unit cell was determined with Patterson search techniques¹⁰⁸⁻¹¹⁰ using the program *AMoRe*.¹¹¹ Electron density calculation and model building proceeded using the program *MAIN*.¹¹² The structure was refined using the program *X-PLOR* to a crystallographic R-value of 21.1% ($R_{\text{free}} = 29.6\%$) with bond deviations of 1.7° from ideally.¹¹³

Ring puckering parameters of the complexed inhibitor were calculated using the program PLATON. Atomic coordinates of the complex have been deposited in the Protein Data Bank under accession code 1JH1.

6.5 Computational Docking and Modeling

The following steps preprocessed the ligand for docking experiments. First, the coordinates of the reference compound **16** were extracted from the PDB file and transformed into SYBYL mol2 file format. The res file format of the crystallographic data of compound **14b** were transformed to SYBYL mol2 file format using BABEL.¹¹⁴ The two structures were loaded into the visualisation tool InsightII and modified by combining the *N*-sulfonylated amino acid moiety from the X-ray structure of **14b** with the 5-(4-chlorophenyl)-6H-1,3,4-thiadiazine-2-amine moiety from the PDB file. The "new" inhibitor structure of **14b** now provided reference coordinates to cdMMP-8. Correct atom types including hybridization states (mol2 notation)¹¹⁵ as well as correct bond types were defined. Hydrogen atoms were added to all atoms with reasonable geometries and formal charges were assigned. The ligand was centered and an energy minimization was performed using the command "Optimize".

For the receptor (cdMMP-8), a so-called receptor description file (rdf) was edited. The file contains information on chains, substructures and hetero atoms to consider, on how to resolve ambiguities in the PDB file (alternate location indicators), on how to add hydrogens to polar atoms in the active site of cdMMP-8, etc. A template that contains physico-chemical information about the amino acids was assigned to each amino acid of cdMMP-8. All assignments were made according to default rules.

The docking package FlexX (GMD-SCAI, Germany) was used under standard conditions (autodock mode) in combination with the molecule visualization program InsightII version 98' (MSI, Germany).

6.6 *In vitro* Assays

6.6.1 MMP Inhibition Assay

Enzymatic activity was measured using a modified version of a resonance energy transfer fluorogenic assay.¹¹⁶ Progress curves were monitored by following the increase in fluorescence at 393 nm ($\lambda_{\text{ex}} = 328$ nm), induced by the cleavage of the (7-methoxycoumarin-4-yl)acetyl-Pro-Leu-Gly-Leu-(3-[2,4-dinitro-phenyl]-L-2,3-diaminopropionyl)-Ala-Arg-NH₂ (Mca-Pro-Leu-Gly-Leu-Dpa-Ala-Arg-NH₂) fluorogenic substrate by MMPs. Enzyme inhibition assays were carried out in MRB which consisted of 50 mM HEPES/NaOH, pH 7.0, 10 mM CaCl₂ and 0.02% (w/v) PEG 8000 at 25°C. MMP microfluorometric profiling assay was done in white U-bottomed 96-well plates (Microfluor 1 White, Dynex, USA) with a final substrate concentration of 6 μ M Mca-peptide, approximately 0.3 to 5 nM MMP with variable inhibitor concentrations and 2% DMSO vehicle. From a 1.5 mM stock (100% DMSO) the inhibitors were serially diluted with MRB to 15, 10, 5, 3, 1, 0.6, 0.3, 0.1, 0.05, 0.01 and 0.005 μ M final assay concentration. Column 1, rows A through H, contained only DMSO for the "enzyme-only" wells in the assay. After preincubation for 30 min at 25°C the reaction was started by addition of substrate, and the plate was read on a SpectraFluor Plus (Tecan, Germany) plate reader with excitation at 330 nm and emission at 405 nm with the gain set to 150. Each measurement was done in triplicate to ensure statistically significant results. The experiment was further controlled for background fluorescence of the substrate, for fluorescence of fully cleaved substrate and for fluorescence quenching or augmentation from solutions containing the test compounds.

6.6.2 Determination of the K_i -Values

Datapoints from eight different MMPs generated on the SpectraFluor Plus were directly visualized on a master Excel spreadsheet. The response of inhibition was determined for each inhibitor concentration by comparing the amount of hydrolysis (fluorescence units generated over 30 minutes of hydrolysis) of wells containing compound with the "enzyme-only" wells in column 1. With the program GraFit (Erithacus Software Limited) a

4 parameter logistic fit to the dose-response data was used to calculate IC_{50} values for each compound.

For each MMP, initial rate measurements in the absence of inhibitor were made for eight different substrate concentrations. From these data, K_m values were determined by non-linear fit using the program GraFit. The K_m values determined for MMP-1, cdMMP-2, cdMMP-8, MMP-9, cdMMP-12, cdMMP-13, cdMMP-14 and the ectodomain of MMP-14 were 40.3, 9.1, 5.9, 1.8, 27.3, 7.5, 6.8, and 7.5 μM . Evaluation of the kinetic data was performed as reported by Copeland *et al.* and Horovitz & Levitzki.^{117,118} Assuming Michaelis-Menten kinetics, the K_i -values were calculated using the equation:

$$K_i = \frac{IC_{50}}{\left(1 + \frac{[S]}{K_m}\right)}$$

7 Literature

- [1] Kuntz, I. D., Meng, E. C., Shoichet, B. K. (1994) Structure-based molecular design. *Acc. Chem. Res.* 27, 117-123.
- [2] Dixon, J. S. (1992) Computer-aided drug design: getting the best results. *Trends Biotech.* 10, 357-363.
- [3] Robertus, J. (1994) Structure-based drug design ten years on. *Nat. Struct. Biol.* 1, 352-354.
- [4] Bains, W. (1996) Using bioinformatics in drug discovery. *Trends Biotech.* 14, 37-39.
- [5] Cherfils, J., Janin, J. (1993) Protein docking algorithms: simulating molecular recognition. *Curr. Opin. Struct. Biol.* 3, 265-269.
- [6] Zask, A., Levin, J. I., Killar, L. M., Skotnicki, J. S. (1996) Inhibition of matrix metalloproteinases: Structure based design. *Curr. Pharm. Des.* 2, 624-661.
- [7] Matthews, B. W. (1988) Structural basis of the action of thermolysin and related zinc peptidases. *Acc. Chem. Res.* 21, 333-340.
- [8] Bode, W., Gomis-Rüth, F. X. Stöcker, W. (1993) Astacins, serralysins, snake venom and matrix metalloproteinases exhibit identical zinc-binding environments (HEXXHXXGXXH and Met-turn) and topologies and should be grouped into a common family, the 'metzincins'. *FEBS Lett.* 331, 134-140.
- [9] Woessner, J. F. Jr. (1991) Matrix metalloproteinases and their inhibitors in connective tissue remodeling. *FASEB J.* 5, 2145-2154.
- [10] Birkedal-Hansen, H., Moore, W. G. I., Bodden, M. K., Windsor, L. J., Birkedal-Hansen, B., DeCarlo, A., Engler, J. A. (1993) Matrix metalloproteinases: a review. *Crit. Rev. Oral Biol. Med.* 4, 197-250.

- [11] Ravanti, L., Kähäri, V. M. (2000) Matrix metalloproteinases in wound repair (Review). *Int. J. Mol. Med.* 6, 391-407.
- [12] Bode, W., Fernandez-Catalan, C., Grams, F., Gomis-Rüth, F. X., Nagase, H., Tschesche, H., Maskos, K. (1999) Insights into MMP-TIMP interactions. *Ann. N.Y. Acad. Sci.* 878, 73-91.
- [13] Murphy, G., Willenbrock, F. (1995) Tissue inhibitors of matrix metalloendopeptidases. *Methods Enzymol.* 248, 496-510.
- [14] Lehti, K., Lohi, J., Valtanen, H., Keski-Oja, J. (1998) Proteolytic processing of membrane-type-1 matrix metalloproteinase is associated with gelatinase A activation at the cell surface. *Biochem. J.* 334, 345-353.
- [15] Murphy, G., Knäuper, V., Cowell, S., Hembry, R., Stanton, H., Butler, G., Freije, J., Pendas, A. M., Lopez-Otin, C. (1999) Evaluation of some newer matrix metalloproteinases. *Ann. N. Y. Acad. Sci.* 878, 25-37.
- [16] Van Wart, H. E., Birkedal-Hansen, H. (1990) The cysteine switch: a principle of regulation of metalloproteinase activity with potential applicability to the entire matrix metalloproteinase gene family. *Proc. Natl. Acad. Sci. USA* 87, 5578-5582.
- [17] Mignatti, P., Rifkin, D. B. (1996) Plasminogen activators and matrix metalloproteinases in angiogenesis. *Enz. Prot.* 49, 117-137.
- [18] Cawston, T. (1996) Metalloproteinase inhibitors and the prevention of connective tissue breakdown. *Pharmacol. Ther.* 70, 163-182.
- [19] Ahrens, D., Koch, A. E., Pope, R. M., Steinpicarella, M., Niedbala, M. J. (1996) Expression of matrix metalloproteinase 9 (96-kd gelatinase B) in human rheumatoid arthritis. *Arthritis Rheum.* 39, 1576-1587.

- [20] Overall, C. M., Wiebkin, O. W., Thonard, J. C. (1987) Demonstration of tissue collagenase activity in vivo and its relationship to inflammation severity in human gingiva. *J. Periodontal Res.* 22, 81-88.
- [21] Yong, V. W. (1999) The potential use of MMP inhibitors to treat CNS diseases. *Exp. Opin. Invest. Drugs* 94, 2177-2182.
- [22] Yu, A. E., Hewitt, R. E., Connor, E. W., Stetler-Stevenson, W. G. (1997) Matrix metalloproteinases: novel targets for directed cancer therapy. *Drugs Aging* 11, 229-244.
- [23] Dickens, J. P., Donald, D. K., Kneen, G., McKay, W. R. (1988) Hydroxamic acid based collagenase inhibitors. *European patent* EP0214639.
- [24] Johnson, W. H., Roberts, N. A., Borkakoti, N. (1987) Collagenase inhibitors: their design and potential therapeutic use. *J. Enzyme Inhib.* 2, 1-22.
- [25] Schwartz, M. A., Van Wart, H. E. (1992) Synthetic inhibitors of bacterial and mammalian interstitial collagenases. *Prog. Med. Chem.* 29, 271-334.
- [26] Bode, W., Reinemer, P., Huber, R., Kleine, T., Schnierer, S., Tschesche, H. (1994) The X-ray crystal structure of the catalytic domain of human neutrophil collagenase inhibited by a substrate analogue reveals the essentials for catalysis and specificity. *EMBO J.* 13, 1263-1269.
- [27] Borkakoti, N., Winkler, F. K., Williams, D. H., D'Arcy, A., Broadhurst, M. J., Brown, P. A., Johnson, W. H., Murray, E. J. (1994) Structure of the catalytic domain of human fibroblast collagenase complexed with an inhibitor. *Nat. Struct. Biol.* 1, 106-110.
- [28] Browner, M. F., Smith, W. W., Castelhana, A. L. (1995) Matrilysin-inhibitor complexes: common themes among metalloproteases. *Biochemistry* 34, 6602-6610.

- [29] Grams, F., Reinemer, P., Powers, J. C., Kleine, T., Pieper, M., Tschesche, H., Huber, R., Bode, W. (1995) X-ray structures of human neutrophil collagenase complexed with peptide hydroxamate and peptide thiol inhibitors. Implications for substrate binding and rational drug design. *Eur. J. Biochem.* 228, 830-841.
- [30] Lovejoy, B., Cleasby, A., Hassell, A. M., Longley, K., Luther, M. A., Weigl, D., McGeehan, G., McElroy, A. B., Drewry, D., Lambert, M. H. *et al.* (1994) Structure of the catalytic domain of fibroblast collagenase complexed with an inhibitor. *Science* 263, 375-377.
- [31] Spurlino, J. C., Smallwood, A. M., Carlton, D. D., Banks, T. M., Vavra, K. J., Johnson, J. S., Cook, E. R., Falvo, J., Wahl, R. C., Pulvino, T. A. *et al.* (1994) 1.56 Å structure of mature truncated human fibroblast collagenase. *Proteins* 19, 98-109.
- [32] Stams, T., Spurlino, J. C., Smith, D. L., Wahl, R. C., Ho, T. F., Qoronfleh, M. W., Banks, T. M., Rubin, B. (1994) Structure of human neutrophil collagenase reveals large S₁' specificity pocket. *Nat. Struct. Biol.* 1, 119-123.
- [33] Gooley, P. R., O'Connell, J. F., Marcy, A. I., Cuca, G. C., Salowe, S. P., Bush, B. L., Hermes, J. D., Esser, C. K., Hagmann, W. K., Springer, J. P. *et al.* (1994) The NMR structure of the inhibited catalytic domain of human stromelysin-1. *Nat. Struct. Biol.* 1, 111-118.
- [34] Bode, W., Fernandez-Catalan, C., Tschesche, H., Grams, F., Nagase, H., Maskos, K. (1999) Structural properties of matrix metalloproteinases. *Cell. Mol. Life Sci.* 55, 639-652.
- [35] Beckett, R. P., Whittaker, M. (1998) Matrix metalloproteinase inhibitors 1998. *Exp. Opin. Ther. Patents* 8, 259-282.
- [36] Broadhurst, M. J., Johnson, W. H., Lawton, G., Handa, B. K., Machin, P. J. (1988) Phosphinic acid derivatives. *European patent* EP0276436.

- [37] Brown, P. D. (1994) Clinical trials of a low molecular weight matrix metalloproteinase inhibitor in cancer. *Ann. N. Y. Acad. Sci.* 732, 217-221.
- [38] Darlak, K., Miller, R. B., Stack, M. S., Spatola, A. F., Gray, R. D. (1990) Thiol-based inhibitors of mammalian collagenase. Substituted amide and peptide derivatives of the leucine analogue, 2-[(R,S)-mercaptomethyl]-4-methylpentanoic acid. *J. Biol. Chem.* 265, 5199-5205.
- [39] Markwell, R. E., Hunter, D. J., Ward, R. W. (1989) Peptides with collagenase inhibiting activity. *European patent* EP0320118.
- [40] Markwell, R. E., Ward, R. W., Hunter, D. J. (1993) Phosphonopeptides with collagenase inhibiting activity. *World patent* WO9309136.
- [41] Odake, S., Morita, Y., Morikawa, T., Yoshida, N., Hori, H., Nagai, Y. (1994) Inhibition of matrix metalloproteinases by peptidyl hydroxamic acids. *Biochem. Biophys. Res. Comm.* 199, 1442-1446.
- [42] Gavuzzo, E., Pochetti, G., Mazza, F., Gallina, C., Gorini, B., D'Alessio, S., Pieper, M., Tschesche, H., Tucker, P. A. (2000) Two crystal structures of human neutrophil collagenase, one complexed with a primed- and the other with an unprimed-side inhibitor: implications for drug design. *J. Med. Chem.* 43, 3377-3385.
- [43] Vassiliou, S., Mucha, A., Cuniasse, P., Georgiadis, D., Lucet-Levannier, K., Beau, F., Kannan, R., Murphy, G., Knäuper, V., Rio, M. C., Basset, P., Yiotakis, A., Dive, V. (1999) Phosphinic pseudo-tripeptides as potent inhibitors of matrix metalloproteinases: a structure-activity study. *J. Med. Chem.* 42, 2610-2620.
- [44] Grams, F., Crimmin, M., Hinnes, L., Huxley, P., Pieper, M., Tschesche, H., Bode, W. (1995) Structure determination and analysis of human neutrophil collagenase complexed with a hydroxamate inhibitor. *Biochemistry* 34, 14012-14020.
- [45] Babine, R. E., Bender, S. L. (1997) Molecular recognition of protein-ligand complexes: applications to drug design. *Chem. Rev.* 97, 1359-1472.

- [46] Rasmussen, H. S., McCann, P. P. (1997) Matrix metalloproteinase inhibition as a novel anticancer strategy: a review with special focus on batimastat and marimastat. *Pharmacol. Therapeut.* 75, 69-75.
- [47] Eccles, S. A., Box, G. M., Court, W. J., Bone, E. A., Thomas, W., Brown, P. D. (1996) Control of lymphatic and hematogenous metastasis of a rat mammary carcinoma by the matrix metalloproteinase inhibitor batimastat (BB-94). *Cancer Res.* 56, 2815-2822.
- [48] Beattie, G. J., Smyth, J. F. (1998) Phase I study of intraperitoneal metalloproteinase inhibitor BB94 in patients with malignant ascites. *Clin. Cancer Res.* 4, 1899-1902.
- [49] Krüger, A., Soeltl, R., Sopov, I., Kopitz, C., Arlt, M., Magdolen, V., Harbeck, N., Gänsbacher, B., Schmitt, M. (2001) Hydroxamate-type matrix metalloproteinase inhibitor batimastat promotes liver metastasis. *Cancer Res.* 61, 1272-1275.
- [50] Brown, P. D. (1997) Matrix metalloproteinase inhibitors in the treatment of cancer. *Med. Oncol.* 14, 1-10.
- [51] Nemunaitis, J., Poole, C., Primrose, J., Rosemurgy, A., Malfetano, J., Brown, P., Berrington, A., Cornish, A., Lynch, K., Rasmussen, H., Kerr, D., Cox, D., Millar, A. (1998) Combined analysis of studies of the effects of the matrix metalloproteinase inhibitor marimastat on serum tumor markers in advanced cancer: selection of a biologically active and tolerable dose for longer-term studies. *Clin. Cancer Res.* 4, 1101-1109.
- [52] Steward, W. P. (1999) Marimastat (BB2516): current status of development. *Cancer Chemother. Pharmacol.* 43, S56-60.
- [53] Beckett, R. P., Davidson, A. H., Drummond, A. H., Huxley, P., Whittaker, M. (1996) Recent advances in matrix metalloproteinase inhibitor research. *Drug Disc. Today* 1, 16-26.

- [54] Lombard, M. A., Wallace, T. L., Kubicek, M. F., Petzold, G. L., Mitchell, M. A., Hendges, S. K., Wilks, J. W. (1998) Synthetic matrix metalloproteinase inhibitors and tissue inhibitor of metalloproteinase TIMP-2, but not TIMP-1, inhibit shedding of tumor necrosis factor-alpha receptors in a human colon adenocarcinoma (Colo 205) cell line. *Cancer Res.* 58, 4001-4007.
- [55] MacPherson, L. J., Bayburt, E. K., Capparelli, M. P., Carroll, B. J., Goldstein, R., Justice, M. R., Zhu, L., Hu, S., Melton, R. A., Fryer, L., Goldberg, R. L., Doughty, J. R., Spirito, S., Blancuzzi, V., Wilson, D., O'Byrne, E. M., Ganu, V., Parker, D. T. (1997) Discovery of CGS-27023A, a non-peptidic, potent, and orally active stromelysin inhibitor that blocks cartilage degradation in rabbits. *J. Med. Chem.* 40, 2525-2532.
- [56] Michaelides, M. R., Curtin, M. L. (1999) Recent advances in matrix metalloproteinase inhibitors research. *Curr. Pharm. Design* 5, 787-819.
- [57] Nelson, A. R., Fingleton, B., Rothenberg, M. L., Matrisian, L. M. (2000) Matrix metalloproteinases: biologic activity and clinical implications. *J. Clin. Oncol.* 18, 1135-1149.
- [58] Nelson, N. J. (1998) Inhibitors of angiogenesis enter phase III testing. *J. Natl. Cancer Inst.* 90, 960-963.
- [59] Zook, S. E., Dagnino, R. Jr., Deason, M. E., Bender, S. L., Melnick, M. J. (1997) Metalloproteinase inhibitors, pharmaceutical compositions containing them and their pharmaceutical uses, and methods and intermediates useful for their preparation, *World patent* WO9720824.
- [60] Santos, O., McDermott, C. D., Daniels, R. G., Appelt, K. (1997) Rodent pharmacokinetic and anti-tumor efficacy studies with a series of synthetic inhibitors of matrix metalloproteinases. *Clin. Exp. Metastasis* 15, 499-508.
- [61] Shalinsky, D. R., Brekken, J., Zou, H., McDermott, C. D., Forsyth, P., Edwards, D., Margosiak, S., Bender, S., Truitt, G., Wood, A., Varki, N. M., Appelt, K. (1999)

- Broad antitumor and antiangiogenic activities of AG3340, a potent and selective MMP inhibitor undergoing advanced oncology clinical trials. *Ann. N. Y. Acad. Sci.* 878, 236-270.
- [62] Ghosh, S. S., Mobashery, S. (1991) N-acyl peptide metalloproteinase inhibitors and methods of using the same. *World patent* WO9105555.
- [63] Jacobsen, E. J., Mitchell, M. A., Hendges, S. K., Belonga, K. L., Skaletzky, L. L., Stelzer, L. S., Lindberg, T. J., Fritzen, E. L., Schostarez, H. J., O'Sullivan, T. J. *et al.* (1999) Synthesis of a series of stromelysin-selective thiadiazole urea matrix metalloproteinase inhibitors. *J. Med. Chem.* 42, 1525-1536.
- [64] Bols, M., Binderup, L., Hansen, J., Rasmussen, P. (1992) Inhibition of collagenase by aranciamycin and aranciamycin derivatives. *J. Med. Chem.* 35, 2768-2771.
- [65] Golub, L. M., McNamara, T. F., D'Angelo, G., Greenwald, R. A., Ramamurthy, N. S. (1987) A non-antibacterial chemically-modified tetracycline inhibits mammalian collagenase activity. *J. Dent. Res.* 66, 1310-1314.
- [66] Greenwald, R. A., Moak, S. A., Ramamurthy, N. S., Golub, L. M. (1992) Tetracyclines suppress matrix metalloproteinase activity in adjuvant arthritis and in combination with flurbiprofen, ameliorate bone damage. *J. Rheumatol.* 19, 927-938.
- [67] Tanaka, T., Metori, K., Mineo, S., Matsumoto, H., Satoh, T. (1990) Studies on collagenase inhibitors: II. Inhibitory effects of anthraquinones on bacterial collagenase. *J. Pharm. Soc. Jpn.* 110, 688-692.
- [68] Whittaker, M., Christopher, D. F., Brown, P., Gearing, A. J. H. (1999) Design and therapeutic application of matrix metalloproteinase inhibitors. *Chem. Rev.* 99, 2735-2776.
- [69] Novikova, A. P., Perova, N. M., Chupakhin, O. N. (1991) Synthesis and properties of functional derivatives of 1,3,4-thiadiazines and condensed systems based on these compounds (review). *Khim. Geterot. Soedin.* 11, 1443-1457.

- [70] Pfeiffer, W. D. (1998) Thiadiazines (review). In *Methods of Organic Chemistry (Houben-Weyl)*, 4th ed.; Büchel, K. H., Falbe, J., Hagemann, H., Hanack, M., Klamann, D., Kreher, R., Kropf, H., Regitz, M., Schaumann, E., Eds.; Georg Thieme Verlag, Stuttgart, E9c, 483-529.
- [71] Thorwart, W., Gebert, U., Schleyerbach, R. Bartlett, R. (1988) 5-(3-alkyl-5-tert.butyl-4-hydroxyphenyl)-2-amino-6H-1,3,4-thiadiazine, Verfahren zu ihrer Herstellung, die sie enthaltenen Arzneimittel und ihre Verwendung. *German Patent* DE3702756.
- [72] Coates, W. J., Prain, H. D., Reeves, M. L., Warrington, B. H. (1990) 1,4-bis(3-oxo-2,3-dihydropyridazin-6-yl)benzene analogues: potent phosphodiesterase inhibitors and inodilators. *J. Med. Chem.* 33, 1735-1741.
- [73] Brown, R. C., Dixon, J., Robinson, D. (1988) Verfahren zur Herstellung von pharmazeutisch aktiven Verbindungen. *German Patent* DD253426.
- [74] Pfeiffer, W. D., Dilk, E., Bulka, E. (1977) Über die Umsetzung von 4-Alkylthiosemicarbaziden mit α -Halogenketonen. *Z. Chem.* 17, 218-220.
- [75] Pfeiffer, W. D., Dilk, E., Bulka, E. (1978) Zur Reaktivität von 2-tert. Butylamino- und 2-(2,2,4-Trimethyl-pent-4-yl)amino-1,3,4-thiadiazinen. *Z. Chem.* 18, 65-66.
- [76] Szulzewsky, K., Pfeiffer, W. D., Bulka, E., Rossberg, H., Schulz, B. (1993) The crystal-structures of 2-isopropylamino-6-methyl-5-phenyl-6H-1,3,4-thiadiazine and 2-isopropylamino-6-methyl-5-phenyl-6H-1,3,4-selenadiazine. *Acta Chem. Scand.* 47, 302-306.
- [77] Jira, T., Pfeiffer, W. D., Lachmann, K., Epperlein, U. (1994) Synthesis and HPLC separation of chiral 1,3,4-thiadiazines and 1,3,4-selenadiazines. *Pharmazie* 49, 401-406.
- [78] Cheng, M., De, B., Pikul, S., Almstead, N. G., Natchus, M. G., Anastasio, M. V., McPhail, S. J., Snider, C. E., Taiwo, Y. O., Chen, L., Dunaway, C. M., Gu, F.,

- Dowty, M. E., Mieling, G. E., Janusz, M. J., Wang-Weigand, S. (2000) Design and synthesis of piperazine-based matrix metalloproteinase inhibitors. *J. Med. Chem.* 43, 369-380.
- [79] Bose, P. K. (1924) Thiadiazines. Part 1. Condensation of thiosemicarbazide with ω -bromo-acetophenone. *J. Indian Chem. Soc.* 1, 51-62.
- [80] Busby, R. E., Dominey, T. W. (1980) The rearrangement of 2-amino-1,3,4-thiadiazines to 3-amino-2-thiazol-imines. Part 1. The rates of rearrangement of a series of 5-alkyl- and 5-aryl-2-amino-1,3,4-thiadiazines at 30 and 50 °C. *J. Chem. Soc. Perkin Trans.* 2, 890-899.
- [81] Haas, A. (1982) A new classification principle: The periodic system of functional groups. *Chem. Ztg.* 106, 239-248.
- [82] Thornber, C. W. (1979) Isosterism and molecular modifications in drug design. *Chem. Soc. Rev.* 8, 563-572.
- [83] Schröder, J., Wenzel, H., Stammler, H. G., Stammler, A., Neumann, B., Tschesche, H. (2001) Novel heterocyclic inhibitors of matrix metalloproteinases: three 6H-1,3,4-thiadiazines. *Acta Cryst.* C57, 593-596.
- [84] Cremer, D., Pople, J. A. (1975) A general definition of ring puckering coordinates. *J. Amer. Chem. Soc.* 97, 1354-1358.
- [85] Boeyens, J. C. A. (1978) The conformation of six-membered rings. *J. Cryst. Mol. Struct.* 8, 317-320.
- [86] Allen, F. N., Kennard, O., Watson, D. G., Brammer, L., Orpen, A.G., Taylor, R. (1992) *International tables for crystallography*, Vol. C. edited by A. J. C. Wilson, Kluwer Academic Publisher, Dordrecht, 691-705.
- [87] Stöcker, W., Grams, F., Baumann, U., Reinemer, P., Gomis-Rüth, F. X., McKay, D. B., Bode, W. (1995) The metzincins – topological and sequential relations

- between the astacins, adamalysins, serralysins, and matrixins (collagenases) define a superfamily of zinc-peptidases. *Protein Sci.* 4, 823-840.
- [88] Rarey, M., Kramer, B., Lengauer, T., Klebe, G. (1996) A fast flexible docking method using an incremental construction algorithm. *J. Mol. Biol.* 261, 470-489.
- [89] Schmitt, J. D., Sharples, C. G. V., Caldwell, W. S. (1999) Molecular recognition in nicotinic acetylcholine receptors: the importance of π -cation interactions. *J. Med. Chem.* 42, 3066-3074.
- [90] Ma, J. C., Dougherty, D. A. (1997) The cation- π interaction. *Chem. Rev.* 97, 1303-1324.
- [91] Krüger, A., Soeltl, R., Lutz, V., Wilhelm, O. G., Magdolen, V., Rojo, E. E., Hantzopoulos, P. A., Graeff, H., Gänsbacher, B., Schmitt, M. (2000) Reduction of breast carcinoma tumor growth and lung colonization by overexpression of the soluble urokinase-type plasminogen activator receptor (CD87). *Cancer Gene Ther.* 7, 292-299.
- [92] Lee, J., Weber, M., Mejia, S., Bone, E., Watson, P., Orr, W. (2001) A matrix metalloproteinase inhibitor, batimastat, retards the development of osteolytic bone metastases by MDA-MB-231 human breast cancer cells in Balb C nu/nu mice. *Eur. J. Cancer* 37, 106-113.
- [93] Kröger, M., Tschesche, H. (1997) Cloning, expression and activation of a truncated 92-kDa gelatinase minienzyme. *Gene* 196, 175-180.
- [94] Kleine, T., Bartsch, S., Bläser, J., Schnierer, S., Triebel, S., Valentin, M., Gote, T., Tschesche, H. (1993) Preparation of active recombinant TIMP-1 from *Escherichia-Coli* inclusion-bodies and complex-formation with the recombinant catalytic domain of PMNL-collagenase. *Biochemistry* 32, 14125-14131.

- [95] Tschesche, H., Knäuper, V., Krämer, S., Michaelis, J., Oberhoff, R., Reinke, H. (1992) Latent collagenase and gelatinase from human neutrophils and their activation. *Matrix* 1, 245-255.
- [96] Pieper, M., Betz, M., Budisa, N., Gomis-Rüth, F. X., Bode, W., Tschesche, H. (1997) Expression, purification, characterization, and X-ray analysis of selenomethionine 215 variant of leukocyte collagenase. *J. Protein Chem.* 16, 637-650.
- [97] Hiller, O., Lichte, A., Oberpichler, A., Kocourek, A., Tschesche, H. (2000) Matrix metalloproteinases collagenase-2, macrophage elastase, collagenase-3, and membrane type-1 matrix metalloproteinase impair clotting by degradation of fibrinogen and factor XII. *J. Biol. Chem.* 245, 33008-33013.
- [98] Lichte, A., Kolkenbrock, H., Tschesche, H. (1996) The recombinant catalytic domain of membrane-type matrix metalloproteinase-1 (MT1-MMP) induces activation of progelatinase A and progelatinase A complexed with TIMP-2. *FEBS Lett.* 397, 277-282.
- [99] Roderfeld, M., Büttner, F. H., Bartnik, E., Tschesche, H. (2000) Expression of human membrane type 1 matrix metalloproteinase in *Pichia pastoris*. *Protein Expr. Purif.* 19, 369-374.
- [100] Siemens (1989) *P3/VMS 3.43*. Siemens analytical X-ray instruments Inc., Madison, Wisconsin, USA.
- [101] Sheldrick, G. M. (1990) *SHELXTL-Plus*. Program for crystal structure data reduction. Siemens analytical X-ray instruments Inc., Madison, Wisconsin, USA.
- [102] Sheldrick, G. M. (1997) *SHELXS-97*. Program for crystal structure solution. University of Göttingen, Germany.
- [103] Sheldrick, G. M. (1997) *SHELXL-97*. Program for the refinement of crystal structures. University of Göttingen, Germany.

- [104] Farrugia, L. J. (1997) *ORTEP-3* for Windows – a version of ORTEP-III with a graphical user interface (GUI). *J. Appl. Cryst.* 30, 565.
- [105] Mackay, S., Gilmore, C. J., Edwards, C., Steward, N., Shankland, K. (1999) *MaXus*. Computer program for the solution and refinement of crystal structures. Nonius, The Netherlands; MacScience, Japan.
- [106] Otwinowski, Z., Minor, W. W. (1997) Processing of X-ray diffraction data collected in oscillation mode. *Methods Enzymol.* 276, 307-326.
- [107] Spek, A. L. (1990). *PLATON*. An integrated tool for the analysis of the results of a single crystal structure determination. *Acta Cryst.* A46, C-34.
- [108] Huber, R. (1965) Die automatisierte Faltmolekülmethode. *Acta Cryst.* 19, 353-356.
- [109] Hoppe, W. (1957) Die Faltmolekülmethode: Eine neue Methode zur Bestimmung der Kristallstruktur bei ganz oder teilweise bekannten Molekülstrukturen. *Acta Cryst.* 10, 750-751.
- [110] Rossmann, M. G., Blow, D. M. (1962) The detection of subunits within the crystallographic asymmetric unit. *Acta Cryst.* 15, 24-31.
- [111] Navaza, J. (1994) *AMoRe*. An automated package for molecular replacement. *Acta Cryst.* A50, 157-163.
- [112] Turk, D. (1996) *MAIN 96*. An interactive software for density modifications, model building, structure refinement and analysis. In Proceedings from the 1996 meeting of the International Union of Crystallography Macromolecular Computing School. Bourne, P. E., Watenpaugh, K., Eds.; Western Washington University WA.
- [113] Brunger, A. T. (1992) *X-PLOR 3.1*. A system for X-ray crystallography and NMR. Yale University Press; New Heaven CT.

- [114] Walters, P., Stahl, M. (1997) *BABEL*. A molecular structure information interchange hub. Dolata Research Group, Department of Chemistry, University of Arizona Tucson, AZ 85721.
- [115] Tripos Associates, Inc. (1997) SYBYL. Molecular Modeling Software Version 6.4. St. Louis, Missouri, USA.
- [116] Knight, C. G., Willenbrock, F., Murphy, G. (1992) A novel coumarin-labelled peptide for sensitive continuous assays of the matrix metalloproteinases. *FEBS Lett.* 296, 263-266.
- [117] Copeland, R. A., Lombardo, D., Giannaras, J., Decicco, C. P. (1995) Estimating K_i values for tight binding inhibitors from dose-response plots. *Bioorg. Med. Chem. Lett.* 17, 1947-1952.
- [118] Horovitz, A., Levitzki, A. (1987) An accurate method for determination of receptor-ligand and enzyme-inhibitor dissociation constants from displacement curves. *Proc. Natl. Acad. Sci. U.S.A.* 84, 6654-6658.

Table 1. Crystal data and structure refinement for compound **14b**.

Identification code	14b
Measurement device	Nonius KappaCCD
Empirical formula	C ₁₆ H ₁₅ Cl N ₄ O ₃ S ₃ + 0.25 CH ₃ OH
Formula weight	450.96
Temperature	100(2) K
Wavelength	0.71073 Å
Crystal system, space group	Tetragonal P 41 21 2
Unit cell dimensions	a = 10.0460(4) Å alpha = 90.000(3) deg. b = 10.046(2) Å beta = 90.000(4) deg. c = 74.8620(4) Å gamma = 90.000(3) deg.
Volume	7555.2(18) Å ³
Z, Calculated density	16, 1.586 Mg/m ³
Absorption coefficient	0.562 mm ⁻¹
F(000)	3720
Crystal size, colour and habit	0.27 x 0.21 x 0.07 mm ³ , Colorless plates
Theta range for data collection	2.05 to 24.99 deg.
Index ranges	-11<=h<=11, -11<=k<=11, -89<=l<=88
Reflections collected / unique	33232 / 6252 [R(int) = 0.0763]
Completeness to theta = 24.99	97.2%
Absorption correction	Semi-empirical from equivalents
Max. and min. transmission	1.067 and 0.962
Refinement method	Full-matrix least-squares on F ²
Data / restraints / parameters	6252 / 0 / 515
Goodness-of-fit on F ²	1.123
Final R indices [I>2sigma(I)]	R1 = 0.0562, wR2 = 0.0863 [5215]
R indices (all data)	R1 = 0.0789, wR2 = 0.0925
Absolute structure parameter	0.02(8)
Largest diff. peak and hole	0.376 and -0.370 e.Å ⁻³
remarks	Hydrogens of CH ₃ OH were not included.

Table 2. Atomic coordinates ($\times 10^4$) and equivalent isotropic displacement parameters ($\text{\AA}^2 \times 10^3$) for 14b. $U(\text{eq})$ is defined as one third of the trace of the orthogonalized U_{ij} tensor.

	x	y	z	$U(\text{eq})$
Cl(1)	28873(1)	13213(1)	515(1)	29(1)
S(1)	23250(1)	8585(1)	1038(1)	17(1)
S(2)	17747(1)	8244(1)	1132(1)	19(1)
S(3)	19893(1)	10150(1)	1245(1)	32(1)
O(1)	21721(3)	6574(3)	1143(1)	22(1)
O(2)	16464(3)	8567(3)	1060(1)	26(1)
O(3)	17910(3)	7931(3)	1316(1)	24(1)
N(1)	23345(4)	9640(4)	658(1)	19(1)
N(2)	22169(4)	8998(4)	715(1)	17(1)
N(3)	20953(4)	7644(4)	895(1)	15(1)
N(4)	18284(4)	7006(4)	1017(1)	17(1)
C(1)	25834(4)	10657(5)	540(1)	18(1)
C(2)	26933(4)	11367(5)	478(1)	19(1)
C(3)	27468(4)	12335(5)	586(1)	19(1)
C(4)	26943(5)	12629(5)	752(1)	21(1)
C(5)	25858(4)	11907(4)	811(1)	15(1)
C(6)	25296(4)	10915(4)	707(1)	12(1)
C(7)	24100(4)	10195(4)	773(1)	13(1)
C(8)	23798(5)	10206(4)	967(1)	17(1)
C(9)	22073(4)	8414(4)	869(1)	13(1)
C(10)	20797(4)	6857(5)	1041(1)	16(1)
C(11)	19436(4)	6239(4)	1071(1)	15(1)
C(12)	19413(5)	4877(5)	979(1)	23(1)
C(13)	18784(4)	9607(5)	1088(1)	20(1)
C(14)	18835(4)	10295(4)	928(1)	14(1)
C(15)	19860(5)	11296(5)	941(1)	24(1)
C(16)	20468(5)	11321(5)	1102(1)	27(1)
Cl(2)	12435(1)	3414(1)	770(1)	26(1)
S(4)	17997(1)	8360(1)	266(1)	18(1)
S(5)	23323(1)	8339(1)	94(1)	20(1)
S(6)	21194(1)	6260(1)	51(1)	29(1)
O(4)	19676(3)	10433(3)	192(1)	21(1)
O(5)	24403(3)	8544(3)	215(1)	25(1)
O(6)	23569(3)	8027(3)	-89(1)	23(1)
N(5)	17785(4)	7135(4)	635(1)	18(1)
N(6)	18981(4)	7773(4)	591(1)	19(1)
N(7)	20289(4)	9136(4)	428(1)	16(1)
N(8)	22431(4)	9684(4)	93(1)	18(1)
C(17)	15189(4)	6266(5)	731(1)	16(1)
C(18)	14114(4)	5506(5)	791(1)	17(1)
C(19)	13728(4)	4414(4)	692(1)	17(1)
C(20)	14340(4)	4091(4)	534(1)	18(1)
C(21)	15384(4)	4863(5)	473(1)	19(1)
C(22)	15823(4)	5939(4)	573(1)	16(1)
C(23)	17036(4)	6656(4)	513(1)	13(1)
C(24)	17375(4)	6720(5)	320(1)	17(1)
C(25)	19121(4)	8427(4)	443(1)	15(1)
C(26)	20554(5)	9980(4)	290(1)	15(1)
C(27)	22017(4)	10311(5)	261(1)	18(1)
C(28)	22254(5)	11804(5)	257(1)	24(1)
C(29)	22356(4)	7056(4)	182(1)	18(1)
C(30)	22369(4)	6611(4)	354(1)	17(1)
C(31)	21400(5)	5597(5)	379(1)	22(1)
C(32)	20715(5)	5306(5)	227(1)	23(1)
O(7)	25426(5)	15426(5)	0	128(4)
C(33)	24410(6)	14410(6)	0	68(3)

Table 3. Bond lengths [Å] and angles [deg] for 14b.

Cl(1)-C(3)	1.748(4)
S(1)-C(9)	1.742(4)
S(1)-C(8)	1.800(5)
S(2)-O(3)	1.423(3)
S(2)-O(2)	1.432(3)
S(2)-N(4)	1.605(4)
S(2)-C(13)	1.750(5)
S(3)-C(16)	1.689(5)
S(3)-C(13)	1.707(5)
O(1)-C(10)	1.232(5)
N(1)-C(7)	1.275(5)
N(1)-N(2)	1.412(5)
N(2)-C(9)	1.298(5)
N(3)-C(10)	1.361(6)
N(3)-C(9)	1.379(5)
N(3)-H(3)	1.03(5)
N(4)-C(11)	1.449(6)
N(4)-H(4)	0.86(4)
C(1)-C(6)	1.389(6)
C(1)-C(2)	1.394(6)
C(2)-C(3)	1.378(6)
C(3)-C(4)	1.379(6)
C(4)-C(5)	1.383(6)
C(5)-C(6)	1.388(6)
C(6)-C(7)	1.487(6)
C(7)-C(8)	1.486(6)
C(10)-C(11)	1.517(6)
C(11)-C(12)	1.533(6)
C(13)-C(14)	1.387(6)
C(14)-C(15)	1.442(6)
C(15)-C(16)	1.352(6)
Cl(2)-C(19)	1.744(4)
S(4)-C(25)	1.746(4)
S(4)-C(24)	1.810(5)
S(5)-O(5)	1.427(3)
S(5)-O(6)	1.429(3)
S(5)-N(8)	1.621(4)
S(5)-C(29)	1.744(4)
S(6)-C(32)	1.702(5)
S(6)-C(29)	1.724(4)
O(4)-C(26)	1.236(5)
N(5)-C(23)	1.279(5)
N(5)-N(6)	1.400(5)
N(6)-C(25)	1.298(5)
N(7)-C(26)	1.358(5)
N(7)-C(25)	1.377(6)
N(7)-H(7)	1.00(6)
N(8)-C(27)	1.470(6)
N(8)-H(8)	0.76(5)
C(17)-C(22)	1.385(6)
C(17)-C(18)	1.395(6)
C(18)-C(19)	1.379(6)
C(19)-C(20)	1.372(6)
C(20)-C(21)	1.382(6)
C(21)-C(22)	1.387(6)
C(22)-C(23)	1.485(6)
C(23)-C(24)	1.484(6)
C(26)-C(27)	1.523(6)
C(27)-C(28)	1.519(6)
C(29)-C(30)	1.363(6)
C(30)-C(31)	1.421(6)
C(31)-C(32)	1.362(6)
O(7)-C(33)	1.444(11)

C(9) -S(1) -C(8)	94.7(2)
O(3) -S(2) -O(2)	120.99(19)
O(3) -S(2) -N(4)	107.9(2)
O(2) -S(2) -N(4)	106.19(19)
O(3) -S(2) -C(13)	106.5(2)
O(2) -S(2) -C(13)	106.8(2)
N(4) -S(2) -C(13)	107.9(2)
C(16) -S(3) -C(13)	90.7(2)
C(7) -N(1) -N(2)	119.5(4)
C(9) -N(2) -N(1)	122.5(4)
C(10) -N(3) -C(9)	122.2(4)
C(10) -N(3) -H(3)	124(3)
C(9) -N(3) -H(3)	114(3)
C(11) -N(4) -S(2)	122.1(3)
C(11) -N(4) -H(4)	118(3)
S(2) -N(4) -H(4)	115(3)
C(6) -C(1) -C(2)	120.9(4)
C(3) -C(2) -C(1)	118.2(4)
C(2) -C(3) -C(4)	122.3(4)
C(2) -C(3) -Cl(1)	119.4(3)
C(4) -C(3) -Cl(1)	118.4(4)
C(3) -C(4) -C(5)	118.6(4)
C(4) -C(5) -C(6)	121.0(4)
C(5) -C(6) -C(1)	119.0(4)
C(5) -C(6) -C(7)	119.4(4)
C(1) -C(6) -C(7)	121.6(4)
N(1) -C(7) -C(8)	122.9(4)
N(1) -C(7) -C(6)	117.9(4)
C(8) -C(7) -C(6)	119.1(4)
C(7) -C(8) -S(1)	110.2(3)
N(2) -C(9) -N(3)	116.1(4)
N(2) -C(9) -S(1)	123.5(3)
N(3) -C(9) -S(1)	120.4(3)
O(1) -C(10) -N(3)	122.9(4)
O(1) -C(10) -C(11)	119.6(4)
N(3) -C(10) -C(11)	117.3(4)
N(4) -C(11) -C(10)	117.5(4)
N(4) -C(11) -C(12)	109.7(4)
C(10) -C(11) -C(12)	108.2(4)
C(14) -C(13) -S(3)	114.3(4)
C(14) -C(13) -S(2)	124.9(3)
S(3) -C(13) -S(2)	120.8(3)
C(13) -C(14) -C(15)	108.3(4)
C(16) -C(15) -C(14)	113.4(4)
C(15) -C(16) -S(3)	113.3(4)
C(25) -S(4) -C(24)	94.9(2)
O(5) -S(5) -O(6)	120.6(2)
O(5) -S(5) -N(8)	107.7(2)
O(6) -S(5) -N(8)	105.8(2)
O(5) -S(5) -C(29)	106.88(19)
O(6) -S(5) -C(29)	107.3(2)
N(8) -S(5) -C(29)	108.1(2)
C(32) -S(6) -C(29)	90.5(2)
C(23) -N(5) -N(6)	120.6(4)
C(25) -N(6) -N(5)	121.7(4)
C(26) -N(7) -C(25)	123.6(4)
C(26) -N(7) -H(7)	122(4)
C(25) -N(7) -H(7)	114(4)
C(27) -N(8) -S(5)	120.5(3)
C(27) -N(8) -H(8)	128(4)
S(5) -N(8) -H(8)	103(4)
C(22) -C(17) -C(18)	120.0(4)
C(19) -C(18) -C(17)	118.8(4)
C(20) -C(19) -C(18)	121.6(4)
C(20) -C(19) -Cl(2)	119.2(3)
C(18) -C(19) -Cl(2)	119.2(4)
C(19) -C(20) -C(21)	119.5(4)

C(20)-C(21)-C(22)	120.0(4)
C(17)-C(22)-C(21)	120.0(4)
C(17)-C(22)-C(23)	121.4(4)
C(21)-C(22)-C(23)	118.5(4)
N(5)-C(23)-C(24)	123.0(4)
N(5)-C(23)-C(22)	116.7(4)
C(24)-C(23)-C(22)	120.1(4)
C(23)-C(24)-S(4)	109.8(3)
N(6)-C(25)-N(7)	115.3(4)
N(6)-C(25)-S(4)	124.2(3)
N(7)-C(25)-S(4)	120.4(3)
O(4)-C(26)-N(7)	122.7(4)
O(4)-C(26)-C(27)	121.5(4)
N(7)-C(26)-C(27)	115.8(4)
N(8)-C(27)-C(28)	111.2(4)
N(8)-C(27)-C(26)	107.7(4)
C(28)-C(27)-C(26)	111.7(4)
C(30)-C(29)-S(6)	113.2(3)
C(30)-C(29)-S(5)	126.5(3)
S(6)-C(29)-S(5)	120.3(2)
C(29)-C(30)-C(31)	110.7(4)
C(32)-C(31)-C(30)	112.9(4)
C(31)-C(32)-S(6)	112.7(4)

Table 4. Anisotropic displacement parameters ($\text{Å}^2 \times 10^3$) for 14b.
 The anisotropic displacement factor exponent takes the form:
 $-2 \pi^2 [h^2 a^{*2} U_{11} + \dots + 2 h k a^* b^* U_{12}]$

	U11	U22	U33	U23	U13	U12
C1 (1)	22 (1)	39 (1)	26 (1)	3 (1)	2 (1)	-21 (1)
S (1)	14 (1)	19 (1)	18 (1)	4 (1)	-3 (1)	-5 (1)
S (2)	13 (1)	23 (1)	21 (1)	2 (1)	1 (1)	1 (1)
S (3)	26 (1)	38 (1)	30 (1)	-7 (1)	-9 (1)	2 (1)
O (1)	16 (2)	23 (2)	28 (2)	6 (2)	-5 (2)	0 (2)
O (2)	5 (2)	31 (2)	41 (2)	9 (2)	1 (2)	0 (2)
O (3)	21 (2)	32 (2)	18 (2)	2 (2)	5 (1)	6 (2)
N (1)	12 (2)	23 (2)	20 (2)	5 (2)	2 (2)	-5 (2)
N (2)	12 (2)	22 (2)	19 (2)	7 (2)	2 (2)	-5 (2)
N (3)	12 (2)	17 (2)	16 (2)	4 (2)	1 (2)	-5 (2)
N (4)	12 (2)	26 (2)	13 (2)	3 (2)	-2 (2)	-4 (2)
C (1)	18 (3)	13 (3)	23 (3)	0 (2)	-4 (2)	-3 (2)
C (2)	13 (3)	23 (3)	21 (2)	2 (2)	-1 (2)	1 (2)
C (3)	10 (3)	20 (3)	27 (3)	6 (2)	-2 (2)	-8 (2)
C (4)	21 (3)	23 (3)	20 (2)	-1 (2)	-6 (2)	-7 (2)
C (5)	14 (3)	15 (3)	16 (2)	0 (2)	0 (2)	-2 (2)
C (6)	9 (2)	14 (3)	15 (2)	1 (2)	-4 (2)	2 (2)
C (7)	12 (3)	11 (2)	17 (2)	-3 (2)	-1 (2)	1 (2)
C (8)	19 (3)	15 (3)	18 (2)	-3 (2)	2 (2)	-5 (2)
C (9)	11 (3)	16 (3)	11 (2)	-2 (2)	0 (2)	-2 (2)
C (10)	10 (3)	12 (3)	28 (3)	-4 (2)	3 (2)	-1 (2)
C (11)	15 (3)	17 (3)	13 (2)	5 (2)	-1 (2)	0 (2)
C (12)	20 (3)	17 (3)	33 (3)	-1 (2)	3 (2)	-7 (2)
C (13)	12 (3)	23 (3)	26 (3)	-6 (2)	-1 (2)	1 (2)
C (14)	11 (2)	6 (2)	25 (3)	2 (2)	2 (2)	1 (2)
C (15)	19 (3)	15 (3)	37 (3)	1 (2)	2 (2)	0 (2)
C (16)	14 (3)	21 (3)	46 (3)	-7 (3)	-2 (3)	-1 (2)
C1 (2)	16 (1)	24 (1)	37 (1)	7 (1)	3 (1)	-7 (1)
S (4)	16 (1)	19 (1)	18 (1)	4 (1)	-4 (1)	-6 (1)
S (5)	14 (1)	20 (1)	26 (1)	7 (1)	-3 (1)	-6 (1)
S (6)	26 (1)	31 (1)	30 (1)	5 (1)	-6 (1)	-14 (1)
O (4)	18 (2)	22 (2)	23 (2)	8 (2)	-4 (2)	-7 (2)
O (5)	18 (2)	23 (2)	35 (2)	5 (2)	-9 (2)	-7 (2)
O (6)	20 (2)	22 (2)	27 (2)	3 (2)	6 (2)	-3 (2)
N (5)	13 (2)	20 (2)	20 (2)	1 (2)	1 (2)	-6 (2)
N (6)	10 (2)	20 (2)	25 (2)	8 (2)	-2 (2)	-7 (2)
N (7)	10 (2)	22 (2)	14 (2)	4 (2)	-2 (2)	-6 (2)
N (8)	16 (2)	20 (2)	17 (2)	6 (2)	-6 (2)	-5 (2)
C (17)	11 (3)	18 (3)	19 (2)	-1 (2)	-4 (2)	-2 (2)
C (18)	9 (3)	23 (3)	21 (2)	3 (2)	1 (2)	0 (2)
C (19)	8 (3)	16 (3)	26 (3)	9 (2)	-5 (2)	-3 (2)
C (20)	14 (3)	17 (3)	24 (3)	0 (2)	-5 (2)	-7 (2)
C (21)	11 (3)	23 (3)	22 (2)	2 (2)	1 (2)	-2 (2)
C (22)	9 (3)	16 (3)	24 (3)	5 (2)	-7 (2)	-3 (2)
C (23)	15 (3)	9 (2)	16 (2)	-3 (2)	-5 (2)	3 (2)
C (24)	12 (2)	18 (3)	22 (2)	-1 (2)	1 (2)	-5 (2)
C (25)	14 (3)	14 (3)	16 (2)	-1 (2)	1 (2)	-2 (2)
C (26)	18 (3)	16 (3)	12 (2)	0 (2)	-4 (2)	-6 (2)
C (27)	17 (3)	24 (3)	12 (2)	4 (2)	-7 (2)	-12 (2)
C (28)	19 (3)	22 (3)	29 (3)	0 (2)	1 (2)	-10 (2)
C (29)	15 (3)	18 (3)	20 (2)	4 (2)	-6 (2)	-6 (2)
C (30)	11 (2)	13 (3)	28 (3)	0 (2)	4 (2)	-3 (2)
C (31)	20 (3)	21 (3)	26 (3)	7 (2)	5 (2)	1 (2)
C (32)	20 (3)	17 (3)	32 (3)	3 (2)	-2 (2)	-3 (2)
O (7)	156 (6)	156 (6)	72 (5)	-40 (5)	40 (5)	-108 (7)
C (33)	50 (4)	50 (4)	105 (8)	-3 (4)	3 (4)	-23 (5)

Table 5. Hydrogen coordinates ($\times 10^4$) and isotropic displacement parameters ($\text{\AA}^2 \times 10^3$) for 14b.

	x	y	z	U(eq)
H(3)	20260(5)	7730(5)	794(6)	47(16)
H(4)	18090(4)	7020(4)	905(5)	9(12)
H(1A)	25448	9988	466	22
H(2A)	27304	11188	363	23
H(4A)	27320	13312	824	26
H(5A)	25491	12094	926	18
H(8A)	23095	10871	992	21
H(8B)	24605	10464	1035	21
H(11)	19348	6074	1202	18
H(12A)	18592	4407	1011	35
H(12B)	20183	4353	1018	35
H(12C)	19449	4999	849	35
H(14)	18289	10135	826	17
H(15)	20085	11880	846	28
H(16)	21151	11935	1132	32
H(7)	20940(6)	8980(6)	527(8)	80(2)
H(8)	22040(5)	9630(5)	5(6)	30(18)
H(17)	15485	7006	799	20
H(18)	13657	5738	897	21
H(20)	14048	3342	467	22
H(21)	15801	4657	362	22
H(24A)	16573	6525	248	21
H(24B)	18059	6043	292	21
H(27)	22548	9917	361	21
H(28A)	23196	11980	232	35
H(28B)	22013	12189	373	35
H(28C)	21706	12206	163	35
H(30)	22947	6933	445	21
H(31)	21247	5168	490	27
H(32)	20042	4643	221	27

Table 1. Crystal data and structure refinement for **16**.

Identification code	16
Measurement device	Nonius KappaCCD
Empirical formula	C12 H13 Br Cl N3 S
Formula weight	346.67
Temperature	100(2) K
Wavelength	0.71073 Å
Crystal system, space group	Monoclinic P 21/c
Unit cell dimensions	a = 21.3350(6) Å alpha = 90.0000(17) deg. b = 9.3150(2) Å beta = 102.9950(19) deg. c = 14.4910(4) Å gamma = 90.000(3) deg.
Volume	2806.12(13) Å ³
Z, Calculated density	8, 1.641 Mg/m ³
Absorption coefficient	3.254 mm ⁻¹
F(000)	1392
Crystal size, colour and habit	0.50 x 0.30 x 0.30 mm ³ , Colorless Irregular
Theta range for data collection	2.40 to 30.00 deg.
Index ranges	-30 ≤ h ≤ 30, -13 ≤ k ≤ 13, -20 ≤ l ≤ 19
Reflections collected / unique	51635 / 8102 [R(int) = 0.0615]
Completeness to theta = 30.00	93.7%
Absorption correction	Semi-empirical from equivalents
Max. and min. transmission	0.4418 and 0.2930
Refinement method	Full-matrix least-squares on F ²
Data / restraints / parameters	8102 / 0 / 325
Goodness-of-fit on F ²	1.037
Final R indices [I > 2σ(I)]	R1 = 0.0456, wR2 = 0.0813 [6357]
R indices (all data)	R1 = 0.0699, wR2 = 0.0881
Largest diff. peak and hole	1.033 and -0.702 e.Å ⁻³
remarks	H(1A), H(2A), H(4A) and H(5A) were calculated as half occupied.

Table 2. Atomic coordinates ($\times 10^4$) and equivalent isotropic displacement parameters ($\text{\AA}^2 \times 10^3$) for 16. $U(\text{eq})$ is defined as one third of the trace of the orthogonalized U_{ij} tensor.

	x	y	z	$U(\text{eq})$
Br(1)	4541(1)	7176(1)	3717(1)	17(1)
Br(2)	515(1)	2159(1)	1189(1)	19(1)
S(1)	4957(1)	1390(1)	3605(1)	17(1)
S(2)	192(1)	-3664(1)	1315(1)	17(1)
Cl(1)	1226(1)	-1311(1)	3396(1)	23(1)
Cl(2)	3858(1)	-6581(1)	1485(1)	22(1)
N(1)	3739(1)	3018(3)	3737(2)	16(1)
N(2)	4326(1)	3734(3)	3901(2)	15(1)
N(3)	5333(1)	4121(3)	3653(2)	20(1)
N(4)	1405(1)	-2029(3)	1145(2)	17(1)
N(5)	818(1)	-1307(3)	1009(2)	17(1)
N(6)	-184(1)	-967(3)	1310(2)	19(1)
C(1)	3103(1)	-490(3)	4100(2)	18(1)
C(2)	2517(1)	-1174(3)	3988(2)	19(1)
C(3)	1972(1)	-498(3)	3478(2)	19(1)
C(4)	2001(1)	812(3)	3049(2)	21(1)
C(5)	2590(1)	1498(3)	3172(2)	19(1)
C(6)	3148(1)	863(3)	3713(2)	15(1)
C(7)	3761(1)	1660(3)	3896(2)	16(1)
C(8)	4386(1)	922(3)	4300(2)	16(1)
C(9)	4873(1)	3218(3)	3732(2)	18(1)
C(10)	5987(1)	3717(4)	3610(2)	25(1)
C(11)	6473(2)	4258(4)	4429(2)	27(1)
C(12)	7008(2)	4884(4)	4355(3)	43(1)
C(13)	2007(1)	-5538(3)	714(2)	18(1)
C(14)	2580(1)	-6281(3)	828(2)	20(1)
C(15)	3132(1)	-5683(3)	1381(2)	17(1)
C(16)	3119(1)	-4379(3)	1822(2)	19(1)
C(17)	2549(1)	-3629(3)	1691(2)	18(1)
C(18)	1980(1)	-4194(3)	1124(2)	16(1)
C(19)	1373(1)	-3384(3)	968(2)	16(1)
C(20)	747(1)	-4119(3)	585(2)	17(1)
C(21)	272(1)	-1840(3)	1197(2)	16(1)
C(22)	-831(1)	-1472(3)	1326(2)	22(1)
C(23)	-1293(2)	-268(4)	1186(2)	27(1)
C(24)	-1691(2)	-70(4)	1742(3)	30(1)

Table 3. Bond lengths [Å] and angles [deg] for 16.

S(1)-C(9)	1.726(3)
S(1)-C(8)	1.801(3)
S(2)-C(21)	1.720(3)
S(2)-C(20)	1.805(3)
Cl(1)-C(3)	1.742(3)
Cl(2)-C(15)	1.739(3)
N(1)-C(7)	1.285(4)
N(1)-N(2)	1.392(3)
N(1)-H(1A)	0.8800
N(2)-C(9)	1.335(4)
N(2)-H(2A)	0.8800
N(3)-C(9)	1.316(4)
N(3)-C(10)	1.461(4)
N(3)-H(3A)	0.8800
N(4)-C(19)	1.287(4)
N(4)-N(5)	1.395(3)
N(4)-H(4A)	0.8800
N(5)-C(21)	1.349(4)
N(5)-H(5A)	0.8800
N(6)-C(21)	1.306(4)
N(6)-C(22)	1.465(4)
N(6)-H(6A)	0.8800
C(1)-C(2)	1.380(4)
C(1)-C(6)	1.391(4)
C(1)-H(1B)	0.9500
C(2)-C(3)	1.382(4)
C(2)-H(2B)	0.9500
C(3)-C(4)	1.377(4)
C(4)-C(5)	1.384(4)
C(4)-H(4B)	0.9500
C(5)-C(6)	1.401(4)
C(5)-H(5B)	0.9500
C(6)-C(7)	1.474(4)
C(7)-C(8)	1.498(4)
C(8)-H(8A)	0.9900
C(8)-H(8B)	0.9900
C(10)-C(11)	1.478(4)
C(10)-H(10A)	0.9900
C(10)-H(10B)	0.9900
C(11)-C(12)	1.307(5)
C(11)-H(11A)	0.9500
C(12)-H(12A)	0.9500
C(12)-H(12B)	0.9500
C(13)-C(14)	1.382(4)
C(13)-C(18)	1.392(4)
C(13)-H(13A)	0.9500
C(14)-C(15)	1.383(4)
C(14)-H(14A)	0.9500
C(15)-C(16)	1.375(4)
C(16)-C(17)	1.377(4)
C(16)-H(16A)	0.9500
C(17)-C(18)	1.406(4)
C(17)-H(17A)	0.9500
C(18)-C(19)	1.472(4)
C(19)-C(20)	1.493(4)
C(20)-H(20A)	0.9900
C(20)-H(20B)	0.9900
C(22)-C(23)	1.477(4)
C(22)-H(22A)	0.9900
C(22)-H(22B)	0.9900
C(23)-C(24)	1.308(4)
C(23)-H(23A)	0.9500
C(24)-H(24A)	0.9500
C(24)-H(24B)	0.9500

C(9) -S(1) -C(8)	94.55 (14)
C(21) -S(2) -C(20)	94.65 (13)
C(7) -N(1) -N(2)	116.6 (2)
C(7) -N(1) -H(1A)	121.7
N(2) -N(1) -H(1A)	121.7
C(9) -N(2) -N(1)	125.9 (2)
C(9) -N(2) -H(2A)	117.1
N(1) -N(2) -H(2A)	117.1
C(9) -N(3) -C(10)	125.2 (3)
C(9) -N(3) -H(3A)	117.4
C(10) -N(3) -H(3A)	117.4
C(19) -N(4) -N(5)	116.0 (2)
C(19) -N(4) -H(4A)	122.0
N(5) -N(4) -H(4A)	122.0
C(21) -N(5) -N(4)	125.6 (2)
C(21) -N(5) -H(5A)	117.2
N(4) -N(5) -H(5A)	117.2
C(21) -N(6) -C(22)	122.2 (3)
C(21) -N(6) -H(6A)	118.9
C(22) -N(6) -H(6A)	118.9
C(2) -C(1) -C(6)	120.9 (3)
C(2) -C(1) -H(1B)	119.6
C(6) -C(1) -H(1B)	119.6
C(1) -C(2) -C(3)	119.0 (3)
C(1) -C(2) -H(2B)	120.5
C(3) -C(2) -H(2B)	120.5
C(4) -C(3) -C(2)	121.7 (3)
C(4) -C(3) -C1(1)	119.2 (2)
C(2) -C(3) -C1(1)	119.0 (2)
C(3) -C(4) -C(5)	118.9 (3)
C(3) -C(4) -H(4B)	120.6
C(5) -C(4) -H(4B)	120.6
C(4) -C(5) -C(6)	120.6 (3)
C(4) -C(5) -H(5B)	119.7
C(6) -C(5) -H(5B)	119.7
C(1) -C(6) -C(5)	118.8 (3)
C(1) -C(6) -C(7)	121.5 (3)
C(5) -C(6) -C(7)	119.7 (3)
N(1) -C(7) -C(6)	118.0 (2)
N(1) -C(7) -C(8)	121.0 (3)
C(6) -C(7) -C(8)	121.0 (2)
C(7) -C(8) -S(1)	109.00 (19)
C(7) -C(8) -H(8A)	109.9
S(1) -C(8) -H(8A)	109.9
C(7) -C(8) -H(8B)	109.9
S(1) -C(8) -H(8B)	109.9
H(8A) -C(8) -H(8B)	108.3
N(3) -C(9) -N(2)	119.0 (3)
N(3) -C(9) -S(1)	121.6 (2)
N(2) -C(9) -S(1)	119.4 (2)
N(3) -C(10) -C(11)	112.5 (3)
N(3) -C(10) -H(10A)	109.1
C(11) -C(10) -H(10A)	109.1
N(3) -C(10) -H(10B)	109.1
C(11) -C(10) -H(10B)	109.1
H(10A) -C(10) -H(10B)	107.8
C(12) -C(11) -C(10)	123.7 (3)
C(12) -C(11) -H(11A)	118.2
C(10) -C(11) -H(11A)	118.2
C(11) -C(12) -H(12A)	120.0
C(11) -C(12) -H(12B)	120.0
H(12A) -C(12) -H(12B)	120.0
C(14) -C(13) -C(18)	121.2 (3)
C(14) -C(13) -H(13A)	119.4
C(18) -C(13) -H(13A)	119.4
C(13) -C(14) -C(15)	118.9 (3)
C(13) -C(14) -H(14A)	120.6

C(15)-C(14)-H(14A)	120.6
C(16)-C(15)-C(14)	121.4(3)
C(16)-C(15)-Cl(2)	119.7(2)
C(14)-C(15)-Cl(2)	118.9(2)
C(15)-C(16)-C(17)	119.5(3)
C(15)-C(16)-H(16A)	120.2
C(17)-C(16)-H(16A)	120.2
C(16)-C(17)-C(18)	120.7(3)
C(16)-C(17)-H(17A)	119.7
C(18)-C(17)-H(17A)	119.7
C(13)-C(18)-C(17)	118.3(3)
C(13)-C(18)-C(19)	120.9(3)
C(17)-C(18)-C(19)	120.8(3)
N(4)-C(19)-C(18)	117.9(3)
N(4)-C(19)-C(20)	121.8(3)
C(18)-C(19)-C(20)	120.3(2)
C(19)-C(20)-S(2)	108.92(19)
C(19)-C(20)-H(20A)	109.9
S(2)-C(20)-H(20A)	109.9
C(19)-C(20)-H(20B)	109.9
S(2)-C(20)-H(20B)	109.9
H(20A)-C(20)-H(20B)	108.3
N(6)-C(21)-N(5)	119.8(3)
N(6)-C(21)-S(2)	120.6(2)
N(5)-C(21)-S(2)	119.5(2)
N(6)-C(22)-C(23)	110.9(3)
N(6)-C(22)-H(22A)	109.5
C(23)-C(22)-H(22A)	109.5
N(6)-C(22)-H(22B)	109.5
C(23)-C(22)-H(22B)	109.5
H(22A)-C(22)-H(22B)	108.0
C(24)-C(23)-C(22)	121.9(3)
C(24)-C(23)-H(23A)	119.0
C(22)-C(23)-H(23A)	119.0
C(23)-C(24)-H(24A)	120.0
C(23)-C(24)-H(24B)	120.0
H(24A)-C(24)-H(24B)	120.0

Table 4. Anisotropic displacement parameters ($\text{\AA}^2 \times 10^3$) for 16.
 The anisotropic displacement factor exponent takes the form:
 $-2 \pi^2 [h^2 a^2 U_{11} + \dots + 2 h k a^* b^* U_{12}]$

	U11	U22	U33	U23	U13	U12
Br (1)	19 (1)	12 (1)	17 (1)	-2 (1)	0 (1)	0 (1)
Br (2)	24 (1)	12 (1)	18 (1)	2 (1)	-3 (1)	-3 (1)
S (1)	17 (1)	14 (1)	20 (1)	-2 (1)	4 (1)	5 (1)
S (2)	17 (1)	13 (1)	20 (1)	2 (1)	1 (1)	-3 (1)
Cl (1)	18 (1)	29 (1)	21 (1)	-2 (1)	3 (1)	-4 (1)
Cl (2)	18 (1)	28 (1)	21 (1)	3 (1)	3 (1)	2 (1)
N (1)	16 (1)	14 (1)	17 (1)	1 (1)	2 (1)	2 (1)
N (2)	14 (1)	14 (1)	18 (1)	-3 (1)	4 (1)	2 (1)
N (3)	16 (1)	16 (1)	28 (1)	-4 (1)	5 (1)	1 (1)
N (4)	18 (1)	15 (1)	16 (1)	0 (1)	2 (1)	-2 (1)
N (5)	19 (1)	13 (1)	18 (1)	1 (1)	3 (1)	-3 (1)
N (6)	20 (1)	15 (1)	20 (1)	-2 (1)	2 (1)	-4 (1)
C (1)	19 (1)	15 (1)	19 (1)	0 (1)	-1 (1)	5 (1)
C (2)	23 (1)	13 (1)	19 (1)	0 (1)	3 (1)	-1 (1)
C (3)	15 (1)	23 (2)	17 (1)	-5 (1)	4 (1)	-2 (1)
C (4)	18 (1)	23 (2)	19 (1)	2 (1)	0 (1)	5 (1)
C (5)	21 (1)	18 (2)	18 (1)	7 (1)	2 (1)	3 (1)
C (6)	16 (1)	15 (1)	14 (1)	-1 (1)	2 (1)	3 (1)
C (7)	18 (1)	15 (1)	14 (1)	-2 (1)	3 (1)	3 (1)
C (8)	15 (1)	14 (1)	17 (1)	1 (1)	-1 (1)	4 (1)
C (9)	20 (1)	18 (1)	13 (1)	0 (1)	1 (1)	6 (1)
C (10)	16 (1)	28 (2)	32 (2)	-10 (1)	8 (1)	1 (1)
C (11)	25 (2)	25 (2)	29 (2)	-2 (1)	2 (1)	7 (1)
C (12)	35 (2)	33 (2)	56 (3)	-2 (2)	-2 (2)	-7 (2)
C (13)	18 (1)	19 (1)	16 (1)	-1 (1)	0 (1)	-3 (1)
C (14)	22 (1)	18 (1)	18 (1)	1 (1)	3 (1)	-2 (1)
C (15)	16 (1)	20 (1)	17 (1)	7 (1)	4 (1)	0 (1)
C (16)	16 (1)	24 (2)	15 (1)	2 (1)	2 (1)	-6 (1)
C (17)	22 (1)	16 (1)	17 (1)	-1 (1)	4 (1)	-7 (1)
C (18)	18 (1)	19 (1)	12 (1)	2 (1)	4 (1)	-2 (1)
C (19)	19 (1)	14 (1)	12 (1)	0 (1)	0 (1)	-6 (1)
C (20)	18 (1)	14 (1)	19 (1)	-1 (1)	2 (1)	-2 (1)
C (21)	21 (1)	15 (1)	11 (1)	-1 (1)	2 (1)	-3 (1)
C (22)	18 (1)	23 (2)	22 (1)	0 (1)	1 (1)	-3 (1)
C (23)	26 (2)	30 (2)	26 (2)	7 (1)	8 (1)	1 (1)
C (24)	33 (2)	21 (2)	39 (2)	-1 (1)	16 (2)	2 (1)

Table 5. Hydrogen coordinates ($\times 10^4$) and isotropic displacement parameters ($\text{\AA}^2 \times 10^3$) for 16.

	x	y	z	U(eq)
H(1A)	3372	3472	3534	19
H(2A)	4338	4607	4138	19
H(3A)	5238	5042	3624	24
H(4A)	1775	-1583	1340	20
H(5A)	803	-429	781	20
H(6A)	-99	-43	1379	22
H(1B)	3481	-949	4445	22
H(2B)	2489	-2094	4258	23
H(4B)	1624	1238	2676	25
H(5B)	2615	2408	2887	23
H(8A)	4321	-131	4289	19
H(8B)	4550	1223	4966	19
H(10A)	6082	4102	3020	30
H(10B)	6017	2657	3588	30
H(11A)	6392	4145	5043	32
H(12A)	7101	5011	3750	52
H(12B)	7303	5211	4907	52
H(13A)	1623	-5952	350	22
H(14A)	2594	-7186	532	24
H(16A)	3500	-3999	2215	22
H(17A)	2541	-2721	1987	22
H(20A)	812	-5171	587	21
H(20B)	570	-3809	-75	21
H(22A)	-824	-1942	1941	26
H(22B)	-971	-2193	819	26
H(23A)	-1302	381	678	32
H(24A)	-1689	-711	2253	36
H(24B)	-1983	714	1634	36